AN ABSTRACT OF THE THESIS OF

Gary E. Clapp for the degree of Doctor of Philosophy

in Chemistry presented on April 15, 1991

Title : Reactive Intermediates : I. The Mechanisms of Photodehalogenation of Three Tetrachloronaphthalenes II. Structure and Electronic Effects in Some Selected Carbenes

Abstract approved: Redacted for Privacy

Dr. Peter K. Freeman

The photodechlorination of three tetrachloronaphthalenes (TCNs) has been studied at the excitation wavelength of 300 nm. Irradiation of 1,2,3,4-, 1,4,6,7-, and 1,3,5,8-tetrachloronaphthalene leads to dechlorination. Regioselective dechlorination is accomplished when phololyses are carried out in the presence of electron transfer reagents. Photolyses in the absence of electron transfer reagents yield very different regioselectivity suggesting the possibility of a different mechanism for this reaction. The observed increase in quantum yield, with increasing concentration of TCN, oxygen quenching of dechlorination, lack of fluorescence, and a strong phosphorescence spectra implies formation of an excimer between triplet state and ground state TCN as the key reactive intermediate. The photolyses accomplished in the presence of triethylamine (TEA) suggest the possibility of singlet exciplexes (TCN-TEA) participating in the formation of products. The photolyses carried out in micellar media imply the triplet can also participate in the product forming step by direct bond cleavage. It has been interpreted that the excimer is a weakly polarized and bound complex which dechlorinates to give similar products as is observed in

straight triplet dechlorination (micellar). Computer modeled intermediates did not prove as insightful as might be anticipated owing to the lack of sophisticated computational programs available for these size molecules.

The effect of conjugation with π systems, with cyclopropyl units, and with a remote site (in homoconjugate sense) on activation parameters and reactivity of carbenes was investigated. Remote site carbene interaction was characterized by relating the observed reactivity to a saturated analog. The mechanistic pathways are thought to arise from two routes: a pyrozole route and a carbene to carbene rearrangement. The conjugation effects on the reactive parameters of carbenes were found to arise from the following: the interaction of molecular orbitals of a π or cyclopropyl system with the carbene carbon and orientation of the polar DMSO solvent.

Reactive Intermediates: I. The Mechanisms of Photodehalogenation of Three Tetrachloronaphthalenes II. Structure and Electronic Effects in Some Selected Carbenes

by

Gary E. Clapp

A THESIS

submitted to

Oregon State University

In partial fulfillment of

the requirements for the

degree of

Doctor of Philosophy

Completed April 15, 1991

Commencement June 1991

APPROVED:

Redacted for Privacy

Professor of Chemistry in Charge of Major

Redacted for Privacy

Head of Department of Chemistry

Redacted for Privacy

Dean of Graduate School

Date thesis is presented April 15, 1991

Typed by Gary E. and Mary J. Clapp

Acknowledgement

As we venture forth into the next stage of life I am reminded of all the people and friends we have come to know here at Oregon State University. We are leaving behind too many friends to thank individually so for those not mentioned specifically, I leave this thought: All that makes us individuals are the fragments of the people we have known in the past, therefore, the person that I am leaves here with a part of you.

These are a few of the people and things that make or made it happen: Rodger, Belaid, P. K. Freeman (the Boss), G. J. Gleicher (the graduate student's friend), Free Nelson (Boo Chicago), Christina, Alan, Mischenko, Alan (again), The Waddle (great mechanic), Mokler (who's he?), Siggel (the Enforcer), the Yaegers, Amedio (rangy), Harry Carey, Minne*soda*, Harmon, Letterman, Hamrick, Tonka Toys, SNL, Sci-fi, Chemistry, Golf, Softball, Grapes (especially pinot), My brothers; the golden boys we're young, we're tough, we're good-looking, and we'll be there!, Toske?, and of course my immediate family: Mother, Father, Grandparents (Trixie), Brothers Tony, Ron, Steve and, last but not least, my lovely wife MJ.

I wish to extend my deepest feelings to my two closest friends, "The Chief" and Mary Jean; for putting up with all this turmoil and trouble. It just goes to show you that even a blind pig occasionally finds an acorn and Hey, "it beats a poke in the eye with a sharp stick". The survival has made us strong.

TABLE OF CONTENTS

LIST OF FIGURES

FIGURE Page

FIGURE Page

LIST OF TABLES

TABLE Page

Reactive Intermediates: I. The Mechanisms of Photodehalogenation of Three Tetrachloronaphthalenes II. Structure and Electronic Effects in Some Selected Carbenes

Chapter I. The Mechanisms of Photodehalogenation of Three Tetrachloronaphthalenes

Introduction

The first recorded observation of products resulting from the reaction of chlorine with naphthalene in the presence of a catalyst was 1833.[1] Patented use of chlorinated naphthalenes began just prior to World War I.[2-4] In general, use of polychlorinated naphthalenes (PCNs) are similar to those of polychlorinated biphenyls (PCBs). PCNs have been employed by the electrical industry as separators in storage batteries, high temperature flame resistant condenser and coil seals, and binders in electrical grade ceramics. They are also employed as water-proofing, flame-retarding, fungicidal and insecticidal inhibiting agents for wood, paper, and textile products.[5] Production of PCNs is estimated to be thousands of tons per year dating from the early 1900s to approximatly 1970.[6,7] Today the family of PCNs include halowaxes, nibren waxes, and clonacire waxes. PCNs have been employed in many industries because of their associated physical properties. Commercially, PCNs are produced by chlorinating naphthalene with chlorine gas in the presence of Fe (III) or Sb (V) chloride. During the process the temperature is increased from 80 °C to 200 °C while the mixture is agitated. When the degree of chlorine uptake is

accomplished, the reaction is quenched by neutralization with aqueous alkali. The products are then washed and vacuum dried. Theoretically, this can produce approximately 75 different PCNs which makes the direct chlorination to produce pure chlorinated naphthalenes an undesirable synthetic route. Therefore, an indirect method is needed to produce desired isomers of polychloronaphthalenes.

The toxicological and environmental hazards of PCNs were reviewed by Kimbrough[8] and Kover[9]. PCNs have been linked to various diseases such as chloracne, x-disease in cattle, and chick oedema.[10-15] PCNs and many other haloarenes have been implicated as the cause of many diseaeses. Massive outbreaks of chloracne occured during World War I when Germany put chlorinated naphthalenes to use as substitutes for natural waxes and rubber. Large outbreaks also appeared in the late 1930's and early 1940's as a result of the manufacture and use of electrical cables whose covering was a fabric impregnated with penta and hexachloronaphthalenes.[16,17,18] Most reports of chloracne are associated with external contact; however, it has been shown that PCN's fumes are by far the most potent, solutions less so, and non-friction contact with the solid is of little importance.[16] The acnegenic activity in man has been shown to be positive in every area of the body tested.[17] Liver disease can occur independently of chloracne.[18] The disease will manifest itself after just 4-6 months of exposure and liver failure can ensue resulting in death.[19]

In 1941, the term x-disease was used to describe an unknown condition seen in many cattle. The disease was later attributed to the intake of highly chlorinated naphthalenes resulting in poisoning. The first symptoms of

poisoning reported were weakness, excessive lacrimation, diarrhea, and large discharges from the nostrils. A chronic cough, poor appetite, and hyperkeratosis of the skin would follow. The degeneration of the pancreas, liver, gall bladder, and renal-cortex cells were also observed.[8,20] Cats, dogs, rats, and chickens impregnated or fed with PCNs that contained high degrees of chlorination quickly began to show symptoms of x-disease. No x-disease symptoms were found after the same test feeding and impregnation with mono and dichloronaphthalenes.

Metabolism

An extensive study on the metabolism of PCNs with rabbits was done by Cornish and Bloch.[21] The authors administered a variety of chloronaphthalenes to rabbits and monitored the urine for the next several days. The results show that the lower chlorinated compounds were readily metabolized and the higher chlorinated analogs could not be detected. The authors conclude that these compounds were metabolized *via* pathways that yield products not easily identified, are deposited and cumulate in tissues, or they are excreted slowly over long periods of time and not detected during the testing period. This seems to agree with the studies of Ruzo. Ruzo *et al.* fed pigs and frogs Halowax 1031, a mixture of chlorinated naphthalenes; the major metabolites isolated are phenolic products.[22,23] The authors assign the transformation (Pathway M) to the metabolic route of disposal of lower chlorinated naphthalenes. No isolation of the hexachloro derived products are observed in

Pathway M

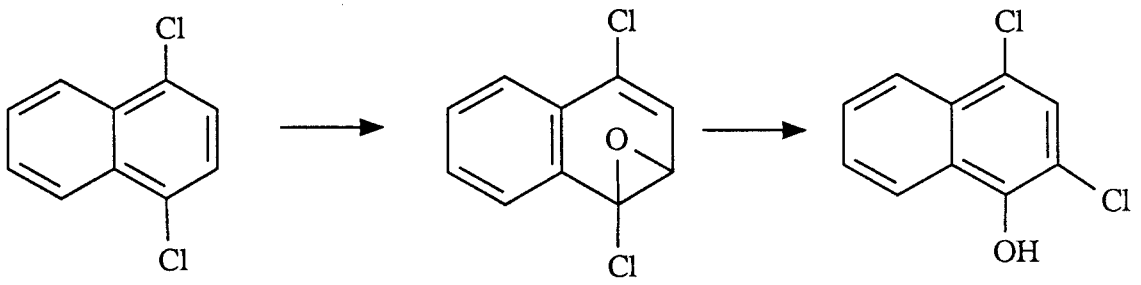

the urinary analysis. This again is in contrast to the lower chlorinated analogs. Although metabolic pathways of PCNs have not been fully elucidated, it is clear that the relationship between toxicity and the number of chlorines present on the ring is one which increases with higher degrees of chlorination.[24,25] Therefore, it is deemed prudent to investigate chlorinated naphthalenes (**1**, **2**, and **3**) which could serve as models for the higher chlorinated analogs.

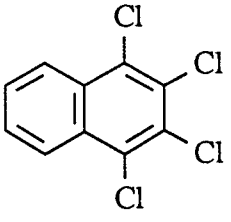

1

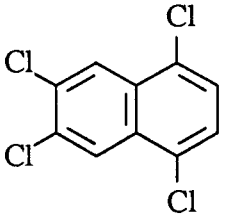

2

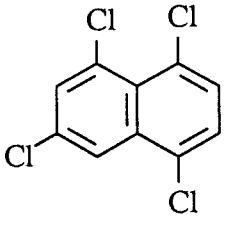

3

Project Goals

In light of the environmental and health problems associated with exposure to PCNs, a clear understanding of the physical behavior of aromatic halides is critical. The photochemical transformations of aryl halides in general is not thoroughly understood. The major photochemical process that occurs in

halogenated aromatics is dehalogenation. Since the toxicity is known to decrease with decreasing chlorination, perhaps the photochemical reactivity may provide a method for detoxification (dechlorination) of PCNs and other aryl halides.

The photochemical excitation of the haloarene leads to the first excited singlet state. The excited singlet state possesses sufficient energy to induce carbon-halogen bond cleavage (Equation I.1).[5] Haloarenes can also undergo

Equation I.1

$$ArX \xrightarrow{light} ArX^1 \longrightarrow Ar\cdot + X\cdot \longrightarrow Products$$

intersystem crossing from the singlet to the triplet state. The triplet state has been reported to participate in the dehalogenation of halo substituted benzenes.[26,27] The extent to which both reactive states are participating in the dehalogenation process (Equation I.2) may be addressed by measuring the intersystem crossing efficiency (ϕ_{isc}). Intersystem crossing efficiency is defined by the number of singlet excited state molecules that cross to the triplet excited state relative to the total number of excited state singlets produced ($k_{isc}/(k_{sd} + k_r + k_{isc})$). Intersystem crossing efficiencies for tetrachlorobiphenyls are found to be unity.[28] Bunce has determined that polychloronaphthalenes dehalogenate through a triplet manifold but does not address the energetics of the bond cleavage in detail.[29,30]

Equation I.2

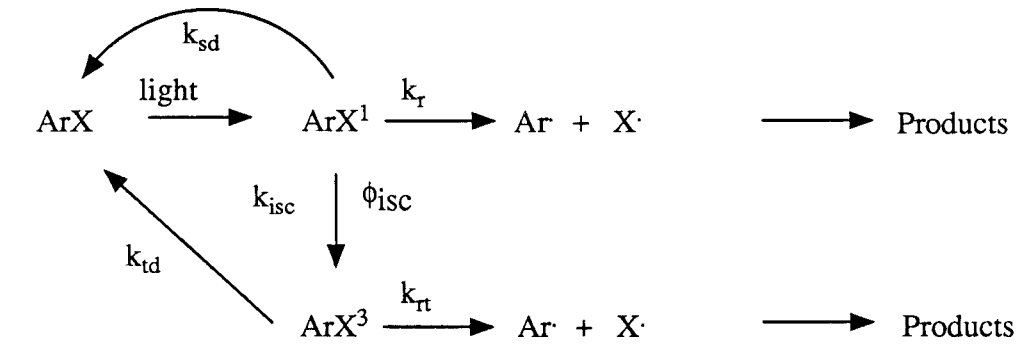

Soumillion and DeWolf suggest products arise from both singlet and triplet manifolds.[31] The possibility of dual mechanisms raises an important energy question. Triplet state energies have been calculated to be far less than aryl-halide bond energies.[32] In order to explain the triplet state reactivity Soumillion and DeWolf postulated the formation of radical ion pairs *via* a triplet excimer. The radical anion could then lose chloride anion and lead to products. Freeman and Ramnath also invoked excimer formation as a product determining intermediate in the photodehalogenation of pentachlorobenzene (Equation I.3).[33] D: represents a generic donor molecule. If D: = ArX there is an excimer formation prior to dehalogenation and if D: = any other electron donor species there is an exciplex formation that leads to product.

Equation I.3

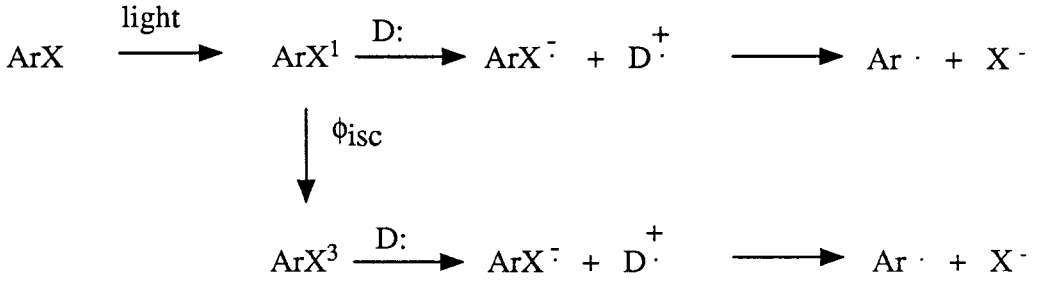

Chloronaphthalene and naphthalene are known to form excimeric species and the associated triplet excimeric spectra have been reported.[34] Bunce also suggests the possibility of an excimer or exciplex π complex being formed in the photolysis of chloronaphthalenes.[29] Bunce further suggests that the electron transfer complex (excimer or exciplex) may correspond to the "π-dimer" known to exist for many aromatic compounds. The π excimer is expected to be a sandwich type of dimer with the two aromatic molecular nuclei occupying parallel planes.[35] The question of planarity between nuclei of aromatic species is supported by the studies of Hirayama.[36] Hirayama studied the effect on fluorescence (singlet) intramolecular excimer formation in a series of diphenyl and triphenyl alkanes (Ph-$(CH_2)_n$-Ph and Ph_2-CH-$(CH_2)_n$-Ph). Hirayama concludes that excimer formation only occurs in a parallel sandwich configuration with a large degree of overlapping of the two π systems. The formation of excimer is most favored when $n = 3$ and $R = 3.2$ Å. Hirayama referred to this as the $n = 3$ rule. While no excimer spectra was obtained for systems where $n \neq 3$, the author did leave open the question of a weakly bound excimeric complex with only a partial overlap of the electron clouds at a distance greater than 3.2 Å. Lim monitored the formation of excimeric

1,n-di-α-naphthyl alkanes in isooctane through phosphorescence (triplet) studies.[37] The fact that the 1,1-di-α-naphthylmethane with two skewed rings exhibits excimer phosphorescence similar to the naphthalene triplet excimer supports the conclusion that both excimers are of skewed structure. Therefore, singlet excimer formation is thought to be coplanar and triplet excimer is thought to be a skewed type of structure.

Photoreactions of many aromatic halides have been studied by several research groups. However, a broader understanding of the mechanisms involved is required. As part of a broad investigation of the photodehalogenation of environmentally significant aryl halides, the chloronaphthalene system was chosen for study. The specific goal of this study is to elucidate the mechanistic pathways for photodehalogenation.

Photochemistry and Spectroscopy of Polychloronaphthalenes

Chloronaphthalenes exhibit a moderate absorption in the 300 nm region that has been assigned to a π-π^* transition. As in other halogenated aromatics, interaction of the lone pair electrons of the halogen with the π system leads to an excited state that may contain some carbon-halogen antibonding character such that bond cleavage might be expected. The excitation incident at 300 nm does possess sufficient energy to cause rupture of the carbon-halogen bond.[38]

The absorption of light by polychloronaphthalenes (PCNs) in solution is expected to lead to excited singlet states. The upper excited singlet states (s_{1+x}) should cascade down to the lowest excited state singlet (s_1). This decay occurs in the time domain of 10^{-12} sec.[39] Singlet processes do not appear to be as

important as triplet processes due to the intersystem crossing efficiencies in higher chlorinated analogs.[29,30] Both naphthalene and chloronaphthalene exhibit singlet and triplet emission spectra.[34] The only reported spectra for tetrachloronaphthalene is the triplet derived phosphorescence and lifetimes previously measured by Giachino.[40a,b] Heavily chlorinated biphenyls demonstrate similar behavior in that only phosphorescence spectra is observed. Tetrachlorobiphenyls show no singlet spectra due to the efficient intersystem crossing to the triplet state. Wagner reports the existence of only one reactive state for several tetrachlorobiphenyls, the triplet, derived from the linearity of Stern-Volmer plots.[28]

Bunce and Ruzo report the quantum yield for the photodechlorination of chloronaphthalene is reduced by approximately 60 % in the presence of atmospheric oxygen, while in the presence of the sensitizer benzophenone the quantum yield is essentially unchanged. The authors conclude that a triplet state is the principal precursor to product.[29] The predominance of triplet derived products seems reasonable in view of the high phosphorescence to fluorescence ratio of 5.2 observed in chloronaphthalene and a very low value 0.09 for naphthalene.[29] This is attributed to the presence of the heavy atom and the well known heavy atom effect for catalysis of intersystem crossing in aromatic systems.[39]

Chloronaphthalenes are found to undergo photochemical fragmentations. Chloride ion formation has been observed in the photolysis of 1-chloronaphthalene in ethanol. It is inferred that the chloride formation arises from HCl formation. Irradiation of the same compound in benzene affords small amounts of 1-phenylnaphthalene. Kulis *et al.* observed photoreduction of

1-chloronaphthalene in methanolic KOH and found the quantum yield to be dependent upon the concentration of base. The authors conclude that there is an electron transfer process operative in the dehalogenation of chloronaphthalene.[41] Similar photoreactions for bromonaphthalene and bromoquinone in basic media have been reported as well.[29]

Quantum yields for photodechlorinations of 1- and 2-chloronaphthalene in CH_3OH, CH_3CN, and C_6H_{12} are reported to be comparable which suggests a similar lability for the chlorine atom in both environments. Bunce and Ruzo found that photolysis of 1,2-dichloronaphthalene gives approximately equal amounts of the monochloro products at small conversions. The authors conclude there is little positional dependence in the lower chlorinated analogs.[29] An examination of the product array led to the suggestion that indeed there are free radical intermediates involved in the photochemical dehalogenation of chloronaphthalenes. Bunce and Ruzo further suggest that an electron transfer process could be operative. This postulate is supported by the observed increase in quantum yield for photodechlorination of 1-chloronaphthalene in the the presence of triethylamine, a known electron transfer reagent.[42]

Photoinduced Electron Transfer Reactions

The action of amines as reducing agents and electron donors to excited state aromatic compounds has been studied by many researchers.[43] As noted earlier, Bunce *et al.* observed rate acceleration in the photodehalogenation of 1-chloronaphthalene in the presence of triethylamine (TEA).[42] Other aromatic halides demonstrate increased reactivity in the presence of amines or sodium

borohydride.[44,45] Davidson and Goodin suggest that the rate acceleration observed is due to the amine donating an electron to an excited state (singlet or triplet) aromatic halide.[46] The radical anion formed then decomposes to aryl radical and halide anion. Scheme I.1 summarizes the mechanisms reported for the photodehalogenation of several aromatic halides in the presence of TEA.

Scheme I.1

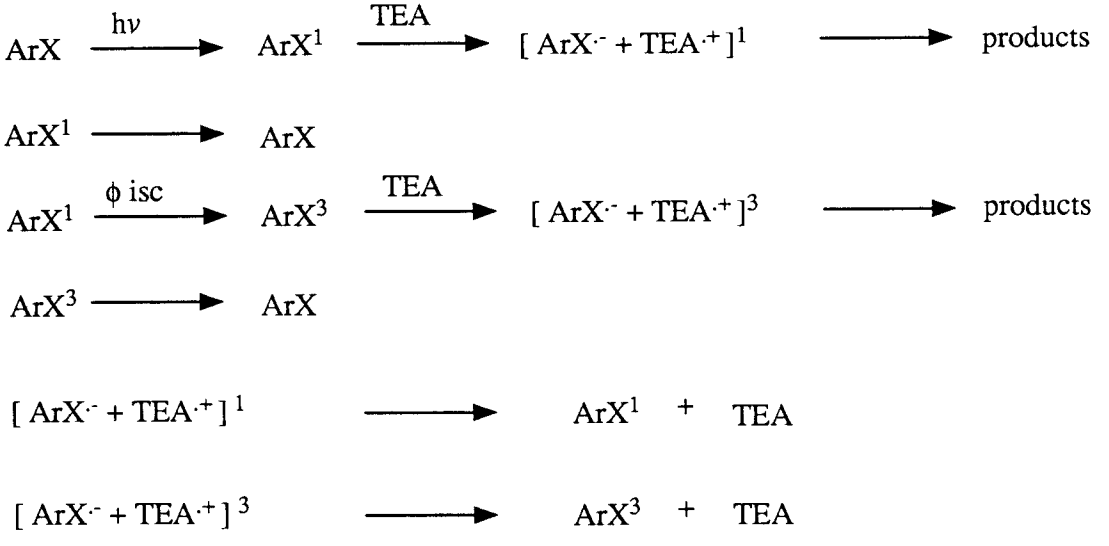

Two studies have been done in an effort to ascertain the mechanism by which the dechlorinated products form after the electron transfer step.[46,47] Deuterium incorporation from various solvents and solvent mixtures containing abstractable hydrogens (deuteriums) led to the following three postulated mechanisms (Scheme I.2). The authors conclude that the hydrogen introduced

Scheme I.2

A) $ArCl^{\cdot -} \longrightarrow Cl^- + Ar^{\cdot} \xrightarrow{RH} ArH + R^{\cdot}$

Homolytic hydrogen abstraction

B) $ArCl^{\cdot -} + H^+ \longrightarrow ArCl{\cdot}H \longrightarrow Cl^{\cdot} + ArH$

Solvent acting as proton donor

C) $ArCl^{\cdot -} + TEA^{\cdot +} \longrightarrow ArCl{\cdot}H + :N(\dot{C}HCH_3)(Et)_2 \longrightarrow Cl^{\cdot} + ArH$

Protonation of exciplex/radical ion pair

into the product arises in part from protonation by triethylamine radical cation and in part from hydrogen abstraction from the bulk solvent.

Barltrop and Bradbury reported the photodehalogenation of Ar-X (X = I, Br, Cl) in the presence of sodium borohydride.[48] Benzene is the only product observed with quantum yields approaching unity. Barltrop suggests the mechanism is a radical chain process. Bunce reported the photochemical dehalogenation of chlorobenzene in the presence of sodium borohydride and also concluded there is a radical chain process operative.[47] The chain process occurs when the phenyl radical abstracts a hydrogen from BH_4^- to give the chain carrier $BH_3^{\cdot -}$. This work is in contrast to the results obtained by Epling and Florio.[49a,b] Epling and Florio found hydride transfer to the excited state aromatic to be consistent with their results. Deuterium studies that were carried out by Freeman and Ramnath on the pentachlorobenzene reaction with sodium borohydride demonstrate that hydrogen transfer takes place after a bimolecular electron transfer step. The authors reach this conclusion from the observations

that the quantum yields for sodium borohydride and borodeuteride are essentially the same and that the quantum yield is linearly dependent upon borohydride or deuteride concentration.[33]

A useful method for determining lifetimes and spin states of reactive species is employment of diene sensitized experiments. Quenching experiments were carried out by Bunce *et al.* in order to measure the triplet lifetimes of chloronaphthalenes.[29] Many dienes were used and most experiments were met with little or no success. The employment of 1,3-cyclohexadiene (E_t = 50 Kcal/mol), biacetyl (E_t = 55 Kcal/mol), and trans stilbene (E_t = 50 Kcal/mol) all demonstrate rate acceleration for the disappearance of starting chloronaphthalene, yet the reaction is quenched by atmospheric amounts of oxygen. The lack of quenching made it impossible to evaluate room temperature, solution, triplet lifetimes. This led Bunce *et al.* to conclude that either energy transfer does not occur despite the energetic favorability, or it is in competition with another process by which decomposition of the excited state species is enhanced. Another suggestion by Bunce *et al.* is the formation of an exciplex followed by an electron transfer. This possibility is not further explored but does provide a pathway to products that is consistent with the observed product array.

Regiochemical Dehalogenation

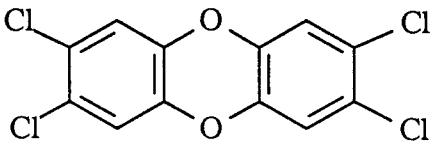

2,3,7,8-TCDD

TCDD = Tetrachlorodibenzodioxin

2,3,7,8-TCDD is reported to be one of the most toxic compounds known to man.[50] Oral LD_{50} values are reported to range from as low as 0.6 μg/kg for female rats to 1.0 mg/kg in frogs. An examination of the structure reveals chlorine substituents at the β and β' position in both ring systems. If there is a connection between toxicity and substitution patterns it becomes essential to control and predict the sites of dehalogenation. Hence, a question: can regiochemical dehalogenation be controlled and/or predicted? Freeman and co-workers have suggested a rationale for the observed regiochemistry in the photodehalogenation of polychloroarenes which react *via* radical anion intermediates (Scheme I.3).[51]

Rationalization is accomplished by considering transition states for two competing pathways leading to the observed products. Freeman suggests the loss of chloride originates from a bent transition state (route A) with some radical localization at C_1.[51] The loss of chloride in a coplanar transition state model (route B) leads to an excited state (an empty sp^2-orbital on C_1 and an extra electron in the π system). The bent transition state model leads to a restoration of the aromatic system forming a phenyl radical and the chloride

Scheme I.3

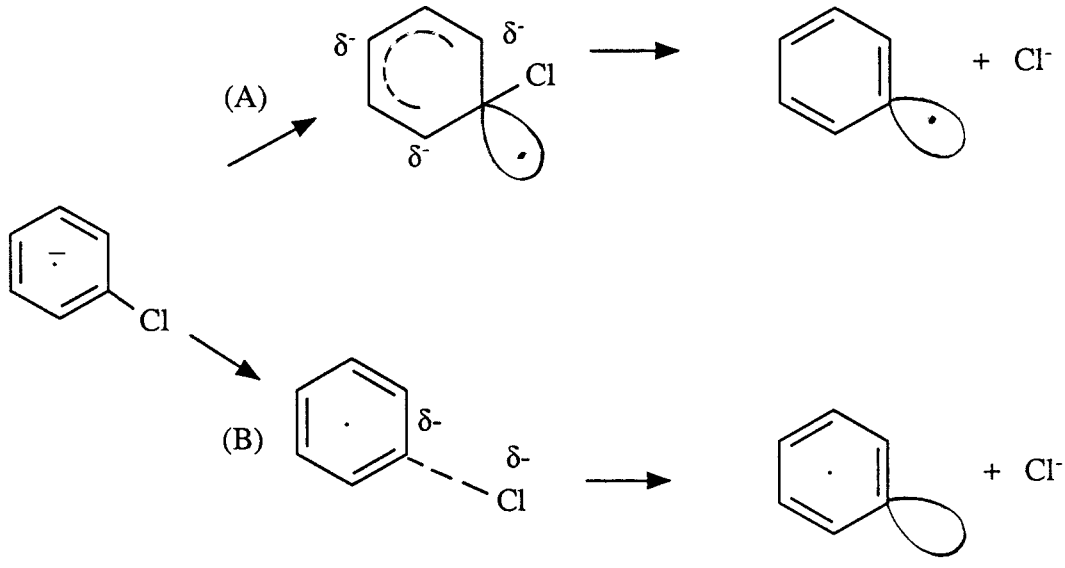

anion as products.

The above transition state model (in route A) now resembles a Wheland type intermediate and it is expected that there will be similarities between the regiochemistry observed for nucleophilic substitution and the regiochemistry of dehalogenation. The reactivity patterns are rationalized by the relative stabilities of all possible Wheland intermediates. Stability is decreased through electron pair repulsion which is created by placement of a halogen on a carbon with partial negative charge.[52] The stability is then assessed by determining which of the intermediates possesses a minimum value for the sum of the charge on carbons that bear an ipso halogen (ΣC_{iX}^2 for the NBMO).[53a,b] This explanation is termed the I_π repulsion theory and has been used to rationalize orientation in nucleophilic substitution at aromatic sites. If employed, this approach predicts the order of stability in Scheme I.4 to be C > D > E. The authors sucessfully used this rationale to analyze the observed relative reactivities in

pentachlorobenzene, triethylamine-mediated, radical-anion photolyses.

Scheme I.4

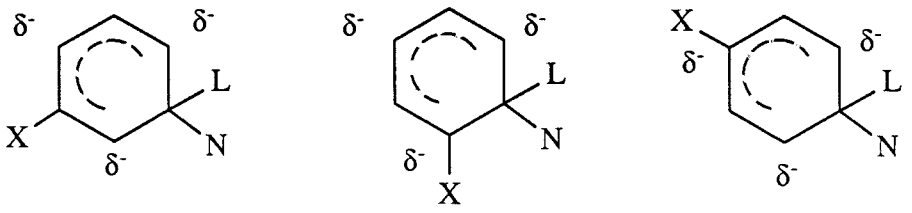

C D E

The pathway proposed by Freeman *et al.* is analogous to the $S_{RN}1$ mechanism for nucleophilic displacement at an aromatic site. $S_{RN}1$ chemistry has been induced chemically, photochemically, and electrochemically.[54] The reactivity of the radical anion formed in the photochemical process can be viewed as analogous to the electrochemical reduction of the haloarene in question. Several papers report attempts to correlate electrochemical reduction potentials with some sort of semi-empirical energy molecular orbital calculation.[54,55] The rate constants for cleavage of the initially formed radical anion are known to vary considerably (half-lives range from hours to nanoseconds) with the nature of the aromatic system and the halogen. Iodide is a better leaving group than bromide which in turn is better than chloride.

The formation and cleavage of the radical anion into the aryl radical and halide anion can be viewed as being initiated by an electron transfer reaction. The transferred electron is thought to first occupy the lowest unoccupied orbital (π^* orbital) of the aromatic system. As the bond is stretched a transition from π^* to σ^* occurs. The bond is cleaved leaving one unpaired electron in the σ-HOMO of the aryl fragment, and two electrons in the atomic 2p orbital of the departing halogen. Calculations of Savéant show that as the carbon-halogen

bond distance increases, stabilization of the carbon-halogen σ* orbital occurs. Virtually no stabilization of the π* orbital is observed. The authors use this observation to rationalize and correlate the reported reduction potentials with free energies of activation derived from σ* stabilization energy.[54,55]

The computations of Gallardo *et al.*[55d] also support a π* radical anion as the first step in electron transfer processes involving haloarenes. The electron is promoted to the anti-bonding σ* orbital in order to break the carbon-halogen bond. This is believed to involve the stretching of the carbon-halogen bond in order to produce the electron transfer. Transfer will take place at the crossing point of the π* and σ* energy surfaces. This is a forbidden transition but can take place if vibronic coupling is sufficient to bring the two surfaces close in energy. After crossing, bond breaking would take place very quickly.

Symons is also a proponent of a π* to σ* transition as the mode of bond cleavage. Symons, in his work on the dehalogenation of aromatic halides argues that, in order to break the carbon-halogen bond in the radical anion, the electron must be transferred from the π system (presumably the LUMO) to the anti-bonding orbital of the bond being cleaved.[56]

Geer and Farwell do not agree with a π* to σ* transition and make use of CNDO/2 calculations in order to evaluate what type of orbital (σ or π) receives the initial electron. The authors conclude the first electron enters a σ* anti-bonding orbital. The logic cited for this conclusion is the correlation observed between half wave potentials and calculated lumo σ energies.[55a]

Another recent publication suggests the π* to σ* transition results in the departure of chloride anion.[57] The departure is proposed to be heterolytic and the term mesolytic is used to describe radical cation and anion heterolytic bond

cleavages. The radical cationic process is further decribed by the term catiomesolytic and the radical anion by the term anionmesolytic.

From the point of view of the initially formed radical anion, the vast majority of reactions result in departure of chloride anion. It is thought that the most stable products are formed in such a process (thermodynamics as the driving force). However, it was recently postulated that the fragmentation process is controlled by factors other than product stability, arguing instead for a kinetically controlled process.[57,58] The kinetic control would involve the ability of the system to delocalize a charge across the bond that is to be cleaved. For radical anions, this ground state parameter, would be represented by the preexisting polarization in the site of eventual bond cleavage. The kinetic explanation turned out to be difficult to address in aromatic halide processes due to the lone pairs of electrons present on the halide. The lone pairs are able to spin-orbit couple with the aromatic system making them an integral part of the ground state and excited state electronics. Therefore, ground state calculations at the semiempirical level may not be sophisticated enough to handle this problem.

In summary, the literature illustrates two possibilities of bond cleavage for the proposed anionmesolytic reaction: the electron either enters a π^* orbital (I) or the electron enters a σ^* orbital (II). In case I the π^* orbital eventually passes the electron to the σ^* leading to bond cleavage in a concerted fashion or stepwise mode. In case II the anti-bonding σ^* orbital captures the electron and then dehalogenates directly. None of the computational models address the possibility of an sp^3 hybridized carbon, as the transition state, involved in the rate determining step of dehalogenation. Incidentally, no work is reported about

attempts to establish the position of the transition state along the reaction coordinate.

Chlorine Atom Abstraction

In 1963 the work of Lorenz *et al.* showed that several aromatic halides are reactive towards trialkyltin hydride.[59] No proposed mechanism is reported but under the reaction conditions employed it seems likely that there is some radical character to the reaction. Since this early report, the reactivity of trialkyl- and triaryltin hydrides and their use in radical generation has been studied extensively.[60] Grady and co-workers, in an investigation of substituent effects in the reduction of substituted benzyl chlorides by the tri-*n*-butyltin radical, observed a large positive rho value (0.81).[60b] The observed rho value is supportive of an atom transfer process with appreciable charge separation in the transition state (Scheme I.5) analogous to the hydrogen atom transfer previously reported.[61]

Scheme I.5

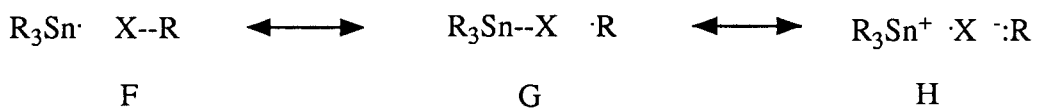

A study by Blackburn and Tanner shows a smaller substituent dependence in the corresponding reduction of benzylic bromides (rho = 0.22).[62] However, a larger dependence is observed in the case of substituted benzylic iodides (rho = 1.05). This is not considered consistent with a direct atom transfer process. The carbon-iodine bond is a weaker bond than the

corresponding bromine and chlorine bonds and, therefore, should be associated with a more exothermic process. A largely exothermic process is associated with an early transition state process and should demonstrate a smaller substituent effect.[63] Possible changes in mechanism can be inferred from these observations. Additional support for a change in mechanism between iodides *vs.* bromides and chlorides in hydride reductions is found by Kochi and co-workers.[64]

The observed reactivity of the trialkyl- or triaryltin radical towards chlorine containing compounds is supportive of a model where the chlorine atom is transferred to the tin directly. Calculated differences of energy tend to support a charge build up in the transition state shown in resonance form H. Charge build up is also supported by the observed rho values and substituent effects in Hammett studies reported on substituted benzylic chlorides.[65]

Chapter II. The Photochemistry of 1,2,3,4-, 1,4,6,7-, and 1,3,5,8-Tetrachloronaphthalene

Photochemistry

The recent past has seen an increase in the attention given to the photochemistry of chlorinated compounds such as chlorinated pesticides, PCBs, and, to a lesser extent, PCNs. Given the high chemical stability and toxic nature of these compounds, photochemical breakdown initiated by the active part of the solar spectrum would seem to be a real possibilty. Photodegradation of PCNs and related compounds may lead to their detoxification and, upon subsequent treatment, to their removal from the environment. It is known that chlorinated aromatic compounds undergo reductive dechlorination, dimerization, and solvent substitution as major reaction pathways to product.[29] The photolysis of 1-chloronaphthalene in a mixture of n-hexane and ethanol is reported to yield chloride anion (HCl) and naphthalene. The chloride yield is shown to increase with increasing ethanol concentration.[66] Small amounts of binaphthyl are also reported. The photolysis of monochloronaphthalene in degassed KOH solutions of 80% aqueous methanol has been carried out using incident light of 280 nm. Naphthalene was the isolated product.[67] The quantum yield was reported to be dependent upon base concentration. The reaction was also seen to take place in neutral media, however, the neutral media reaction demonstrates a lower quantum yield.[41]

Ruzo and Bunce studied a series of chlorinated naphthalenes using 300 nm light.[29a,c] The results, using methanol, cyclohexane, and acetonitrile-water

(4-1, V-V) as solvents, are summarized in the Table II.1. The authors report a

Table II.1 Reported PCN Photoreactivity.

PCN	Solvent	Φ	% dehalo.	Binaphthyl	solvent sub.
1	CH_3OH	0.005	74	25	-
1	CH_3OH-O_2	0.002	76	23	-
1	C_6H_{12}	-	88	12	-
1	CH_3CN-H_2O	-	<1	94	5
2	CH_3OH	0.007	58	38	4
2	CH_3OH-Ph_2CO	0.007	2	97	1
2	C_6H_{12}	-	72	28	-
2	CH_3CN-H_2O	-	2	94	4
1,2	CH_3OH	0.012	32	66	2
1,2	CH_3OH-Ph_2CO	0.014	28	68	4
1,8	CH_3OH	-	86	12	1
1,3,5,8	CH_3OH	-	80	18	1
1,2,3,4	CH_3OH	-	80	16	2

wide range of dechlorination, dimerization, and substitution products. The major organic compounds are indicative of the involvment of free-radical intermediates. The sensitized experiments in the presence of benzophenone or with atmospheric oxygen are considered indicative of a triplet excited state species as the principal precursor leading to product. The attempts to determine triplet lifetimes of PCNs by employment of the triplet quenchers, trans-stilbene, 1,3-cyclohexadiene, and biacetyl lead to unusual behavior, in that quantum yields for the loss of starting material are enhanced.[68,69] However, triplet lifetimes can be measured

in a glass of EPA (diethyl ether, isopentane, and ethyl alcohol) at 77 °K (Table II.2).[40]

Table II.2 Triplet Lifetimes of Chloronaphthalenes in EPA.

Isomer	Lifetime (msec)	k_d s^{-1}
1234	112 ± 3	8.93
1357	49 ± 2	20.4
1458	11.4 ± 0.2	87.7
2367	76 ± 3	13.2

If we are to make a real world application of this work we need to consider a model system that will be similar to the natural environment. A good model for environmental photochemistry is aqueous acetonitrile. Photolysis of chloronaphthalene in this system yields products of hydroxylation, chlorobinaphthyl, and hydroxylated dimers.[29a,70] The presence of oxygen suppressed the formation of products except for small amounts of 1-naphthol and naphthalene. Armed with this information, it is reasonable to postulate two pathways to product. Pathway one is an electron transfer type of activation leading to chloride and radical formation. Pathway two is a direct homolytic bond fission. It should be noted that the reactive species might arise from an excited state singlet or triplet.

$$ArCl \xrightarrow{h\nu} ArCl^* \xrightarrow{X} Ar\cdot + Cl^- + X^{\cdot+} \qquad \text{Pathway 1}$$

$$ArCl \xrightarrow{h\nu} ArCl^* \longrightarrow Ar\cdot + Cl\cdot \qquad \text{Pathway 2}$$

It is our intention to investigate these processes in the hope of better

characterizing the reactive intermediates. In view of the quantity of polychlorinated naphthalenes in our environment and the associated metabolic activity, it seems reasonable to study the photochemistry of some selected PCNs. A proper selection of compounds to study involves evaluation of the inherent ground state UV absorption spectrum of the individual PCNs. PCNS that demonstrate UV absorption in the region of 300 nm are good compounds to study because they allow for the use of the solar spectrum as a possible tool for the destruction of selected PCNs. Ultraviolet absorption data exists for a wide variety of PCNs (Table II.3).[5]

Table II.3 UV Data for Some Selected PCNs.

	λ (nm)	
PCN	B_b band	L_a band
nap.	218s, 221	257, 265, 274, 285
1-nap.	219s, 223	264, 273, 284, 295
2-nap.	221s, 225	257, 267, 277, 288
123	217s, 230s, 234	268, 278, 289, 300
138	217s, 222s, 230s, 235	275, 281, 298, 300
146	217s, 222s, 227s, 233	275, 285, 296, 309
1234	227s, 232, 238	274, 285, 296, 309
1358	221s, 238	285, 297, 308, 321
1467	223s, 228s, 241s, 245	280, 290, 302, 314
12345678	240s, 260s, 268s, 275	310, 322, 332, 345

An examination of the table demonstrates that as the number of chlorines affixed to the naphthalene ring system is increased, the λ_{max} moves to longer wavelength. A selection of test compounds of intermediate chlorination allows us to make inferences about the possibility of environmental application without creating an environmental hazard.

Results and Discussion

The three tetrachloronaphthalenes (TCNs) chosen for this investigation are 1,2,3,4- (1), 1,4,6,7- (2), and 1,3,5,8-tetrachloronaphthalene (3). This selection accomplishes two important goals. It allows for ease of product identification (seven total trichloronaphthalene products) and minimizes the inherent toxicity, disposal, and handling problems of the higher chlorinated analogs.

In an effort to characterize the product determining intermediates generated in the photodechlorination of polyhaloarenes, several experiments were conducted. Title compounds were photolyzed in the presence and absence of electron transfer reagents in CH_3CN solvent, in micellar solutions of hexadecyltrimethylammonium bromide (CTAB), and in CTAB solutions containing the electron transfer reagent triethylamine (TEA) at 300 nm. Dehalogenation was also accomplished by treatment of 1, 2, or 3 with lithium p,p'-di-*tert*-butylbiphenyl radical anion, triphenyltin hydride (AIBN initiation), and reduction *via* treatment with elemental potassium. The regiochemistry of dehalogenation was compared and contrasted. Kinetic analysis of the photodechlorination of the title compounds revealed linear relationships which are rationalized in terms of triplet and triplet excimer or exciplex reactivity. Both processes led to dehalogenation of starting materials. Reactive intermediates were modeled through the use of the AM1 calculations.[71] A simple molecular orbital approach to predict the most stable intermediate was also employed.

Acetonitrile Photolyses

The initial photodecomposition of the tetrachloronaphthalenes (TCNs) 1, 2, and 3 in CH_3CN, (300 nm) led to dehalogenation (Scheme II.1). All conversions were kept below 30% loss of starting material. Some of the TEA mediated photolyses went to near 30% conversion due to the reactivity in the concentrated regions of TEA. In order to get reliable gas chromatographic traces and integrations, the most dilute points of the straight photolyses approached 25% conversion. This was not expected to be a problem since the product of dechlorination is another aryl chloride (trichloronaphthalene) that would be expected to be a better complexing agent than the starting TCN. Consequently, if the conversion to trichloronaphthalene was a participant in rate of product formation the result would be an increase in quantum yield. The increase was not observed and no dichloro isomers were detected under these conditions. In Addition, no dimerization or solvent substitution was observed under reaction conditions. Quantum yields of the appearance of product and loss of starting material were followed. Quantum yield is defined as the ratio of moles of species formed or consumed to the moles light absorbed (Equation II.1). We were also concerned about the regiochemistry associated with the various modes of dehalogenation. The regiochemistry of dehalogenation of 1 favored 1,2,4-trichloronaphthalene (4) over 1,2,3-trichloronaphthalene (5) and dehalogenation of 2 favored 1,6,7,-trichloronaphthalene (6) over 1,4,6-trichloronaphthalene (7) by a values of 4.0:1.0 in each case (Table II.24, 25). The dehalogenation of 3 produced all four possible trichloronaphthalene products. Two major trichloro products and two minor ones were formed.

Scheme II.1

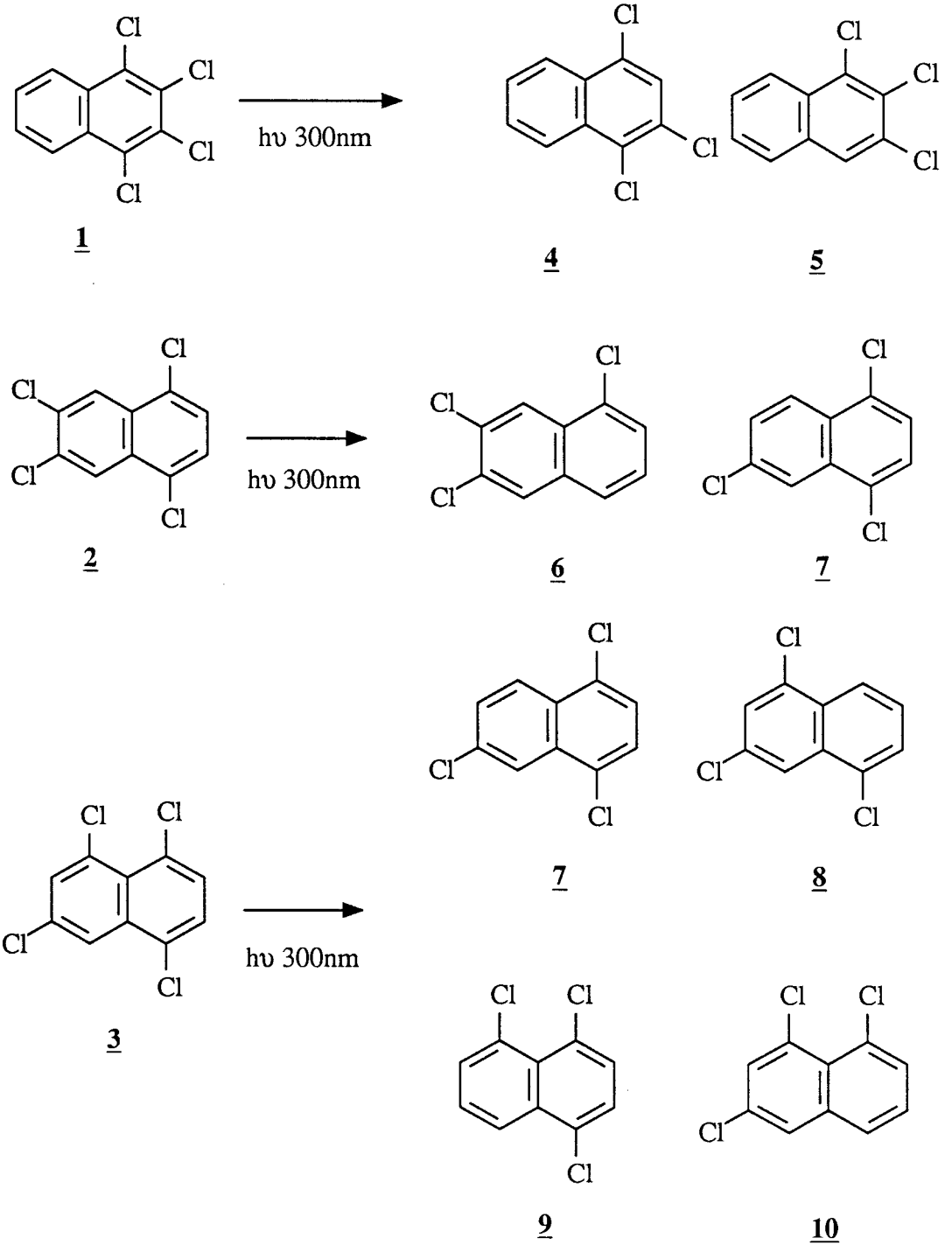

Equation II.1

$$\text{Quantum Yield} = \frac{[\text{ Moles of Product Formed or Starting Material Consumed }]}{[\text{ Moles of Light Absorbed }]}$$

The major trichloro products were identified as 1,4,6-trichloronaphthalene (7) and 1,3,5-trichloronaphthalene (8) and demonstrated an 8:7 ratio of 2.3:1.0 (Table II.26). The minor products were assumed to be 1,4,8-trichloronaphthalene (9) and 1,3,8-trichloronaphthalene (10). Minor products comprised less than 10% of the product formation quantum yield. Isolation for structure identification proved impossible owing to the small amount of products 9 and 10 formed.

Structure Identification

Starting materials were synthesized by standard literature preparation methods and identified by modern NMR techniques.[72] The compounds were further purified by recrystallization and sublimation. Compounds 1, 2, and 3 demonstrate the following spectra: For compounds 1, 2, and 3 the GC/MS is consistent with the empirical formula $C_{10}H_4Cl_4$ m/e = 264 (all Cl_{35}). The ^{13}C spectrum of 1 demonstrates only five ^{13}C resonances. The resonances obtained are 130.32, 130.14, 129.90, 128.72, and 125.41 ppm. The ^{1}H resonances observed are two multiplets that are found centered at 8.29 and 7.69 ppm respectively. The resonances centered at 8.29 were assigned to the para hydrogens (positions 5 and 8) based upon the shifts observed for similar naphthalene ring systems (para hydrogen resonances are typically 0.5 ppm down

field).[72b] The remaining absorption, centered at 7.69 ppm, was assigned to positions 6 and 7.

Compound 2 also demonstrates only five ^{13}C resonances in the NMR. The ^{13}C resonances are centered at 132.92, 130.41, 129.70, 127.02, and 126.23 ppm. The proton spectrum observed is a simple pair of broad singlets that resonate at 8.30 and 7.46 ppm. It is assumed the para hydrogens were resonating at 8.30 ppm (positions 5 and 8) for the same reason as above; the hydrogens at α positions in naphthalene ring systems show absorptions down field of the β position. The resonance at 7.46 is assigned to the hydrogens at positions 2 and 3.

Compound 3 presents a very different problem. The molecule does not possess the same symmetry elements as the two previous compounds and, therefore, all ^{13}C resonances are observed. The resonances found at 134.25, 132.60, 132.10, 131.90, 130.61, 130.48, 129.85, 127.55, 126.70, and 123.95 ppm are the chemical shifts detected. The proton spectra and correlation spectroscopy (HETCORE and COSY) allows for nearly complete structure elucidation. The hydrogen at position 2 is attached to the carbon at 131.90 ppm and demonstrates a doublet (J = 2.0 Hz) centered at 7.63 ppm. The hydrogen of position 4 (8.25 ppm, J = 2.0 Hz) is coupled to the resonance at 7.63 ppm (position 2) and is affixed to the carbon resonance at 123.95 ppm. The two remaining hydrogens (positions 6 and 7) are found as a triplet (doublet of doublets) centered at 7.44 and 7.49 (J = 8.0, 8.0 Hz). The hydrogens at positions 6 and 7 are affixed to the ^{13}C resonances at 127.55 and 130.48 ppm. Other TCNs (1,2,6,8- and 1,2,5,7-) were considered but proton NMR could not be rationalized to even remotely match the observed couplings and absorptions.

No further structure elucidation was deemed necessary.

The products of reduction and photolysis of the starting materials were isolated by preparatory GC. Only small amounts of product were produced, consequently, some of the carbon spectra is incomplete unless it was necessary for further structure proof. All compounds were submitted to a GC/MS analysis. The GC/MS data was consistent for the molecular formula $C_{10}H_5Cl_3$ with a parent m/e of 230 (all Cl_{35}). The molecular ion cluster pattern was consistent with a trichloro substitution due to the natural abundance in the $Cl_{35/37}$ ratio.

The products of decomposition of **1** were identified as 1,2,4- and 1,2,3-trichloronaphthalene (**4** and **5**). Compound **4** was identified by correlation spectroscopy (HETCOSY), ^1H, and ^{13}C NMR. The carbon spectra is 132.17, 131.26, 130.02, 129.73, 128.73, 128.68, 127.72, 127.07, 125.17, and 125.03 ppm. The hydrogen attached to position 3 demonstrates a singlet at 7.66 ppm. Position 5 is a broad doublet of doublets with a small 0.5 Hz coupling (para) making it a doublet of doublet of doublets (J = 8.5, 1.5, 0.5 Hz) centered at 8.27 ppm. The hydrogen at position 8 is also a doublet of doublet of doublets that manifests itself as a doublet of doublets centered at 8.32 ppm (J = 8.0, 1.5, 0.5). The hydrogens at positions 6 and 7 appear as a multiplet centered at 7.68 ppm. A COSY (^1H-^1H correlation) experiment demonstrates couplings of 8.5, 8.0, 1.5, and 1.5 Hz to the resonance at 7.68 ppm. The structure is then assigned to **4**.

Compound **5** was identified as 1,2,3-trichloronaphthalene by analysis of the proton NMR only. A phase sensitive COSY is used to nicely illustrate the proton relationships. The hydrogen at position 4 (d, 7.92 ppm) demonstrates 0.5

Hz transannular coupling to position 8[72] and a positive NOE to another resonance assigned to position 5. Position 5 (7.76 ppm, d,d,d J = 8.0, 2.0, 1.0 Hz) appears as a doublet of doublets but is later seen to also couple in a para relationship to position 8. Position 8 is also observed to be a doublet of doublets under standard proton conditions but the COSY experiment reveals a 1.0 Hz coupling to position 5 and the 0.5 Hz coupling to position 4 already noted above. The resonance associated with the chemical shift at 8.23 ppm is, therefore, assigned to be a d,d,d,d (J = 8.5, 2.0, 1.0, 0.5 Hz). The phase sensitive COSY also allows the assignment of the coupling constants for the hydrogens at positions 6 and 7. The multiplet observed is, in reality, two d,d,d. The hydrogen at position 7, (J = 8.5, 8.0, 2.0 Hz), is assigned to the resonance centered at 7.62 ppm and the hydrogen at position 6, (J = 8.0, 8.5, 2.0) is assigned to the resonance at 7.57 ppm. The ^{13}C was not assigned but resonances of 132.13, 131.50, 130.45, 130.15, 128.44, 128.02, 127.73, 127.38, 127.34, and 124.93 are observed.

The products obtained from dechlorination of compound **2** were identified as **6** and **7**. Compound **6** (1,6,7-trichloronaphthalene) was identified by assignment of proton resonances and coupling constants. The hydrogen at position 2 is doublet of doublets (J = 7.3, 2.0 Hz) centered at 7.59 ppm. Position 3 is occupied by a hydrogen with a triplet spectra (doublet of doublets). The triplet (7.42 ppm) is coupled into the resonance at 7.59 ppm (position 2, J = 7.3 Hz) and the resonance centered at 7.67 ppm (position 4, J = 7.8 Hz). Position 4 demonstrates coupling into positions 2, (2.0 Hz), position 3, (7.8 Hz), and position 8 (0.5 Hz). Also the hydrogen at position 4 shows a positive NOE with another hydrogen at position 5. Positions 5 and 8 appear as

broadened singlets at 7.97 and 8.38 ppm respectively, however, small couplings of 1.0 and 0.5 Hz can be found in the COSY for position 8 and 1.0 Hz for position 5. The hydrogen at position 5 also demonstrates a positive NOE with position 4. The ^{13}C spectrum observed is 133.20, 131.32, 130.81, 129.79, 128.99, 128.13, 127.14, 127.01, 125.95, and 125.79 ppm.

1,4,6-trichloronaphthalene, (7) demonstrates proton resonances from postions 2 and 3 as a doublet of doublets ($J = 8.2$ Hz) centered at 7.48 and 7.52 ppm. Position 5 is coupled into both positions 7 and 8. The observed splitting is a broadened doublet ($J = 2.0$ Hz) with a small 0.8 Hz coupling (para) centered at 8.29 ppm. Position 7 is a doublet of doublets ($J = 9.1$ and 2.0 Hz) centered at 7.59 ppm. Position 8 is identified as a doublet of doublets ($J = 9.1$, 0.8 Hz) that appears as a doublet at 8.24 ppm. The only ^{13}C spectrum obtained is the carbons that are connected to hydrogens 128.76, 127.07, 126.86, 126.18, and 124.04.

The final compound that was identified is 1,3,5-trichloronaphthalene **8**. Identification was accomplished by proton NMR. The proton at position 2 demonstrates a doublet ($J = 2.0$ Hz) at 7.64 ppm. Position 2 is coupled into position 4. Position 4 is 2.0 Hz coupled into position 2 and 0.5 Hz coupled into position 8 and resonates at 8.23 ppm. The proton at position 6 is a doublet of doublets ($J = 7.5$, 1.5 Hz) and is found at 7.67 ppm. Position 7 is an observed triplet at 7.50 ppm but is really another doublet of doublets ($J = 7.5$, 8.5 Hz). The position of the final hydrogen (8) is assigned by the observed transannular coupling to 4 ($J = 0.5$ Hz) and the coupling to positions 6 and 7 ($J = 1.5$, 8.5 Hz). The assignment is given to the resonance found at 8.18 ppm.

Data Interpretation

Quantum yields (Tables II.4-6) with respect to the number of moles of **1**, **2**, or **3** which react, increased with increasing concentration of tetrachloronaphthalene over the range 1×10^{-4} to 4×10^{-3} M. Quantum Yields with respect to the amount of product formed were also followed and demonstrated a similar trend (Tables II.4-6).

Table II.4 Photolysis of 1,2,3,4-TCN in CH_3CN at 300 nm.

TCN[a]	[TCN][b]	$[TCN]^{-1}$	Q.Y. pd[c]	Q.Y. sm[d]	$Q.Y.^{-1}pd$	$Q.Y.^{-1}sm$
1234	240	417	58.5	64.7	1710	1550
	103	971	49.6	55.9	2020	1790
	82.4	1210	44.4	47.8	2250	2090
	71.0	1410	39.8	29.5	2510	2330
	50.5	1980	29.5	33.8	3390	2960
	24.5	4080	18.0	20.6	5550	4860
	15.4	6790	11.5	11.7	8710	8530
	10.3	9710	11.6	12.0	8640	8320
	8.20	12100	11.4	11.7	8810	8550
	7.10	14100	11.2	11.6	8950	8650

[a] Isomer of tetrachloronaphthalene. [b] [Value] x 10^5 M. [c] Quantum yield for product appearance x 10^5. [d] Quantum yield for loss of starting material x 10^5.

Table II.5 Photolysis of 1,4,6,7-TCN in CH_3CN at 300 nm.

TCN[a]	[TCN][b]	$[TCN]^{-1}$	Q.Y pd[c]	Q.Y. sm[d]	$Q.Y.^{-1}pd$	$Q.Y.^{-1}sm$
1467	253	396	44.0	59.6	2280	1680
	101	990	39.8	51.0	2510	1960
	75.8	1320	37.1	49.1	2700	2040
	50.5	1980	33.1	43.3	3030	2310
	25.3	3960	20.8	22.6	4810	4430
	15.2	6580	13.8	15.5	7250	6440
	10.1	9900	14.3	15.7	6990	6360
	7.60	13200	14.0	15.4	7120	6500
	5.10	19800	13.1	14.5	7660	6890

[a] Isomer of tetrachloronaphthalene. [b] [Value] x 10^5 M. [c] Quantum yield for product appearance x 10^5. [d] Quantum yield for loss of starting material x 10^5.

Table II.6 Photolysis of 1,3,5,8-TCN in CH_3CN at 300 nm.

TCN[a]	[TCN][b]	$[TCN]^{-1}$	Q.Y pd[c]	Q.Y. sm[d]	$Q.Y.^{-1}pd$	$Q.Y.^{-1}sm$
1358	406	246	63.3	71.4	1580	1400
	325	307	61.6	70.4	1620	1430
	244	410	56.5	60.6	1770	1650
	203	492	50.8	55.9	1970	1790
	163	615	47.2	49.8	2120	2010
	81.4	1230	33.8	36.2	2960	2760
	40.7	2460	20.1	20.6	4980	4860
	32.5	3070	15.5	16.6	6430	6030
	16.3	6140	14.8	15.8	6780	6340
	10.7	9350	13.9	14.5	7190	6890
	8.10	12300	13.9	14.3	7210	7010

[a] Isomer of tetrachloronaphthalene. [b] [value] x 10^5 M. [c] Quantum yield for appearance of product x 10^5. [d] Quantum yield for loss of starting material x 10^5.

A strong agreement between quantum yields for loss of starting material and appearance of product is indicative of similar reaction pathways and a conservation of mass. In regions of greater dilution, linear functions with slope close to zero were observed. This is consistent with two competing pathways to product or loss of starting material: one dependent, and one that is independent, of concentration. (Figures II.1-6)

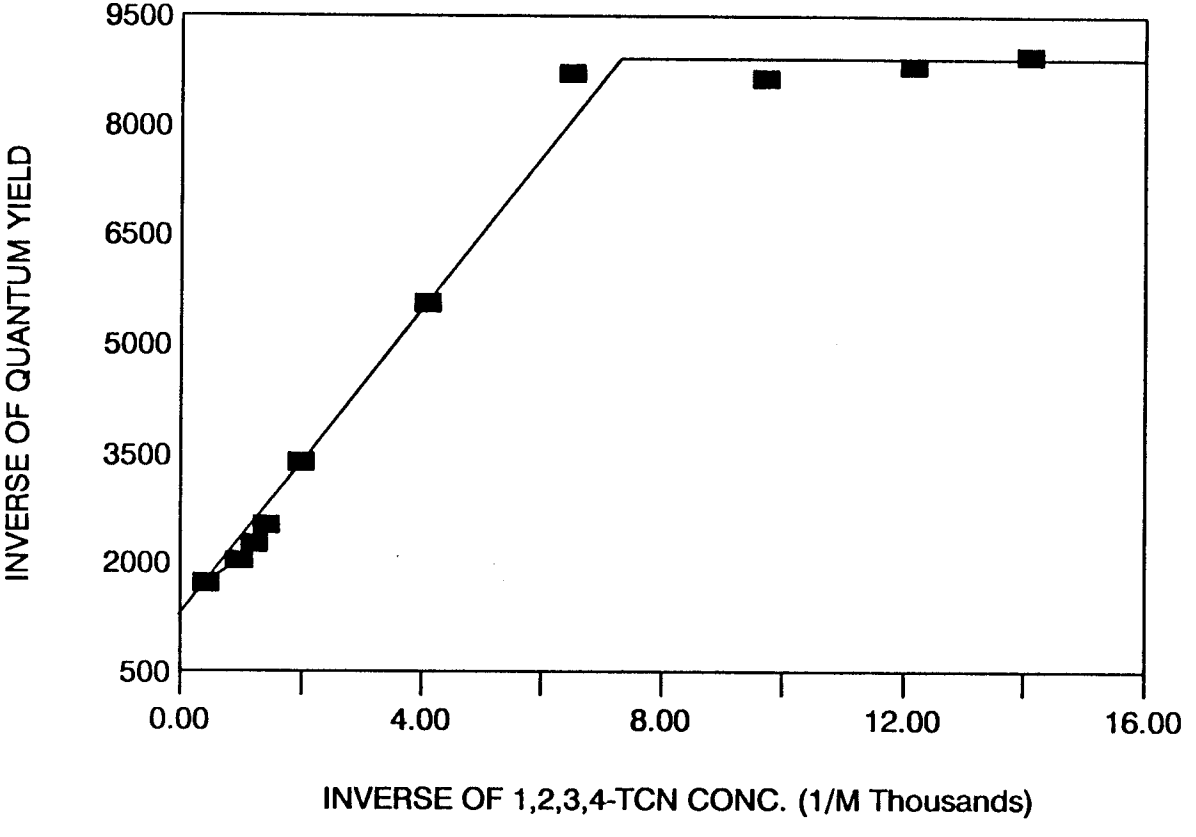

Figure II.1 Product Appearance from Photolysis of 1,2,3,4-Tetrachloronaphthalene at 300 nm.

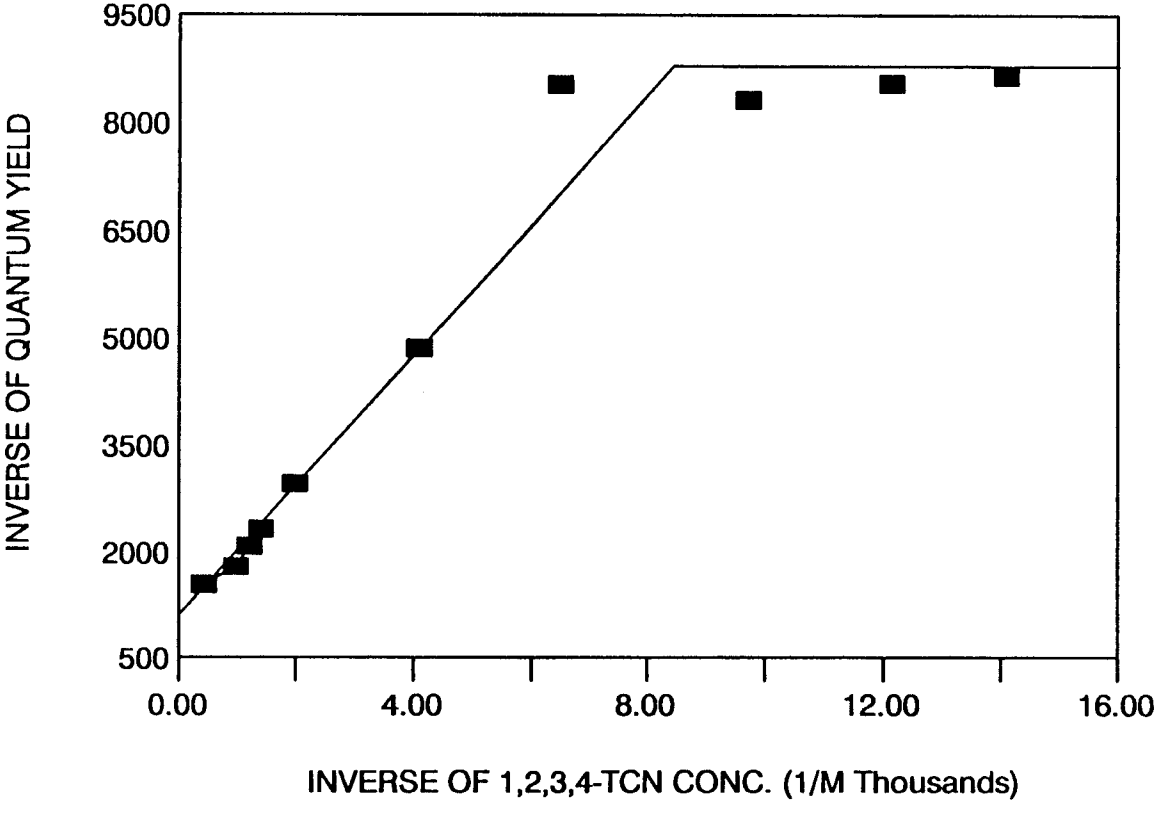

Figure II.2 Loss of 1,2,3,4-Tetrachloronaphthalene from Photolysis at 300 nm.

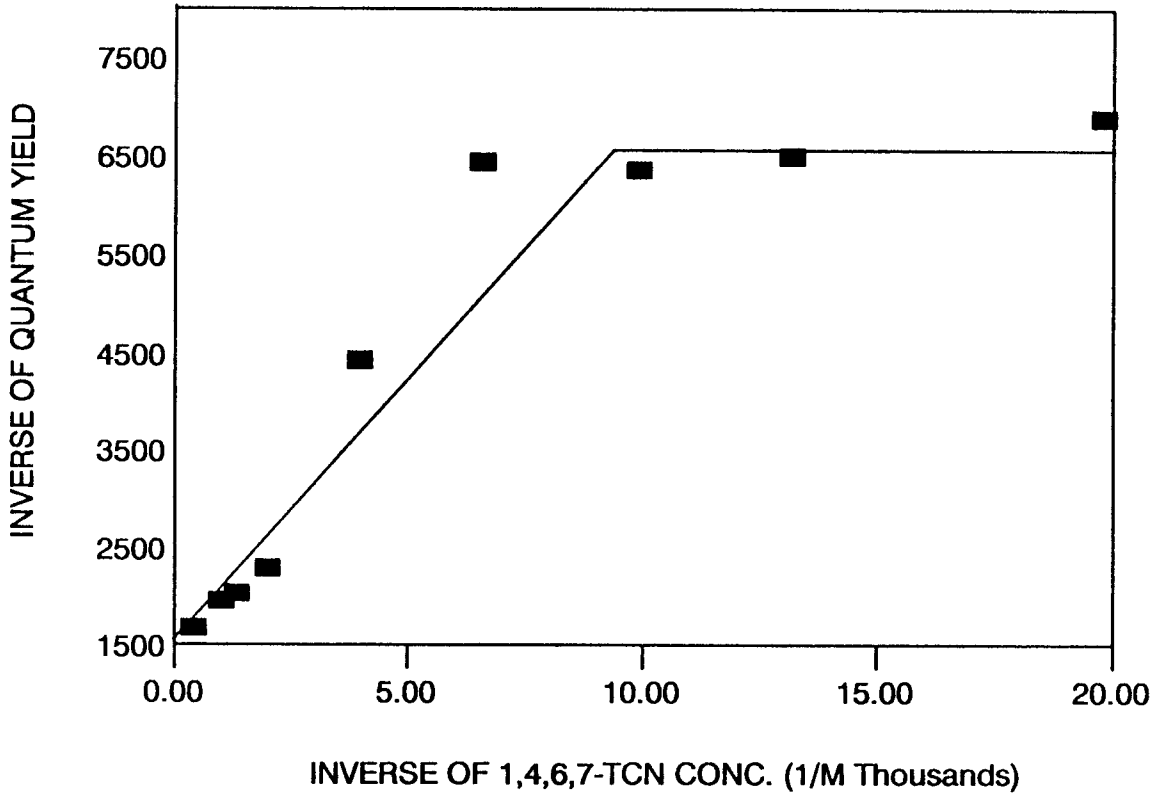

Figure II.3 Product Appearance from Photolysis of 1,4,6,7-Tetrachloronaphthalene at 300 nm.

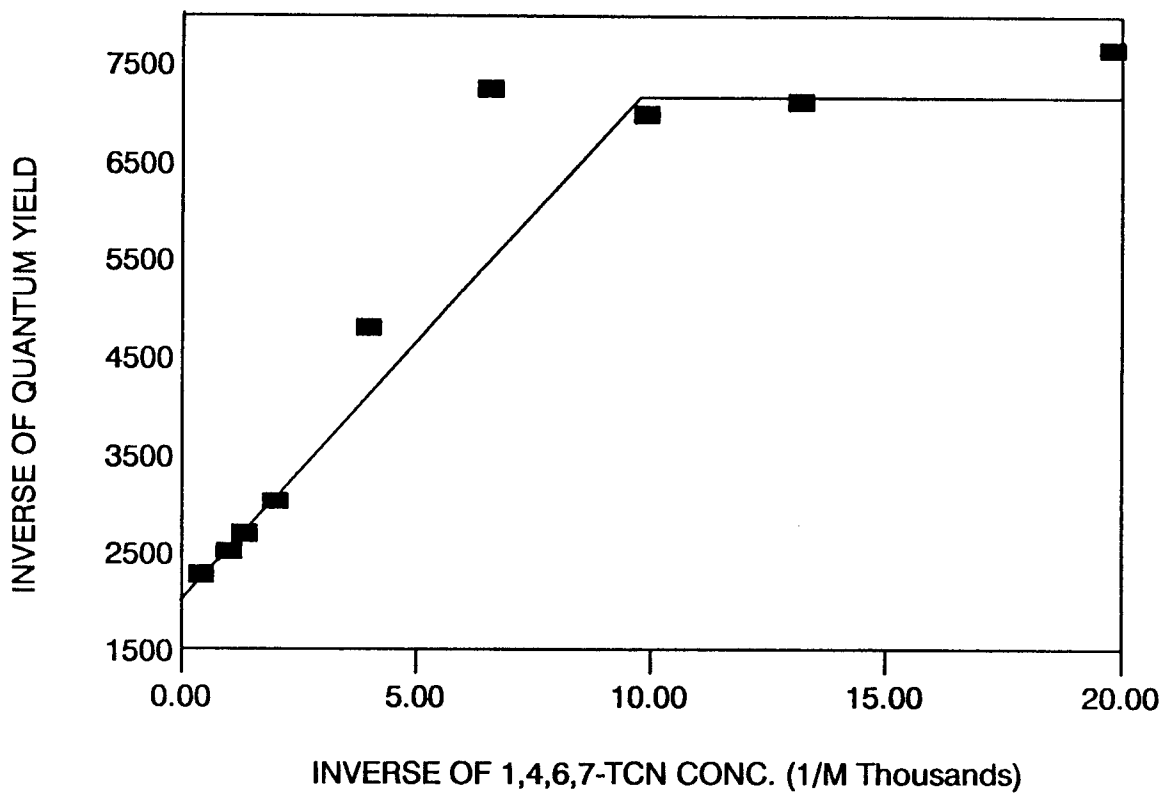

Figure II.4 Loss of 1,4,6,7-Tetrachloronaphthalene from Photolysis at 300 nm.

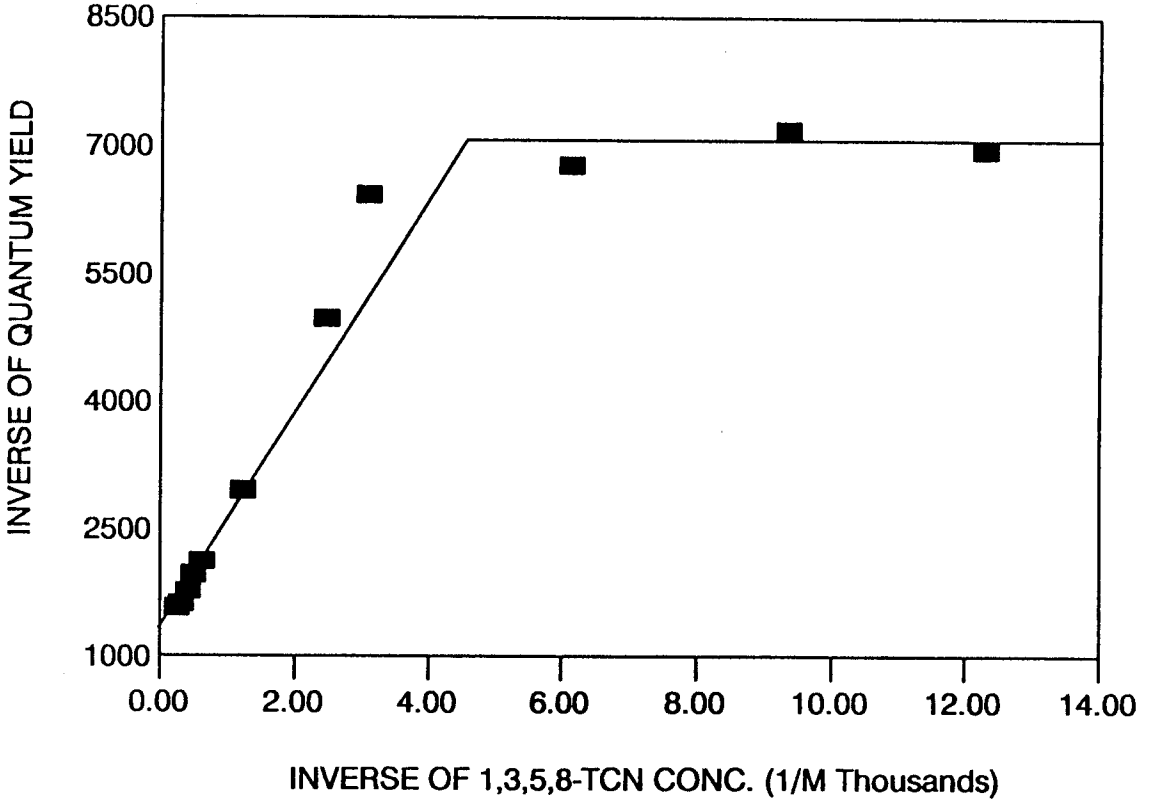

Figure II.5 Product Appearance for Photolysis of 1,3,5,8-Tetrachloronaphthalene at 300 nm.

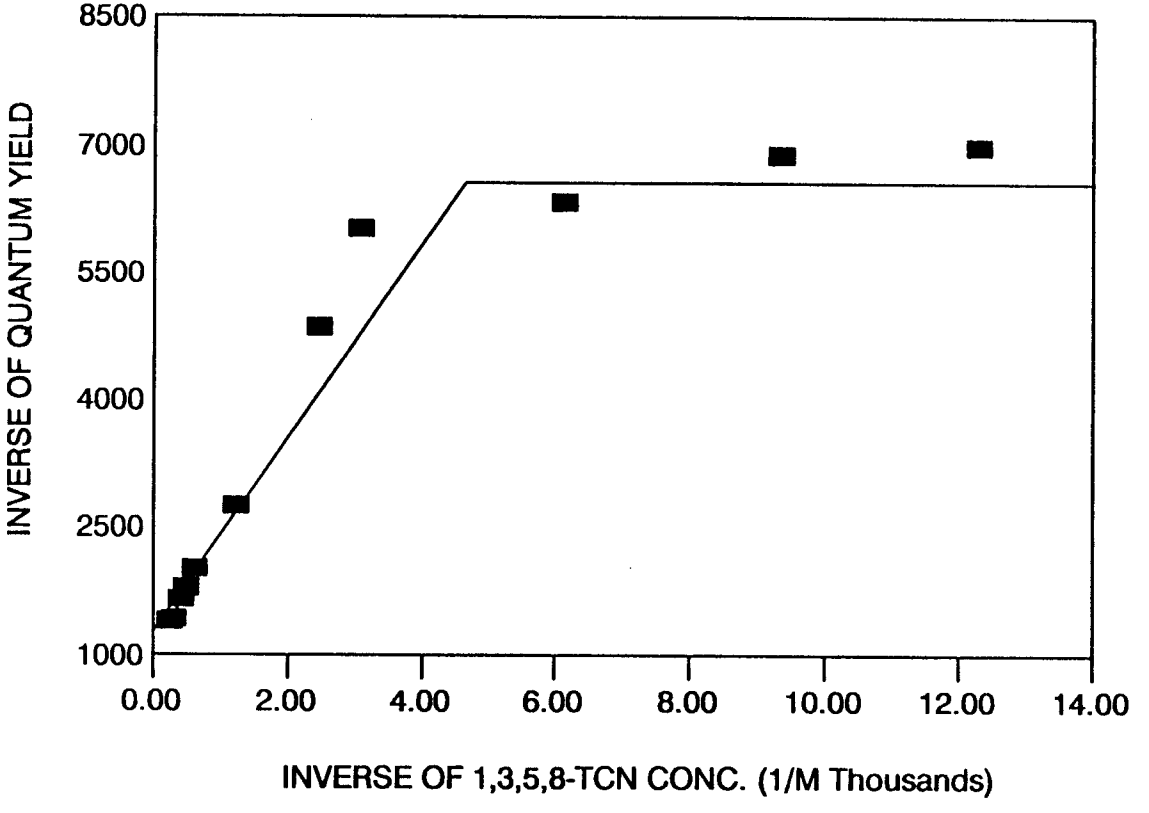

Figure II.6 Loss of 1,3,5,8-Tetrachloronaphthalene from Photolysis at 300 nm.

Discussion and Mechanistic Analysis

Our view of the mechanistic implications of Figures II.1-6 led us to suggest Scheme II.2. Absorption of a photon brings the ground state molecule to the first excited singlet state. The excited singlet is catalyzed to intersystem cross to a triplet spin state by the presence of the four heavy atoms. The lack of observable fluorescence, a strong phosphorescence spectra (Figures II.7, 8 and 9) diene triplet quenching, and oxygen triplet quenching (two-thirds reduced) provide strong evidence for a reactive triplet spin state which is responsible for product formation. The triplet is expected to undergo bond homolysis or react

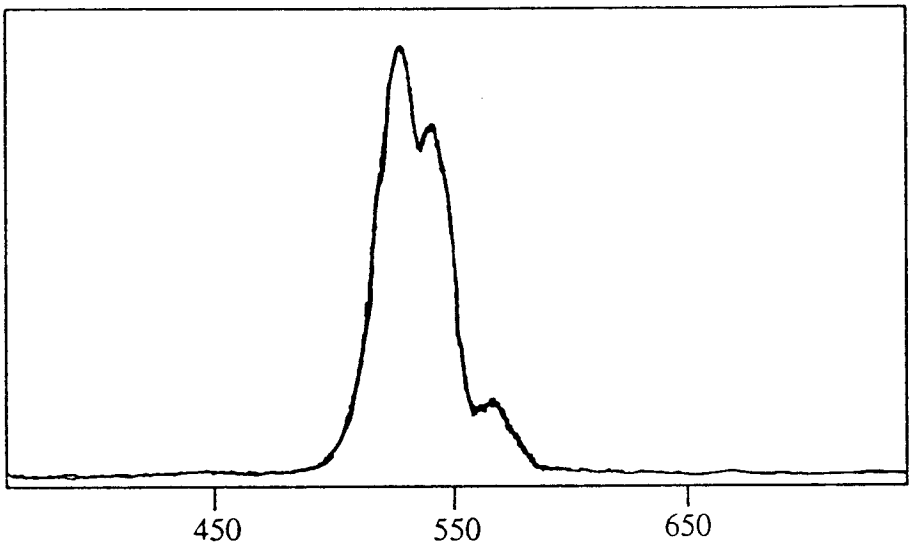

Figure II.7 Phosphorescence of 1,2,3,4-Tetrachloronaphthalene at 77 °K.

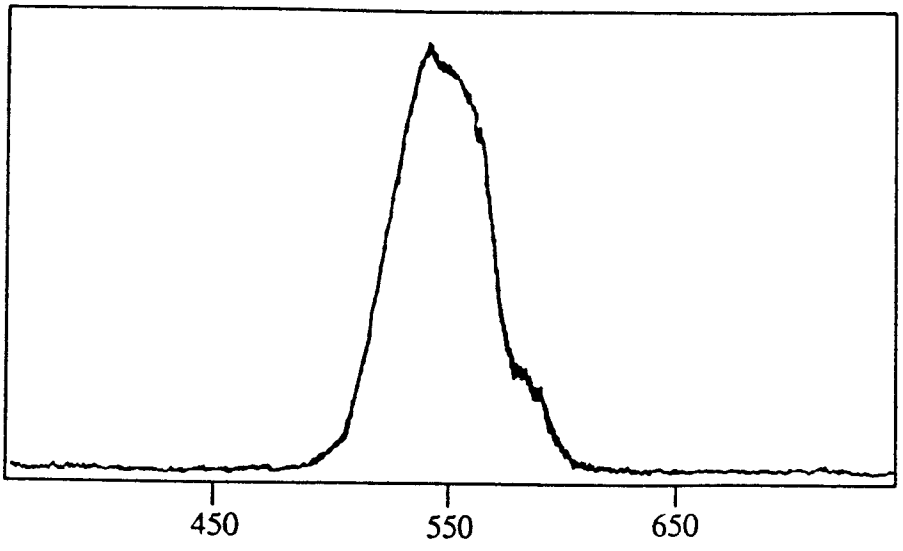

Figure II.8 Phosphorescence of 1,4,6,7-Tetrachloronaphthalene at 77 °K.

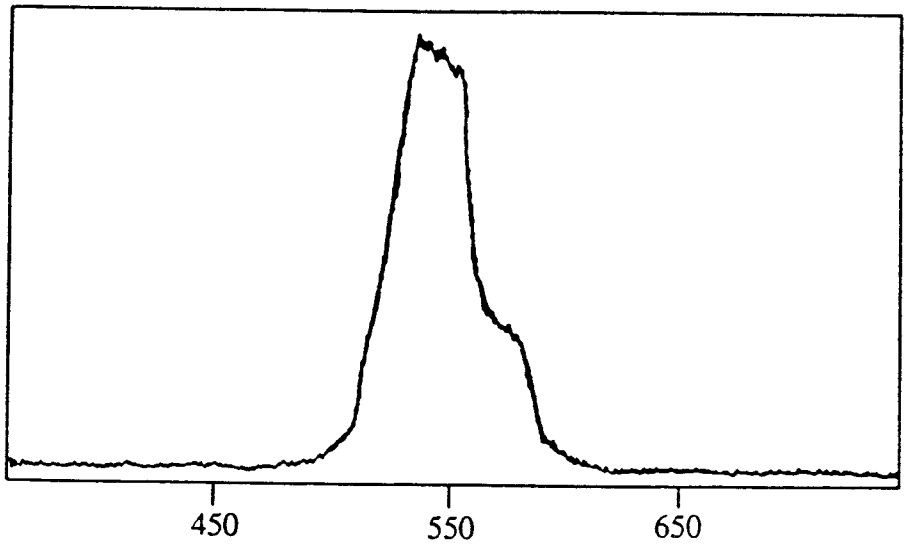

Figure II.9 Phosphorescence of 1,3,5,8-Tetrachloronaphthalene at 77 °K.

with an electron donor species to form a triplet excimer or exciplex.[30,31,73] Carbon-chlorine bond homolysis from the triplet state generates an aryl radical which can lead to product. At first, this was thought to be unlikely because the reactive triplet spin state possesses insufficient energy (470 nm emission equates to 61 Kcal/mol) to account for the phenyl C-Cl bond fission (85-95 Kcal/mol).[74-77] Bond homolysis of the triplet species could occur, however, if the following conditions narrow the energy gap sufficiently: upper vibrational levels of the triplet state contribute energy, strain relief of the ortho Cl-Cl interactions contribute (2.2 Kcal/mol),[78] and peri Cl-H or Cl-Cl (1-8, 4-6) interactions contribute. Calculated energy differences (MMX and AM1) for 1-chloronaphthalene versus 2-chloronaphthalene and 1,8-dichloronaphthalene versus 2,7-dichloronaphthalene are expected to be good models to estimate the 1-8 or 4-6 peri interactions. The MMX and AM1 energy differences estimate the strain in 1,8-dichloronaphthalene to be 6.1 and 6.71 Kcal/mol relative to the 2,7-dichloronaphthalene isomer, respectively. MMX calculations suggest that 1-chloronaphthalene is 3.0 Kcal/mol higher in energy than 2-chloronaphthalene while AM1 calculations provide an energy difference of 1.25 Kcal/mol (Table II.7). PCNs with vicinal peri chlorine substitutions are reported to be more reactive than other isomers.[79] Triplet excimer or exciplex formation is expected to produce some charge separation into radical cation like and radical anion like partners. The radical anion moiety is viewed as the precusor which will undergo bond fission to aryl radical and chloride anion, thus avoiding the more energy demanding bond homolysis.[31]

A kinetic evaluation of Scheme II.2 is accomplished by the use of a steady state approximation for the formation of the singlet, triplet, and excimer

Table II.7 AM1 and MMX Calculation Summary for Estimate of Peri Interaction and Strain Relief.

Model	MMX ΔH_f[a]	AM1 ΔH_f[a]
1-chloronaphthalene	26.20	34.65
2-chlorornaphthalene	23.20	33.47
1,8-dichlorornaphthalene	29.10	33.33
2,7-dichloronaphthalene	23.00	26.62

[a] Kcal/mole.

Scheme II.2

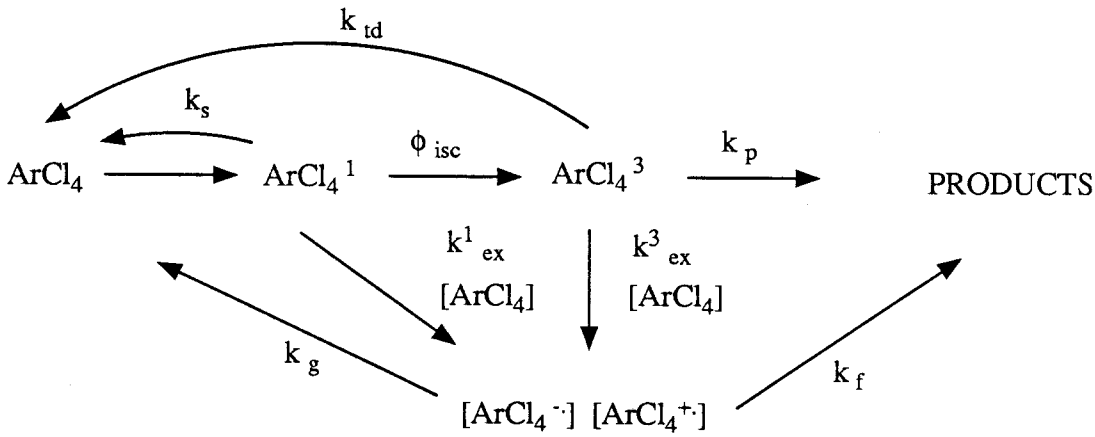

species. The quantum yield of product formation is then represented by Equation II.2, where $k_f/(k_f + k_g) = G$. At high concentrations, it is reasonable to expect $k_p << k_{ex}[ArCl_4](G)$, and then Equation II.2 can be simplified to Equation II.3. An analysis in the concentrated region of Figures II.1-6 will now yield rate ratio information about k_{td}/k_{ex} and information about the intercept $1 / G\,\phi_{isc}$. If ϕ_{isc} is unity, as we expect, then the intercept provides us with information about the efficiency of product formation from excimer. The

fraction G can be cancelled out and the ratio k_{td}/k_{ex} can be obtained by dividing the slope by the intercept. An estimate of k_{td} can be easily measured by phosphorescence experiments; Therefore, k_{ex} can be estimated.[40] The Region

$$\Phi = \phi_{isc} \left(\frac{k_p + k_{ex}[ArCl_4]\,G}{k_p + k_{td} + k_{ex}[ArCl_4]} \right) \qquad \text{Equation II.2}$$

$$\frac{1}{\Phi} = \frac{1}{G\,\phi_{isc}} + \frac{k_{td}}{G\,\phi_{isc}\,k_{ex}\,[ArCl_4]} \qquad \text{Equation II.3}$$

of the graphs that demonstrate a positive slope correspond to concentrations greater than 1×10^{-4} M (high concentration). At concentrations more dilute than 1×10^{-4} a seemingly linear plot is also obtained but demonstrates a slope that appears to be essentially zero. The points obtained in the concentrated region were subjected to a linear regression analysis and the results are plotted along with the more dilute region (zero slope) in Figures II.1-6. The slope/intercept ratio (k_{td}/k_{ex}) in the concentrated region for each compound is then estimated and are listed in the Table II.8. A perusal of Table II.8 reveals that the

Table II.8 Linear Regression Analysis Summary of Least Squares Fit.

compound	slope	intercept	slope/intercept (k_{td}/k_{ex})
1234 TCN (1)	0.836 [a]	1290	6.48×10^{-4}
	0.811 [b]	1130	7.17×10^{-4}
1467 TCN (2)	0.479 [a]	2070	2.31×10^{-4}
	0.395 [b]	1540	2.57×10^{-4}
1358 TCN (3)	1.73 [a]	1170	1.48×10^{-3}
	1.55 [b]	940	1.65×10^{-3}

[a] Values obtained from quantum yield of product formation.
[b] Values obtained from quantum yield for the loss of starting material.

efficiency (reciprocal of the intercept) of excimer formation, for all compounds studied, is between 1 in 1000 and 1 in 2000. This means that for approximately every 1500 excimeric pairs formed only one goes on to form the observed dehalogenated products.

Triplet Lifetimes

Solutions of 1, 2, and 3 were prepared in EPA and allowed to cool to 77 °K (liquid N_2). The resulting glass mixture is excited with 310 nm incident radiation. Emission is monitored from 400 nm to 680 nm after a time evolution of *ca.* five milliseconds (msec). The five msec time frame is selected to ensure that there is no possibility of singlet emission (fluorescence) overlapping the triplet emission (phosphorescence) even though no evidence of fluorescence could be detected at room temperature or in a glass at 77 °K. The decay of the intensity is averaged over 256 scans. Triplet decay is known to be a simple first order rate process, and, therefore, a linear decay in natural log of the

intensity is expected. The slope of the calculated line from Figures II.10, 11, 12 yields the rate constant k_{td}. The value k_{td} is used to estimate the rate k_{ex} and to discern the triplet lifetimes (τ).

Table II.9 Calculated Excimer Rate Formation, from Triplet Data and Regression Analysis.

compound	k_{td} s^{-1}	τ_{msec}	k_{td}/k_{ex}	k_{ex} s^{-1}
1234 TCN	8.97	112[c]	6.48×10^{-4} [a] 7.17×10^{-4} [b]	1.38×10^{4} 1.25×10^{4}
1467 TCN	28.1	35.6	2.31×10^{-4} [a] 2.57×10^{-4} [b]	1.22×10^{5} 1.09×10^{5}
1358 TCN	34.5	29.0	1.48×10^{-3} [a] 1.65×10^{-3} [b]	2.33×10^{4} 2.09×10^{4}

[a] Values obtained from quantum yield of product fromation.
[b] Values obtained from quantum yield for the loss of starting material.
[c] Identicle with previously reported literature result.

An evaluation of the two Tables (Tables II.8, 9) and the Figures II.1-6 reveals some important similarities and some subtle differences. All three compounds (1, 2, and 3) form excimeric species at relatively slow rates (k_{ex}) and are fairly inefficient at forming reaction products. All three TCNs demonstrate a product forming dependence upon concentration of starting material. All three compounds fail to show any singlet spectra (fluorescence) and are 60% quenched by the presence of atmospheric amounts of oxygen. Samples that were not subjected to three freeze-pump thaw cycles (oxygen removal) demonstrated 60% reduced quantum yields. Also, all three TCNs yield a strong triplet derived phosphorescence spectra that is relatively long lived. The intersystem crossing yield experiments were only successful with compound 1 due to the observed reactivity. Compound 1 demonstrated an intersystem

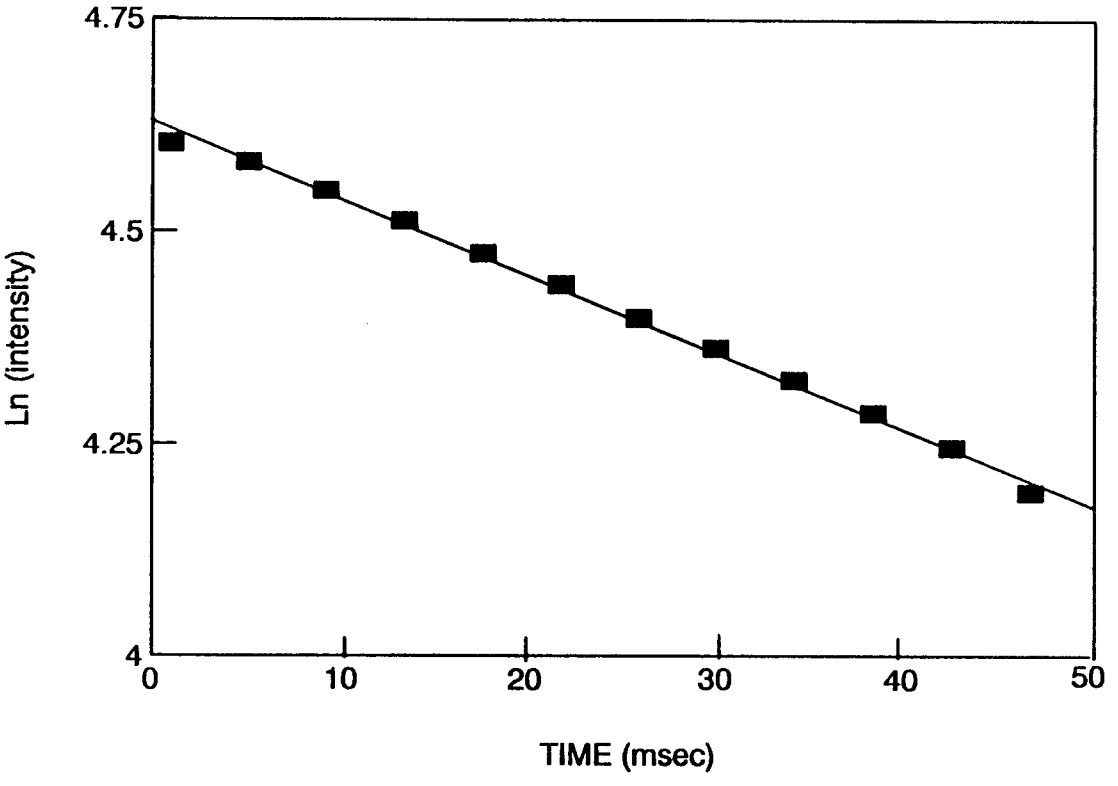

Figure II.10 Least Squares Fit for the Triplet Decay of 1,2,3,4-Tetrachloronaphthalene

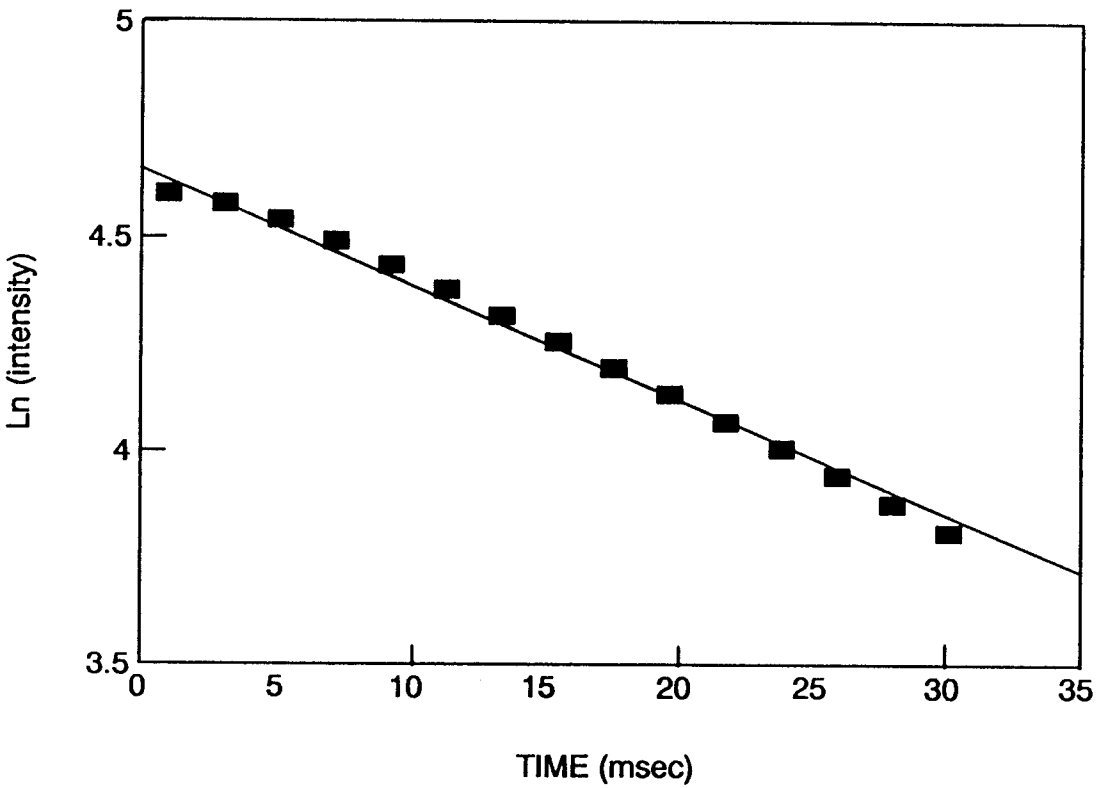

Figure II.11 Least Squares Fit for the Triplet Decay of 1,4,6,7-Tetrachloronaphthalene

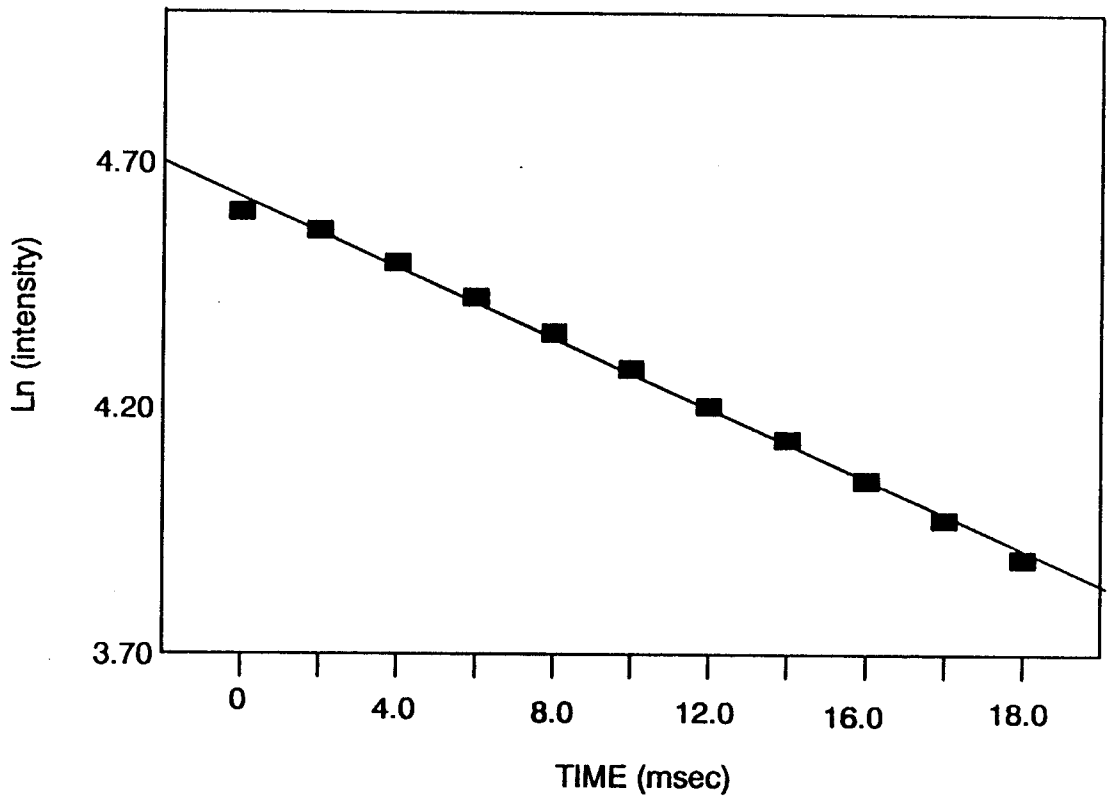

Figure II.12 Least Squares Fit for the Triplet Decay of 1,3,5,8-Tetra-chloronaphthalene

crossing yield of 1.0 ± 0.04. Intersystem crossing yield and quenching expeiments are dealt with in a later section.

The subtle differences are observed in the concentration dependence column (slope), the efficiency of excimer to product formation (intercept), the estimated rate of excimer formation (k_{ex}), and the quantum yields themselves. All compounds give nearly the same quantum yields, however, 3 appears to be slightly more reactive, more sensitive to concentration change, and more efficient at forming product from the excimer all while being the shortest lived species in the glass at 77 °K. Compound 2 appears able to form the excimer at the highest rate but is the least efficient at going on to product and demonstrates the smallest sensitivity to changes in concentration. Compound 1 demonstrates the longest lifetime at 77 °K, a dependence upon concentration that is intermediate relative to 2 and 3, a rate of excimer formation similar to that of 3, and demonstrates a similar efficiency of excimer derived product to that of compound 3.

Triethylamine Photolyses

In a further effort to characterize the postulated radical anion like moiety in the triplet excimer, photolytic runs were conducted in the presence of variable concentrations of triethylamine (TEA) in acetonitrile. The concentration of the individual TCNs are held constant at a level to insure that all incident irradiation is absorbed by the TCN and not the TEA. Also ultraviolet spectrophotometric studies demonstrate no evidence for a ground state complex. TEA is known to be an excellent electron donor species and is expected to

form an exciplex.[51,80] In the case of exciplex formation between 1, 2, or 3 and TEA, earlier work suggests that these exciplexes are quickly separated to solvent separated ions.[81] Studies by Peters and co-workers, employing picosecond decay and conventional laser flash photolysis, found that the initially formed exciplexes in CH_3CN undergo ion-pair separation.[81,82] The existence of solvent separated ions in CH_3CN is also demonstrated through deuterium incorporation.[47,83]

Figures II.13-18 are plots of inverse quantum yield against inverse TEA concentration. A large increase in quantum yield is observed with increasing TEA concentration. The mechanistic picture is depicted in Scheme II.3 The expression representing quantum yield is similar to Equation II.2 except for the addition of the exciplex rate of formation term k_2 [TEA]. At high concentrations of TEA, this term is expected to be the dominant route to product. By employment of the steady state assumption and setting the value $k_n/(k_n+k_m) = G$, the quantum yield, according to Scheme II.3, is represented by Equation II.4. At high concentrations of TEA, $k_p + k_{ex}(ArCl_4)$ F is expected to be much smaller than k_2 [TEA] (G) and this allows the simplification of Equation II.4 to II.5. This is consistent with the plots obtained by plotting the inverse of quantum yield versus the inverse of TEA starting concentration (Tables II.10-12, Figures II.13-18). At elevated concentrations of TEA, the plots obtained are linear with a positive slope. At lower concentrations of TEA, the slope decreases to a point where the conversion to product should become constant (no slope). This is consistent with what is expected from the competition of a bimolecular reaction (TEA-TCN) and the production of product *via* excimer or triplet fragmentation. Use of the portion of the graph where

Scheme II.3

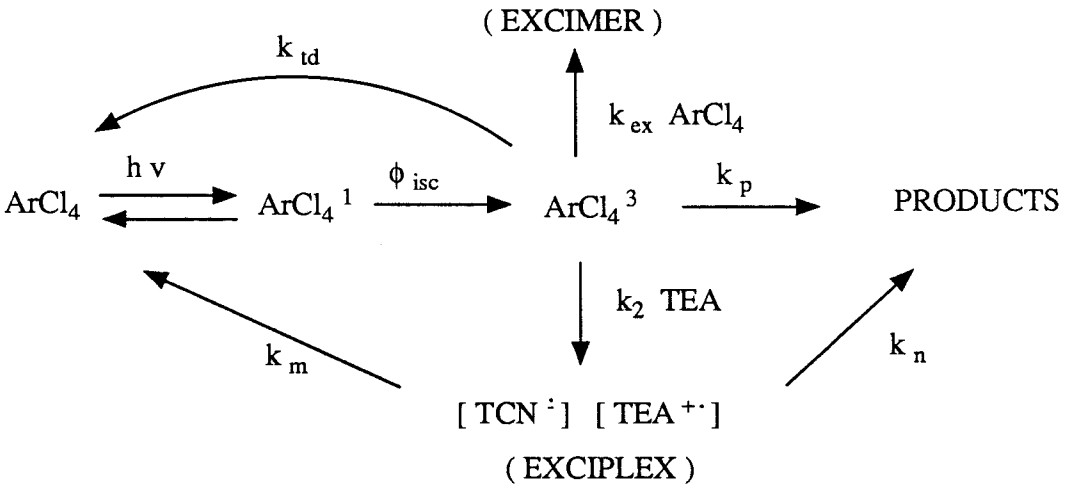

$$\Phi = \phi_{isc} \left(\frac{k_p + k_2 [TEA] G + k_{ex}(ArCl_4)F}{k_p + k_{td} + k_2 [TEA] + k_{ex}(ArCl_4)} \right) \quad \text{Equation II.4}$$

$$\frac{1}{\Phi} = \frac{1}{G \phi_{isc}} + \frac{k_{td}}{G \phi_{isc} k_2 [TEA]} \quad \text{Equation II.5}$$

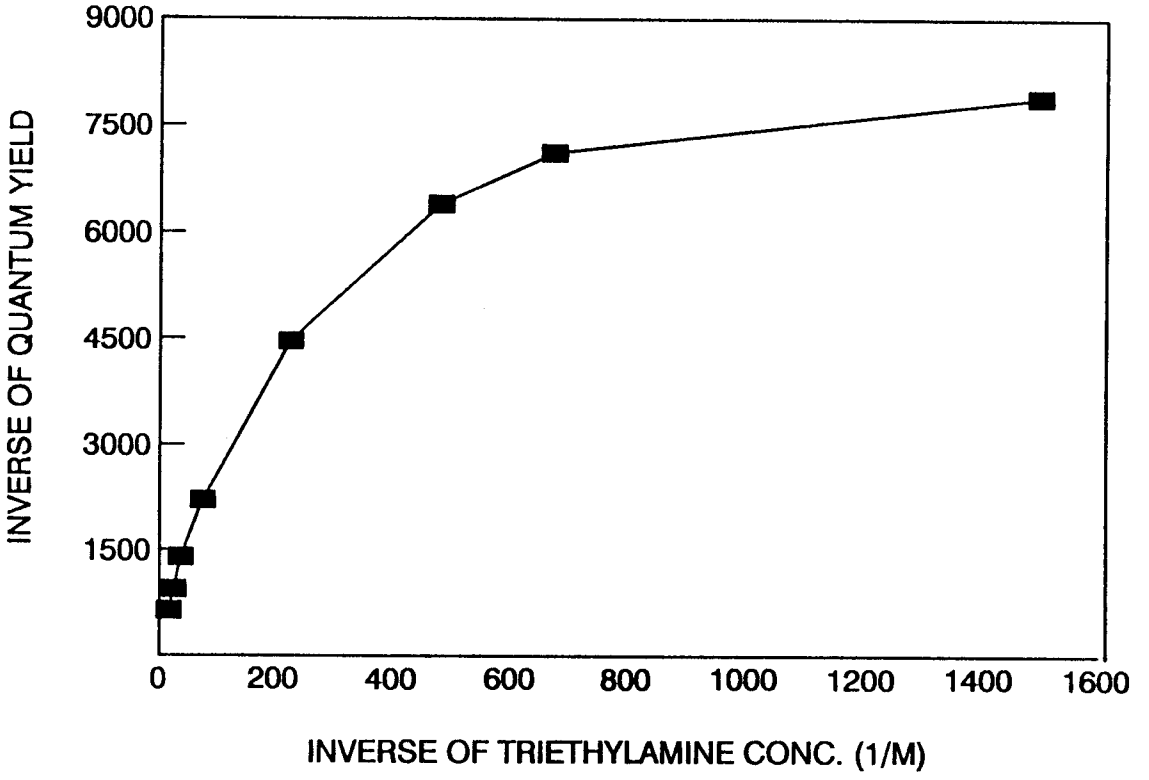

Figure II.13 Product Appearance from Photolysis of 1,2,3,4-Tetrachloronaphthalene in the Presence of Triethylamine at 300 nm.

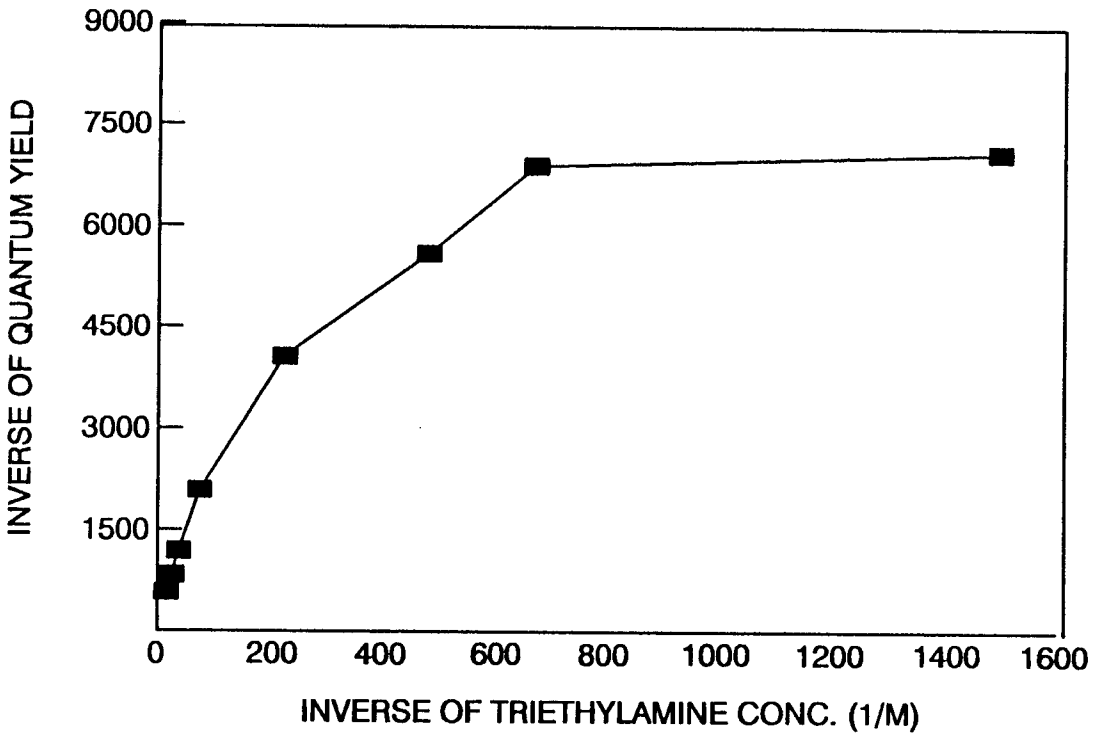

Figure II.14 Loss of 1,2,3,4-Tetrachloronaphthalene from Photolysis in the Presence of Triethylamine at 300 nm.

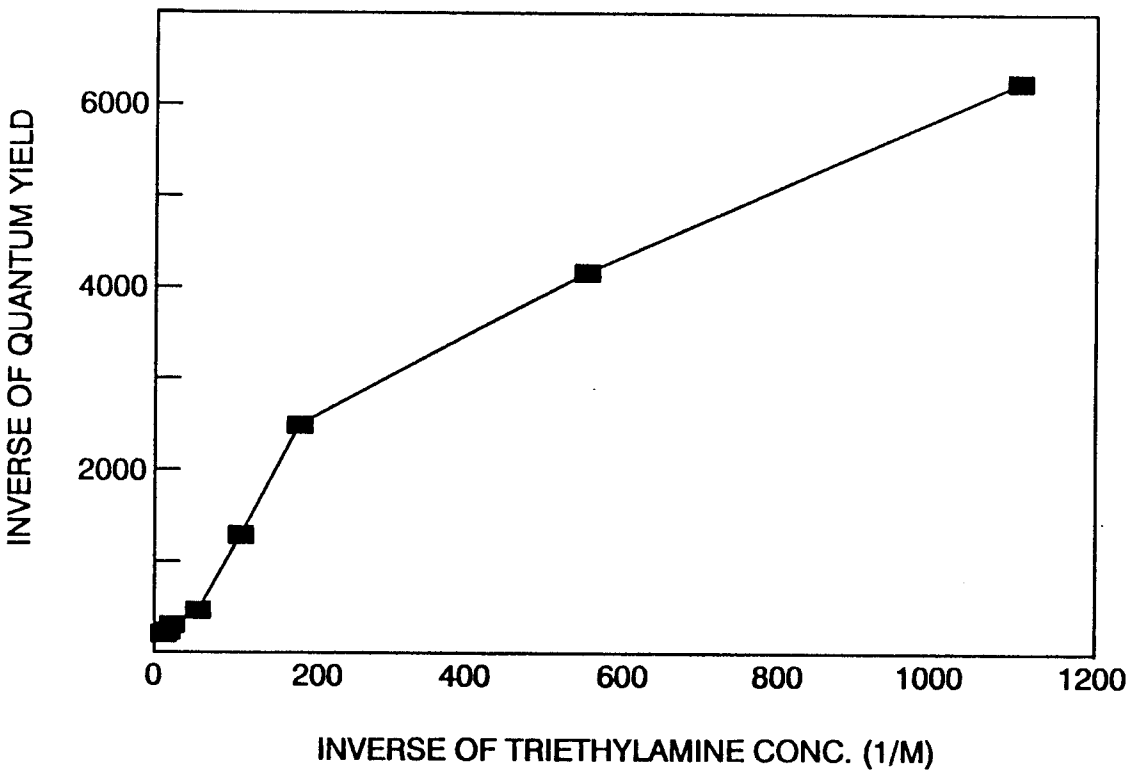

Figure II.15 Product Appearance from Photolysis of 1,4,6,7-Tetrachloronaphthalene in the Presence of Triethylaimne at 300 nm.

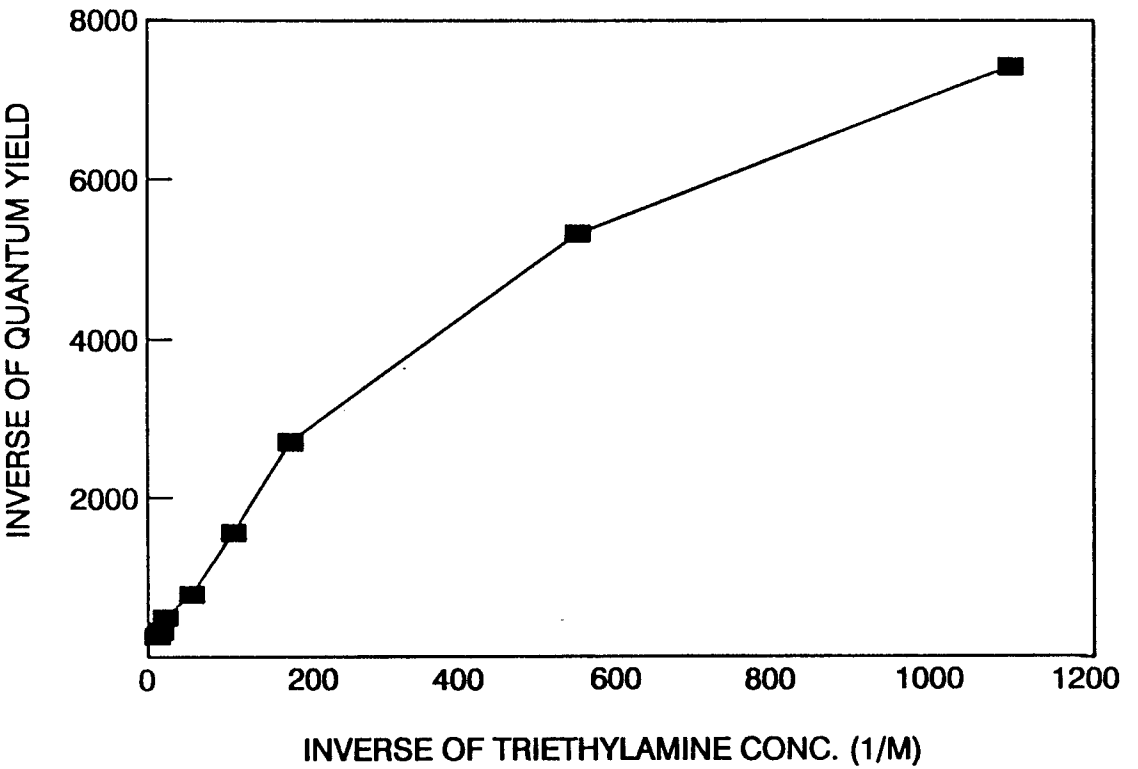

Figure II.16 Loss of 1,4,6,7-Tetrachloronaphthalene from Photolysis in the Presence of Triethylamine at 300 nm.

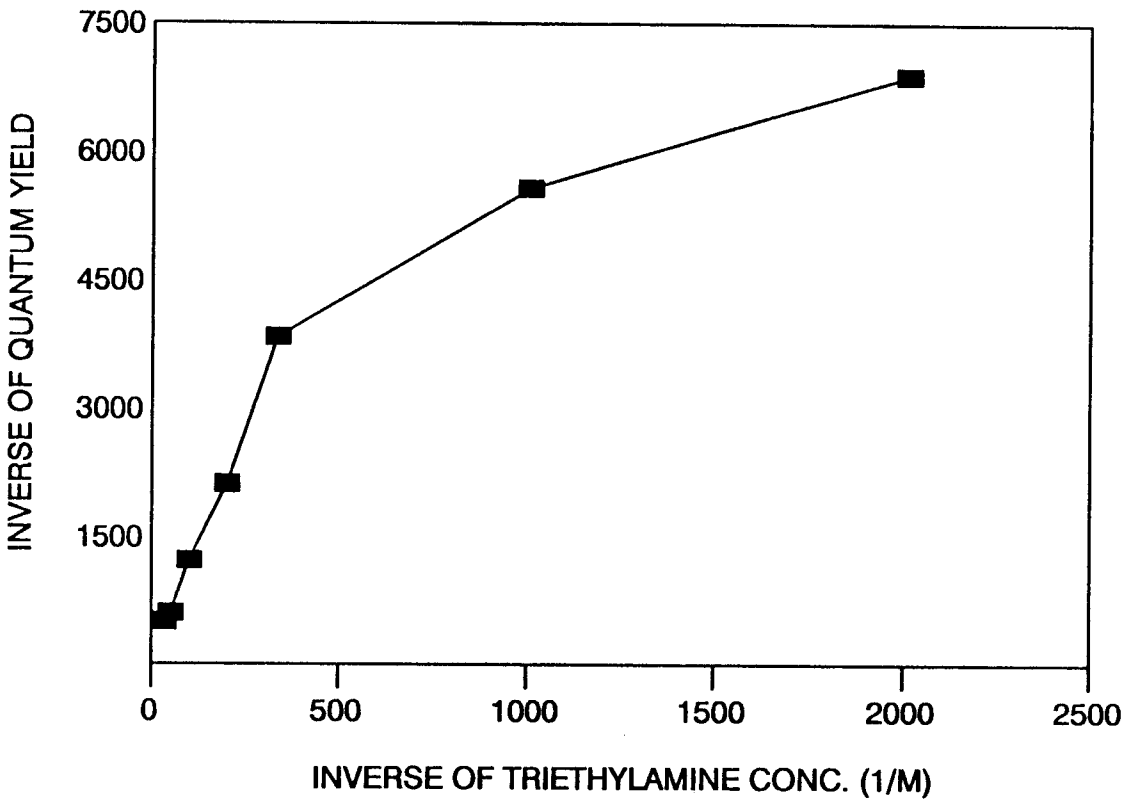

Figure II.17 Product Appearance from Photolysis of 1,3,5,8-Tetrachloronaphthalene in the Presence of Triethylamine at 300 nm.

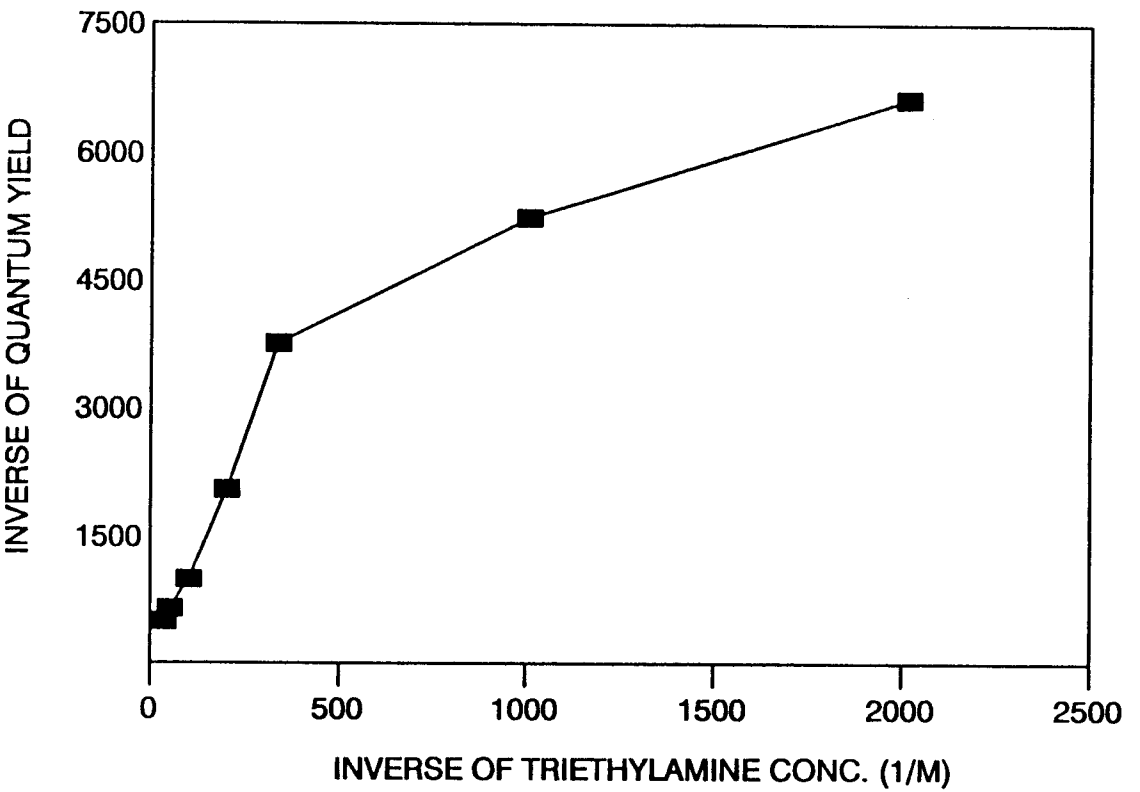

Figure II.18 Loss of 1,3,5,8-Tetrachloronaphthalene from Photolysis in the Presence of Triethylamine at 300 nm.

exciplex formation (TEA-TCN) is dominate and the conditions of Equation II.5 hold true, allows one to evaluate similar constants to those that were extracted from the photolyses without the presence of amine. That is, the intercept is a representation of the efficiency of the exciplex to form product, the slope is an indication of the sensitivity of exciplex formation to concentration, and the ratio of the two (slope/intercept) is the ratio k_{td}/k_2 (Table II.13). A combination of the rate ratio data and the previously measured triplet lifetimes at 77 °K, allows for an estimate to be made of the rate of exciplex formation (k_2, Table II.14).

Table II.10 Photolysis of 1,2,3,4-TCN[a] in CH_3CN/TEA at 300 nm.

$[TEA] \times 10^3$ (M)	$[TEA]^{-1}$ (M)	Quantum Yield $\times 10^5$ Pd[b]	SM[c]	Quantum Yield^{-1} Pd[b]	SM[c]
67.1	14.9	153	171	655	585
40.3	24.8	106	118	948	846
26.9	37.2	71.2	83.3	1400	1200
13.5	74.1	45.3	48.0	2210	2080
4.46	224	22.4	24.6	4460	4060
2.08	480	15.6	17.9	6400	5600
1.49	672	14.1	14.5	7210	6890
0.667	1500	12.9	14.1	7800	7100

[a] Experiment was done at one concentration of TCN, 3×10^{-4} M.
[b] Quantum yield for appearance of products.
[c] Quantum yield for loss of starting TCN.

Table II.11 Photolysis of 1,4,6,7-TCN[a] in CH_3CN/TEA at 300 nm.

[TEA] x 10^3 (M)	[TEA]$^{-1}$ (M)	Quantum Yield x 10^5 Pd[b]	SM[c]	Quantum Yield^{-1} Pd[b]	SM[c]
90.1	11.1	388	493	258	203
63.3	15.8	305	431	328	232
45.3	22.1	202	331	495	302
18.1	55.2	127	215	787	465
9.09	110	63.9	78.1	1570	1280
5.44	184	36.9	40.2	2710	2490
1.81	552	18.8	24.0	5320	4160
0.909	1110	13.5	16.0	7410	6250

[a] Experiment was done at one concentration of TCN, 3 x 10^{-4} M.
[b] Quantum yield for appearance of products.
[c] Quantum yield for loss of starting TCN.

Table II.12 Photolysis of 1,3,5,8-TCN[a] in CH_3CN/TEA at 300 nm.

[TEA] x 10^3 (M)	[TEA]$^{-1}$ (M)	Quantum Yield x 10^5 Pd[b]	SM[c]	Quantum Yield^{-1} Pd[b]	SM[c]
29.7	33.6	198	205	505	489
19.8	50.3	164	156	610	640
9.90	101	81.8	101	1220	988
4.95	202	47.2	48.9	2120	2050
2.98	336	26.1	26.6	3830	3760
0.992	1010	18.0	19.1	5570	5240
0.496	2020	14.5		6620	6620

[a] Experiment was done at one concentration of TCN, 3x10^{-4} M.
[b] Quantum yield for appearance of products.
[c] Quantum yield for loss of starting TCN.

Table II.13 Linear Regression Analysis Summary, Least Squares Fit. TEA/TCN Photolysis at 300 nm.

compound	slope	intercept [c]	slope/intercept (k_{td}/k_2)
1234 TCN (1)	33.9 [a]	68.6	0.494
	31.3 [b]	30.9	1.01
1467 TCN (2)	12.8 [a]	138	0.0930
	10.7 [b]	40.1	0.268
1358 TCN (3)	10.9 [a]	79.4	0.137
	10.8 [b]	26.1	0.414

[a] Values obtained from quantum yield of product formation.
[b] Values obtained from quantum yield for the loss of starting material.
[c] Calculated error in the intercept is large.

Table II.14 Calculated Rates from the Regression Analysis, TEA/TCN Photolysis at 300 nm.

compound	k_{td} s^{-1}	τ_{msec}	k_{td}/k_2	k_2 s^{-1}	k_2 s^{-1} [c]
1234 TCN	8.97	112	0.494	18.1	2×10^{10}
			1.01	8.88	1×10^{10}
1467 TCN	28.1	35.6	0.0930	302	1×10^{11}
			0.268	105	4×10^{10}
1358 TCN	34.5	29.0	0.137	252	7×10^{10}
			0.414	83.3	2×10^{10}

[a] Values obtained from quantum yield of product fromation.
[b] Values obtained from quantum yield for the loss of starting material.
[c] Values calculated from singlet analysis.

A least squares fit (regression analysis) is performed on the five TEA points of highest concentration. The analysis unveils the rate information that is observed in Tables II.13, 14. There is a considerable amount of uncertainty associated with the intercept values. This might be expected with the large increase in slope and the large increase in quantum yields observed in the TEA mediated photolytic runs. The goodness of fit (R), however, allows one to

evaluate the slope values with a little more certainty. The R values were all 0.981 or larger: compound 1, demonstrates R values equal to 0.995 and 0.994, compound 2, R = 0.995 and 0.981, compound 3 yields R values of 0.994 and 0.996 for the appearance of product and loss of starting TCN, respectively. An examination of the slopes and the Figures II.13-18 shows again the similarities of the three TCNs under investigation. All three compounds demonstrate a dependence on the concentration of starting amine (TEA) and a very large increase in the slope is observed relative to the uncatalyzed photolysis runs. One problem that stands out is that the estimation of the rate constant for exciplex formation seems unreasonably low; however, the magnitude of the increase of efficiencies for exciplex product formation relative to that for the excimer is important and should be noted. While the straight photolysis excimer appears to be very inefficient (approximately 1/1500) at moving on to product, the exciplex TEA-TCN is apparently very efficient at producing the dehalogenated product (approximately 1/75). Other differences are also noted.

Another possibility exists, reaction could occur from the singlet excited state if the electron transfer reaction competes with intersystem crossing to the triplet. As TEA is increased, we expect exciplex formation to be the dominate route to product. The Equation II.6 is then simplified to Equation II.7 and the slope divided by the intercept will yield the ratio $(k_{isc} + k_{sd}) / k_2$. An estimate for $k_2 \approx$ intercept/slope x 10^{10}. The value 10^{10} is arrived at by using Turro's estimation of singlet lifetimes, the observed epsilons of the individual TCNs, and assuming that for k_2 to be competitive it would need to be 100 times as faster than k_{isc}. The Turro estimate allows for an evaluation of k_2 from a singlet mechanism seen in Table II.14.[88b] The estimates seen in the table

Scheme II.3a

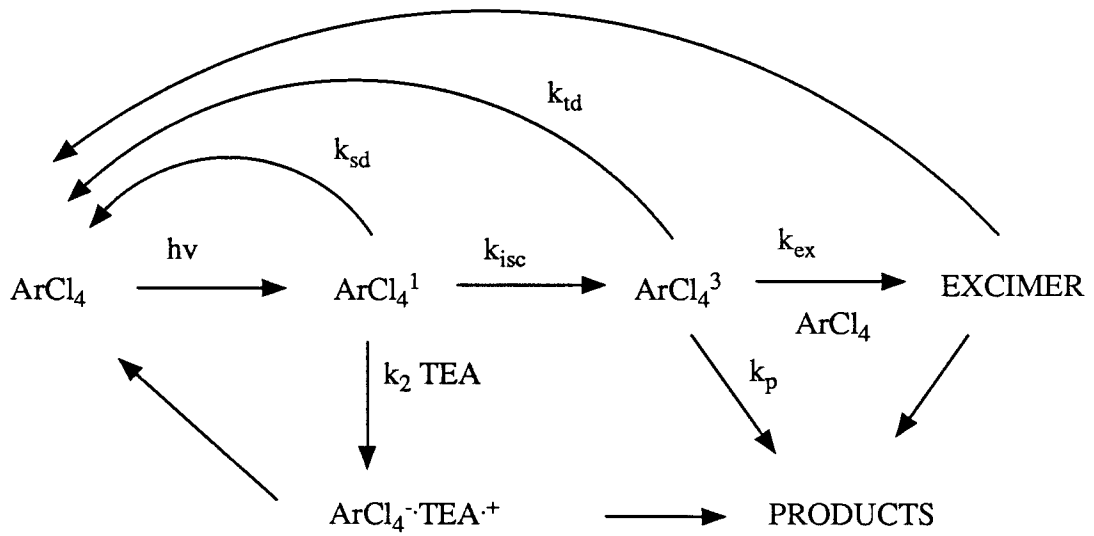

$$\phi = \frac{k_2[TEA]\,G + k_{isc}\left\{\dfrac{k_{ex}(ArCl_4)\,F + k_p}{k_{ex}(ArCl_4) + k_p + k_{td}}\right\}}{k_2[TEA] + k_{isc} + k_{sd}} \qquad \text{Equation II.6}$$

$$\phi = \frac{k_2[TEA]\,G}{k_2[TEA] + k_{isc} + k_{sd}} \qquad \text{Equation II.7}$$

$$\phi^{-1} = \frac{1}{G} + \frac{k_{isc} + k_{sd}}{k_2[TEA]\,G} \qquad \text{Equation II.8}$$

support the possibilty of a singlet exciplex as the principal precursor that leads to product. It seems more reasonable to expect a rate of exciplex formation to approach the diffussion controlled rates observed in the table for the singlet process than the rates estimated for the triplet process.

Interestingly, the regiochemistry of dehalogenation of 2 and 3 is inverted under these conditions relative to the uncatalyzed straight photolyses. Compound 2 favors 6 by a 4.0:1.0 ratio when photolyzed in CH_3CN solvent only and favors 7 by 50:1.0 in excess TEA. Photolysis of 3 yields 8:7 ratio of 2.3:1.0 in the straight photolytic runs and in the presence of excess TEA the regiochemistry inverts to a 7:8 ratio of by 25:1.0. Compound 1 is also more selective under these conditions favoring formation of 3 in both cases with ratios increasing from 4.0:1.0 in the straight photolyses to 10:1 in 0.2 M TEA. This is a result of the efficient electron transfer to the excited state TCN and the ensuing solvent separation leading to an unencumbered radical anion that was suggested by Peters and co-workers.[81] The solvent separated radical anion apparently has a large propensity for dehalogenation.

Sodium Borohydride Photolyses

Irradiation of 2 and 3 in 94% aqueous acetonitrile and excess $NaBH_4$ leads to a significant increase in the quantum yield of dehalogenation. The quantum yield is also increased with increasing amounts of $NaBH_4$ (Figure II.19, 20). The dependence of quantum yield on the concentration of borohydride suggests that the borohydride is involved in the product forming step. The following kinetic scheme is proposed for the $NaBH_4$ mediated

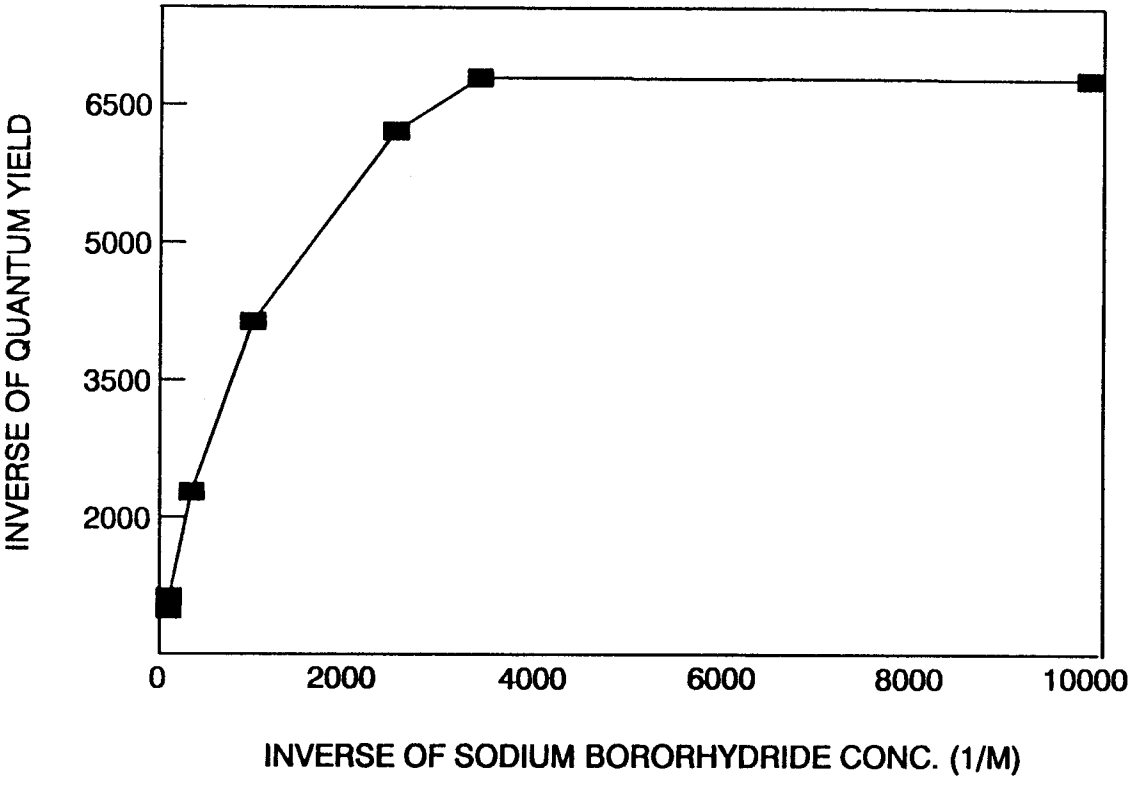

Figure II.19 Loss of 1,3,5,8-Tetrachloronaphthalene from Photolysis in the Presence of Sodium Borohydride at 300 nm.

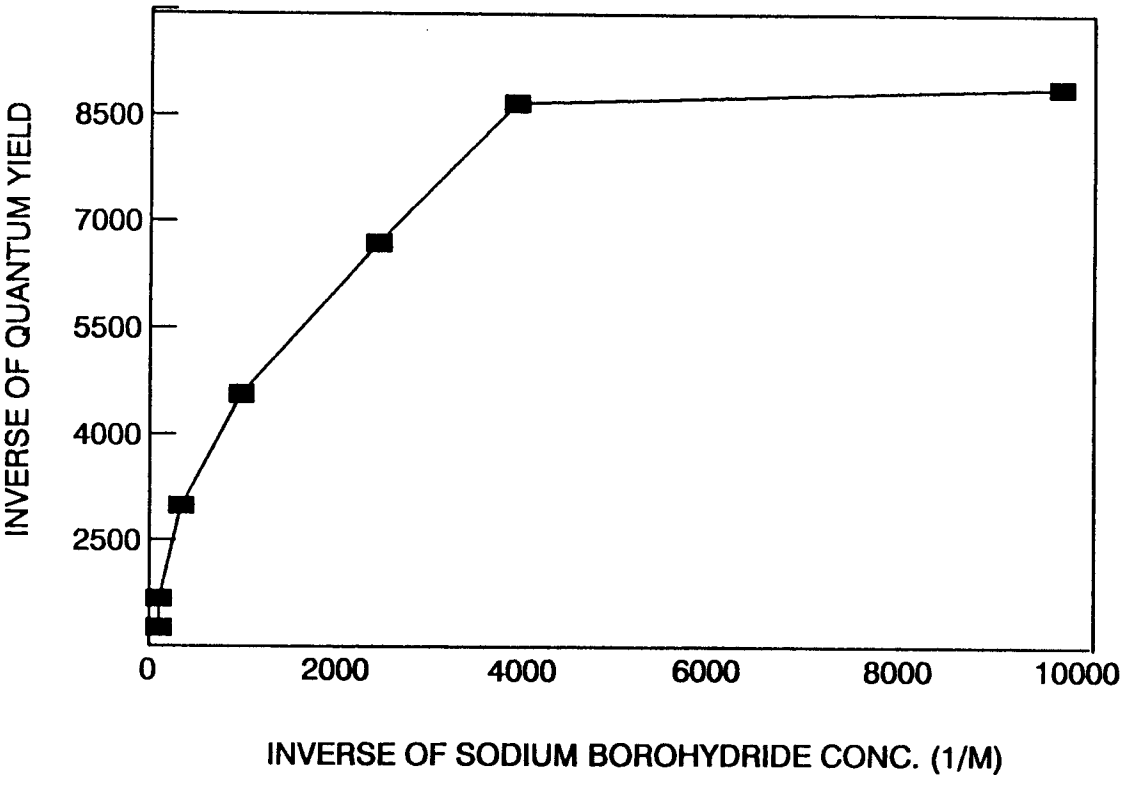

Figure II.20 Loss of 1,4,6,7-Tetrachloronaphthalene from Photolysis in the Presence of Sodium Borohydride at 300 nm.

photodehalogenation. The expression for quantum yield is similar to Equation II.2 except for the inclusion of $k_2\,[BH_4^-]\,[G]$ and the possibility of the singlet reaction $k'_2\,[BH_4^-]\,[G']$ terms. The term G is the fraction of product formed through a triplet manifold and the term G' is the fraction of product formed through the singlet manifold. At high concentrations of borohydride Equation

Scheme II.4

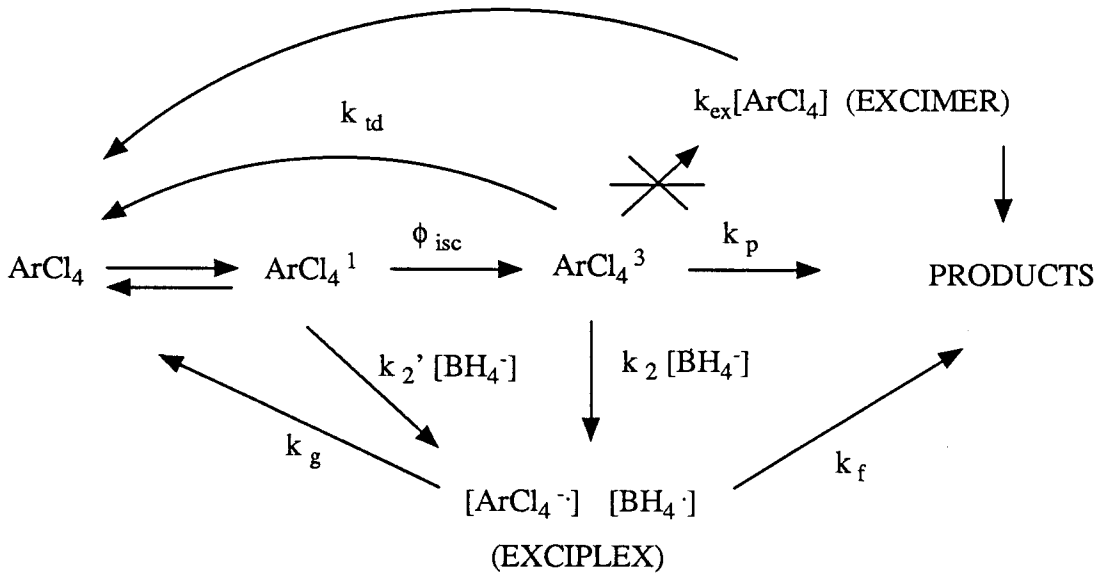

II.3 can be rewritten as in the cases of the TEA photolytic runs to reflect rate ratios. The decreasing slope in the plot of inverse ϕ (quantum yield) versus inverse $[NaBH_4]$ at dilute borohydride concentrations is seen as an indication of the triplet state reactivity competing with the triplet state exciplex for product formation.[33] This is an analogous situation to the TEA mediated product determining intermediate. A clue as to the fate of the exciplexes ($\underline{2}$*-BH_4^-) or ($\underline{3}$*-BH_4^-) is unveiled when the regiodehalogenation is examined. The excited state of $\underline{2}$ forms a charge transfer complex with TEA in acetonitrile as shown in Scheme II.3 which affords products $\underline{7}$:$\underline{6}$ in a 50:1.0 ratio. In the direct

Table II.15 Photolysis of 1,3,5,8-TCN[a] in $CH_3CN/H_2O/NaBH_4$ at 300 nm.

$[BH_4] \times 10^4$ (M)	$[BH_4]^{-1}$ (M)	Quantum Yield x 10^5 SM[b]	Quantum Yield $^{-1}$ SM[b]
409	24.4	85.4	1170
102	97.1	59.5	1680
30.8	325	34.6	2890
10.3	971	22.4	4460
4.10	2440	15.2	6590
2.56	3905	11.3	8890
1.03	9700	11.2	8900

[a] Experiment was done at one concentration of TCN, 3.5×10^{-4} M.
[b] Quantum yield for loss of 1,3,5,8-tetrachloronaphthalene.

Table II.16 Photolysis of 1,4,6,7-TCN[a] in $CH_3CN/H_2O/NaBH_4$ at 300 nm.

$[BH_4] \times 10^4$ (M)	$[BH_4]^{-1}$ (M)	Quantum Yield x 10^5 SM[b]	Quantum Yield $^{-1}$ SM[b]
400	25.0	101	990
101	99.0	88.5	1130
29.4	340	43.9	2280
10.1	990	24.2	4140
4.00	2500	16.1	6220
2.94	3400	14.7	6800
1.01	9900	14.5	6880

[a] Experiment was done at one concentration of TCN, 2.8×10^{-4} M.
[b] Quantum yield for loss of 1,4,6,7-tetrachloronaphthalene.

photolysis of 2, without the presence of an electron transfer reagent, a reversal of selectivity is observed in favor of 6:7 by 4.0:1.0. The excited state of 3

also will yield to the charge transfer complex with TEA in acetonitrile. The observed regiochemical dehalogenation favored 7:8 by 25:1.0 in the TEA/CH_3CN system, while the photolysis of 3 in CH_3CN without TEA favored 8:7 by 2.3:1.0. The change in regioselectivity can be rationalized by a radical anion fragmentation pathway consistent with a Wheland type intermediate. In the sodium borohydride case, Tables II.25-26 show the regiochemistry to be intermediate between direct photolysis and radical anion mediated dehalogenation. A possible explanation for the intermediacy of the product ratios is seen in Scheme II.5. The radical anion/radical borohydride pair, after initial complexation, may either diffuse apart to give an uncomplexed radical anion which may lead to product or may decompose *via* a radical caged pair. The caged pair is thought to be the major pathway in the photodecomposition of pentachlorobenzene in the presence of sodium borohydride.[33] A linear

Scheme II.5

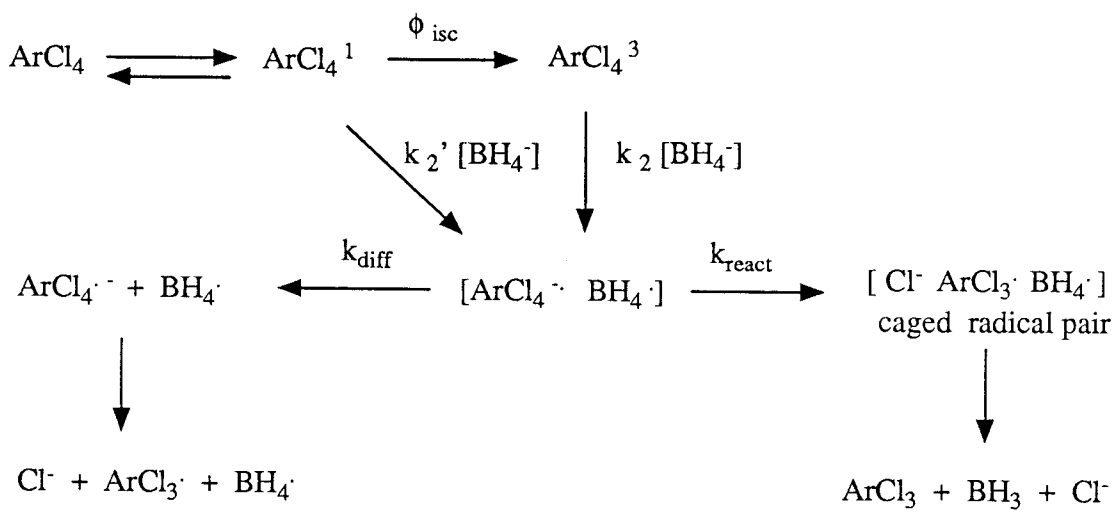

regression analysis is performed on the four most concentrated points of the

photolysis work and the data is again consistent with an excited state aromatic reacting with the ground state borohydride species. The analyses are summarized in the Table II.17, 18. There is again a large uncertainty associated

Table II.17 Linear Regression Analysis of Plot of $1/\Phi$ vresus $1/(NaBH_4)$ for the Photolysis of Tetrachloronaphthalene in Presence of $NaBH_4$.

compound	slope	intercept [b]	slope/intercept (k_{td}/k_2)
1467 TCN (2) [a]	3.4	1200	2.83×10^{-3}
1358 TCN (3) [a]	3.3	935	3.53×10^{-3}

[a] Values obtained from quantum yield for starting material lost.
[b] Calculated error in the intercept is large.

Table II.18 Calculated Rates from Triplet Data and Regression Analysis of Plots of Tetrachloronaphthalene in the presnce of $NaBH_4$ at 300 nm.

compound	k_{td} s^{-1}	τ_{msec}	k_{td}/k_2	k_2 s^{-1b}	k_2 s^{-1c}
1467 TCN [a]	28.1	35.6	2.83×10^{-3}	9.93×10^{3}	5×10^{12}
1358 TCN [a]	34.5	29.0	3.53×10^{-3}	9.78×10^{3}	3×10^{12}

[a] Values obtained from quantum yield of starting material lost. [b] Triplet derived data.
[c] Singlet derived data.

with the calculated intercepts (uncertainty in the intercept values were calculated to be as large as 20% of the intercept itself) which could lead to an erroneous conclusion about the rate of exciplex formation and exciplex to product efficiency. However, the increase in the two slopes relative to the uncatalyzed photolyses is an indication of the sensitivity of the TCNs to the concentration

of sodium borohydride. When compared to the data in the TEA work and the straight photolyses, the borohydride appears to be an effective reducing agent but not as effective as TEA. If the intercepts can be regarded as a reasonable estimate of the efficiency of exciplex to form dehalogenated products, then the exciplex formation (BH_4^-:TCN) leads to product in a more efficient maner than the excimer, but, again, not as efficient as the exciplex TEA:TCN. The goodness of fit, measured by the term R, is calculated from the regression analyses. The R value for 1,4,6,7-TCN is shown to be 0.975 and for 1,3,5,8-TCN is 0.994. An attempt to evaluate the question of singlet or triplet exciplex formation by the estimated rate data does not give a clear cut answer. It does seem unlikely that the rate of exciplex would exceed the diffusion controlled rate of $2 \times 10^{10}\ s^{-1}$, therefore, it would seem more reasonable to conclude that there may be several rate processes occurring at the same time and that it may be impossible to fully characterize all pathways to products.

Micellar Photodehalogenation

In an attempt to generate unencumbered radical anions of 1, 2, and 3, 0.2 M CTAB (cetyltrimethylammonium bromide) solutions were prepared. CTAB is a surfactant consisting of a hydrocarbon chain, which is hydrophobic, and a polar or ionic group, which is hydrophilic. These are the properties that enable the sufactant to form aggregates called micelles. The conventional representation of the formed micelle in an ionic detergent is shown in Figure II.21. The micelle may adopt many shapes, therefore, the representation in the Figure II.21 is an averaged, two dimensional, cross section, of the shere that is thought to be a micelle of CTAB. At the core of the micelle one finds the hydrophobic components of the detergent molecules. The head groups of the CTAB (ammonium) form the interface with the aqueous phase at a region called the Stern-layer, a compact sphere at the outside of the micelle. The Gouy-Chapman layer is just outside of the Stern-layer and contains the unbound counter ions suspended in an aqueous layer. There exists an inherent concentration level for each detergent at which micelles begin to form. This concentration is known as the critical micelle concentraion or CMC. At concentrations greater than the CMC, all detergents from micelles. CTAB forms micelles at concentrations and temperatures reported in Table II.19.[84] The CTAB micelle is similar to the structure seen in Figure II.21 where the TCN is expected to reside in the inner sphere of the micelle and the TEA is expected to reside in the aqueous layer.[85] Poisson statistics have been shown to be

Figure II.21 Micelle Diagram.

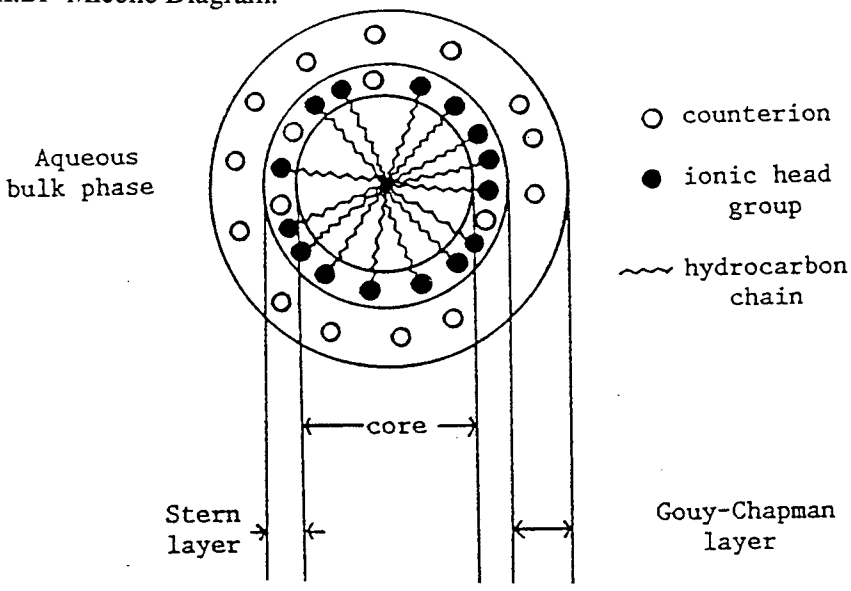

Scheme II.6

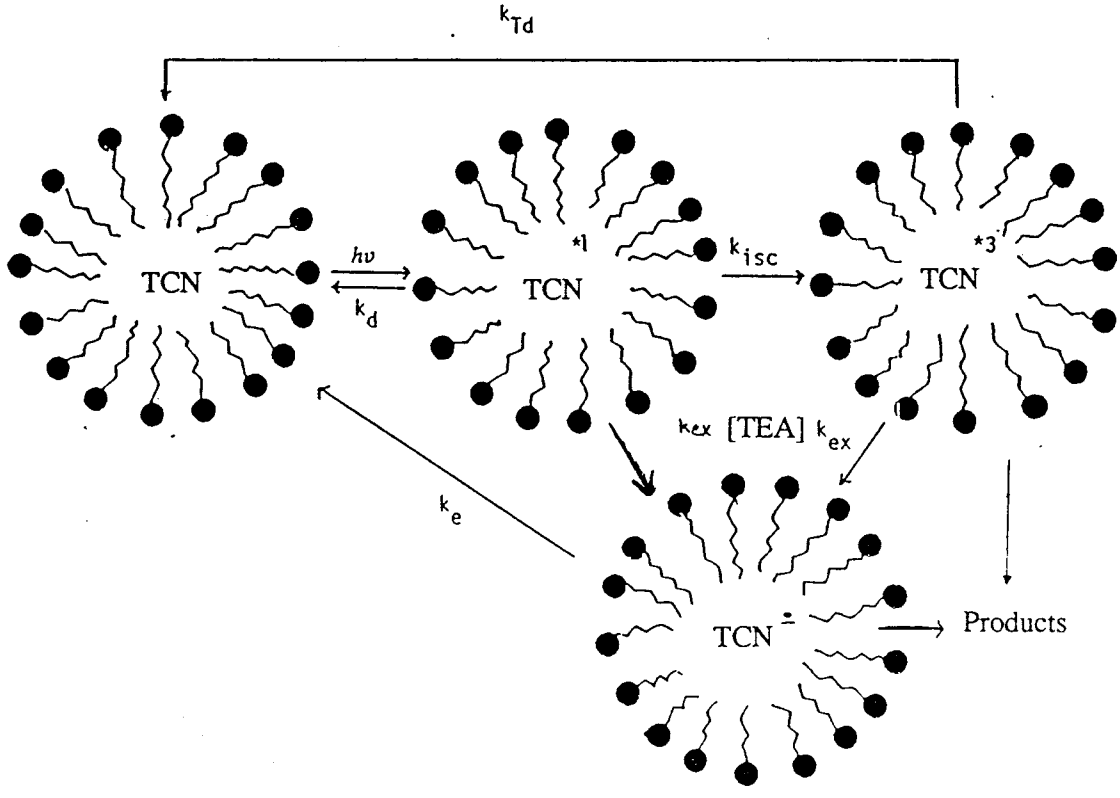

Table II.19 Critical Micelle Concentrations of CTAB at Some Selected Temperatures.

Temperature (°C)	CMC (M)
25	$5.0 - 9.8 \times 10^{-4}$
35	$9.5 - 10.2 \times 10^{-4}$
45	1.16×10^{-3}

appropriate for calculating the occupancy of the micelle (Equation II.9). P(n) is

Equation II.9

$$P(n) = \frac{\langle s \rangle^n}{n!} \exp(-\langle s \rangle)$$

the probability of finding a micelle containing n solute molecules and <s> is the average number of solute molecules per micelle. The mean occupancy number, <s>, is the ratio of the bulk concentration of **1**, **2**, or **3** to the bulk concentration of CTAB micelles in H_2O (Equation II.10) and N_{agg} is the mean aggregation number of CTAB molecules per micelle.[86] The aggregation number,

Equation II.10

$$\langle s \rangle = \frac{[\text{Solute}]}{[\text{Micelles}]}, \qquad [\text{Micelles}] = \frac{[\text{CTAB}] - \text{CMC}}{N_{agg}}$$

N_{agg}, is taken to be 80 for CTAB in this experiment.[87] Under our conditions no

fluorescence was detected, no phosphorescence could be observed, and all micelles were essentially empty or mono-occupied. Bulk concentrations of 1, 2, and 3 and the corresponding microscopic concentrations were optimized with the goal of an occupancy number $\leq$ 1 based upon the calculated Poisson distributions.[88,89] The calculated probability for occupancy of the micelles were 0.002 doubly occupied, 0.150 mono occupied, and 0.848 unoccupied. The three TCNs, 1, 2, and 3 were photolyzed under these conditions in the presence and absence of TEA. The regiochemical dechlorination is examined for clues as to the reactivity. The mechanism is depicted in Scheme II.6.

An excess amount of TEA is spiked into each CTAB/TCN solution. TEA concentration varied from 1:1 to 20:1 in microscopic concentration. Samples photolyzed in the 20:1 microscopic concentration region (0.025 M TEA) demonstrated similar regiochemical dehalogenation to the TEA in CH_3CN photolyses. The TEA has been shown to reside predominatly in the aqueous phase and around the surface of the micelle.[100] Upon irradiation, it is expected that the TEA will transfer an electron to the excited state TCN and thus generate an excited state radical anion within the micellar environment. The positively charged micellar surface will repell the resultant radical cation of the TEA leaving behind a TCN radical anion unencumbered by a counter ion.[31,90] The micelle is then broken by dillution extracted with diethyl ether and analyzed by gas chromatography (GC) and by GC/MS.

The photoreaction within a CTAB micelle in the absence of TEA is expected to be dependent upon the occupancy of the micelle. In our hands TCN solubility could not be induced to be greater than an average mono-occupancy of 15%. Most micelles remain unoccupied (*ca.* 84.8% empty) and a small

fraction (*ca.* 0.2%) doubly occupied. Concentration estimates are reinforced by ultraviolet absorption measurements and previously determined extinction coefficients. Therefore, photodehalogenation in the CTAB solution without TEA is assigned to triplet reactivity of the associated TCN; direct triplet bond homolysis. Products are analyzed in an identical manor to the above procedure. Ratios of products are similar to products derived from triplet and triplet excimer species (Table II.24-26). This remains in contrast to irradiation results in the presence of electron transfer reagents, TEA/CTAB or TEA/CH_3CN. The regiodechlorination of the TEA/CTAB solutions closely resemble the results obtained in the TEA/CH_3CN solutions. Therefore, the mechanism of dechlorination is expected to be similar in both cases. Product ratios from CTAB photolyses for **1**, **2**, and **3** all favored the straight photolysis products **4**, **6**, and **8**. Product ratios observed in TEA/CTAB photolyses favored products similar to those generated in the TEA/CH_3CN runs (Tables II.24-26). It is apparent that an unencumbered (CTAB) radical anion reacts to produce products similar to those of radical anions in CH_3CN/TEA photolyses giving further evidence for solvent separated ions in the triethylamine photolyses. Another point of interest shown here is that the monomer is capable of dechlorination without the activation of excimer formation and that the observed regiochemistry of dechlorination from excimer or monomer is nearly identical.

Photochemical Quenching Studies

Further attempts to characterize the reactive intermediates involved in the dechlorination of starting compounds **1**, **2** and **3** were pursued by the

employment of triplet quenching reagents. If only one reactive excited state (presumably the triplet) is responsible for the observed reactivity, then it should be possible to quench that reactive state with the proper quencher.[91] Compound **1** is photolyzed in the presence of a mixture of *cis*- and *trans*-1,3-pentadiene and quenching was observed. The Stern-Volmer plots obtained (Figure II.22,23) from the data (Table II.20) are linear. However, the two other TCNs (**2** and **3**)

Table II.20 Stern-Volmer Data from 1,2,3,4-Tetrachlorornaphthalene [c] with a Mixture of *cis*- and *trans*-1,3-Pentadiene.

Pentadiene concentration (M)	Φ_o / Φ [a]	Φ_o / Φ [b]
0.0000	1.00	1.00
0.0010	4.00	3.95
0.0025	9.20	9.11
0.0050	18.6	17.5
0.0100	39.4	38.4

[a] Relative quantum yield for product formation. [b] Relative quantum yield for loss of starting material. [c] 3.0×10^{-4} M.

failed to demonstrate quenching when the quantum yield is measured by loss of starting material under the identical conditions (Tables II.21 and Figures II.24-27). The samples that were photolyzed in the concentrated regions of the

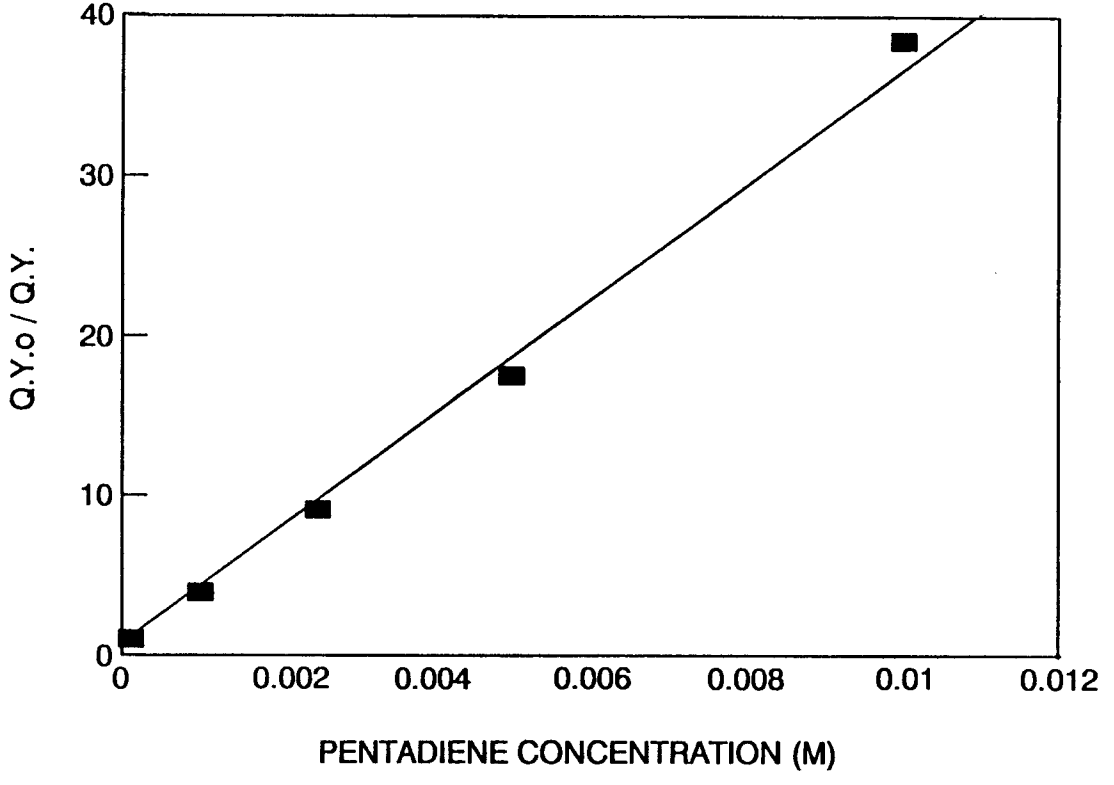

Figure II.22 Stern-Volmer Plot for Loss of 1,2,3,4-Tetrachloronaphthalene in the Presence of a Mixture of Pentadienes at 300 nm.

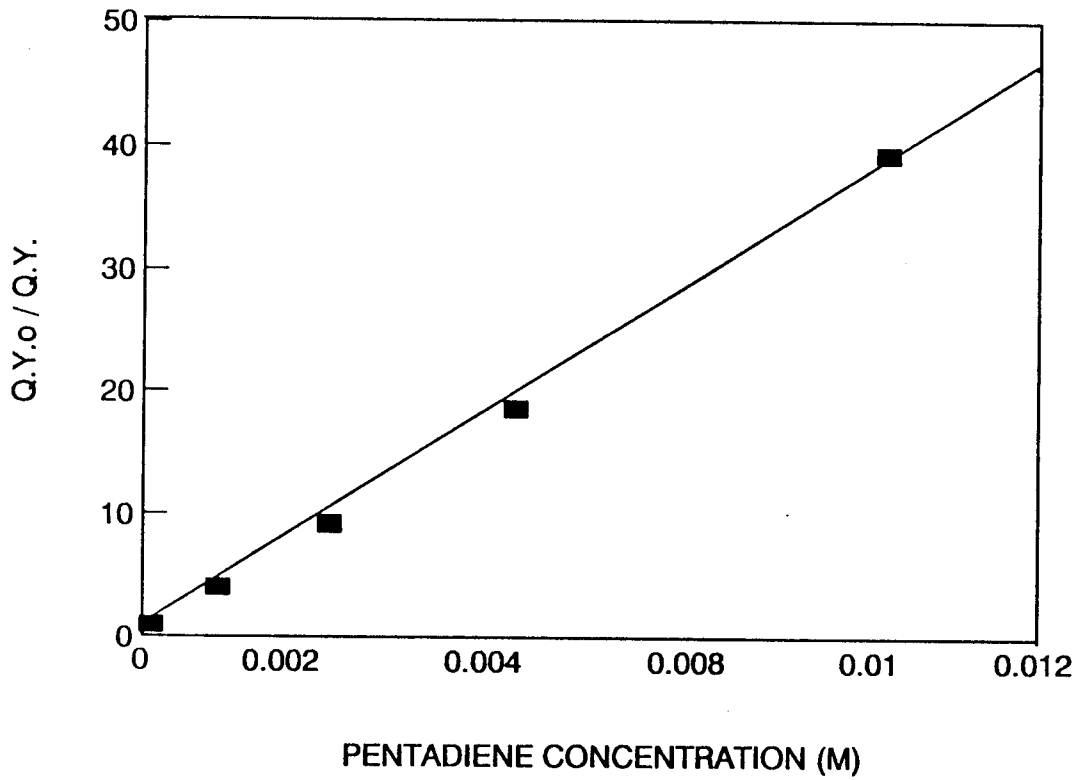

Figure II.23 Stern-Volmer Plot of Product appearance from Photolysis of 1,2,3,4-Tetrachloronaphthalene at 300nm.

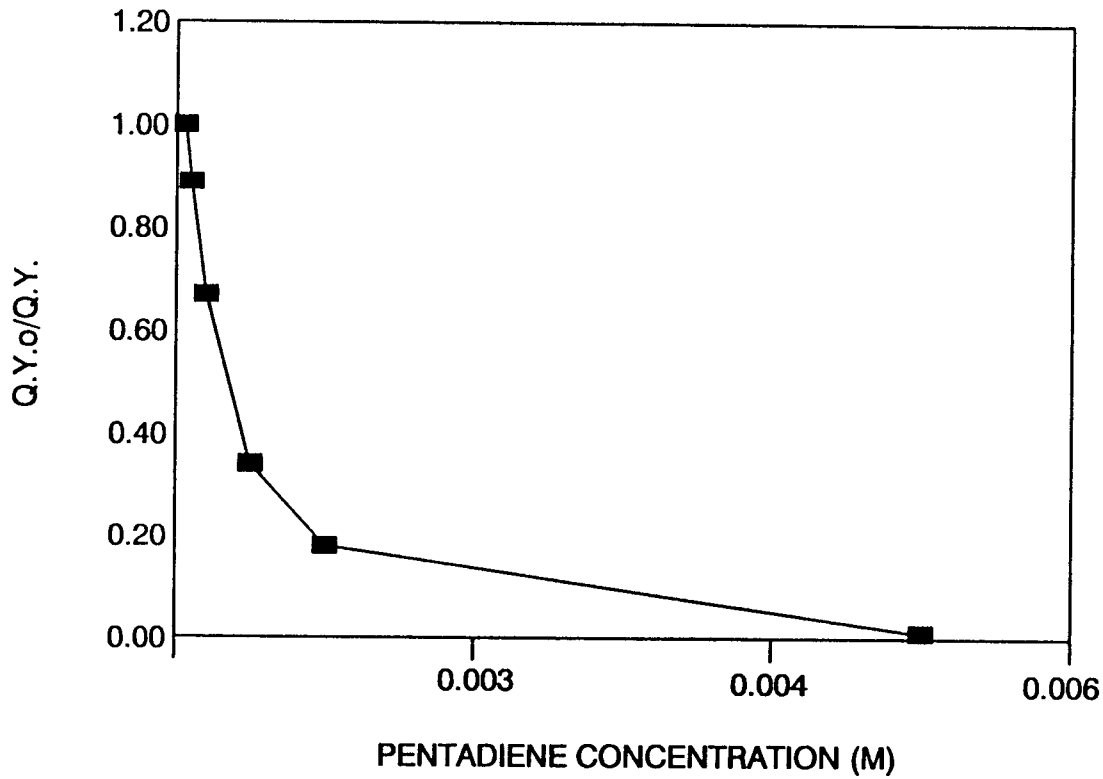

Figure II.24 Stern-Volmer Plot for Loss of 1,4,6,7-Tetrachloronaphthalene in the Presence of a Mixture of Pentadienes at 300 nm.

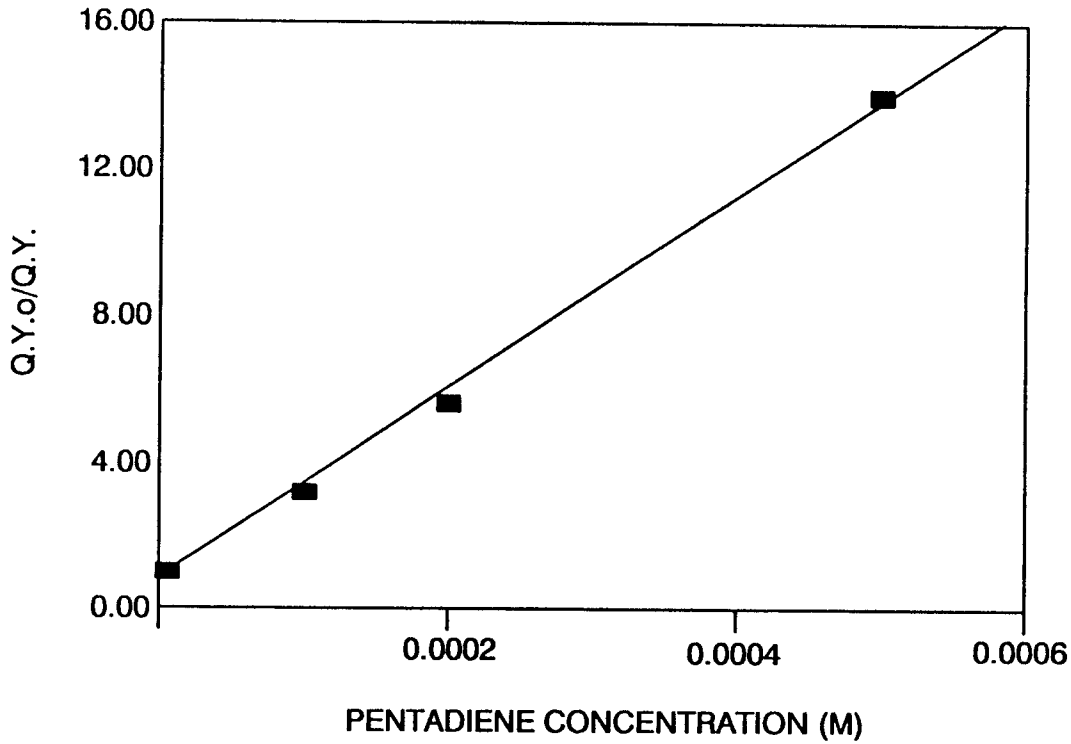

Figure II.25 Stern-Volmer Plot for Product Appearance from Photolysis of 1,4,6,7-Tetrachloronaphthalene at 300 nm.

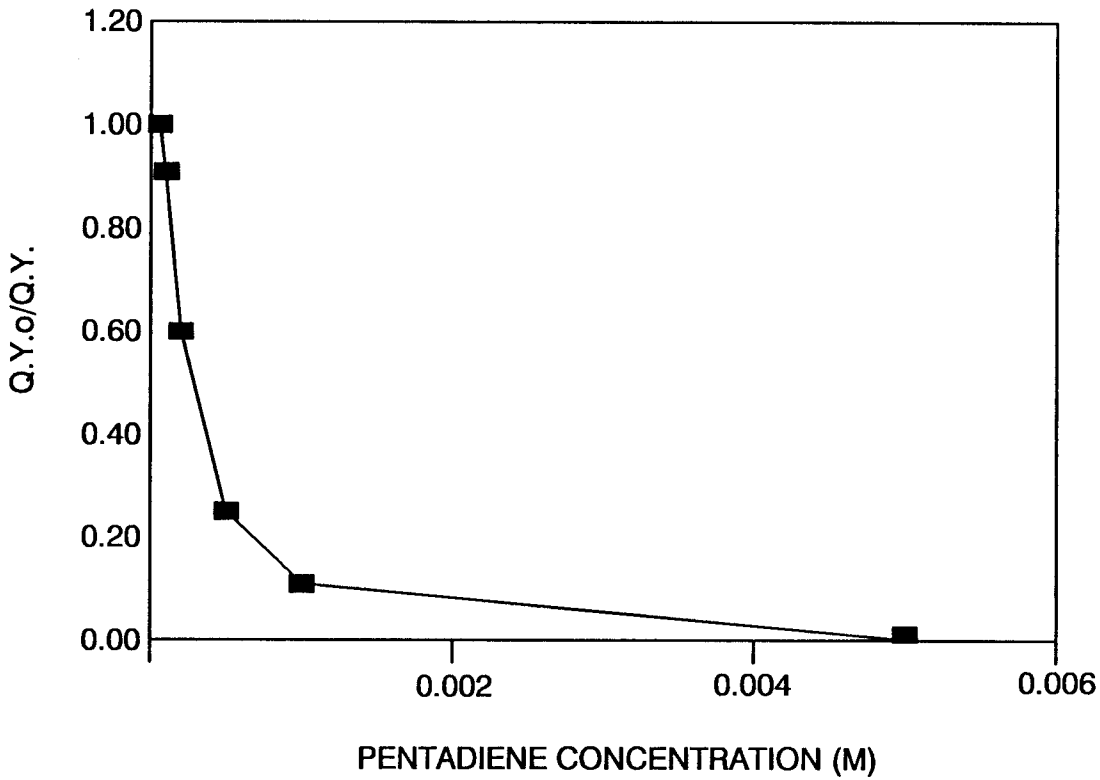

Figure II.26 Stern-Volmer Plot for Loss of 1,3,5,8-Tetrachloronaphthalene in the Presence of a Mixture of Pentadienes at 300 nm.

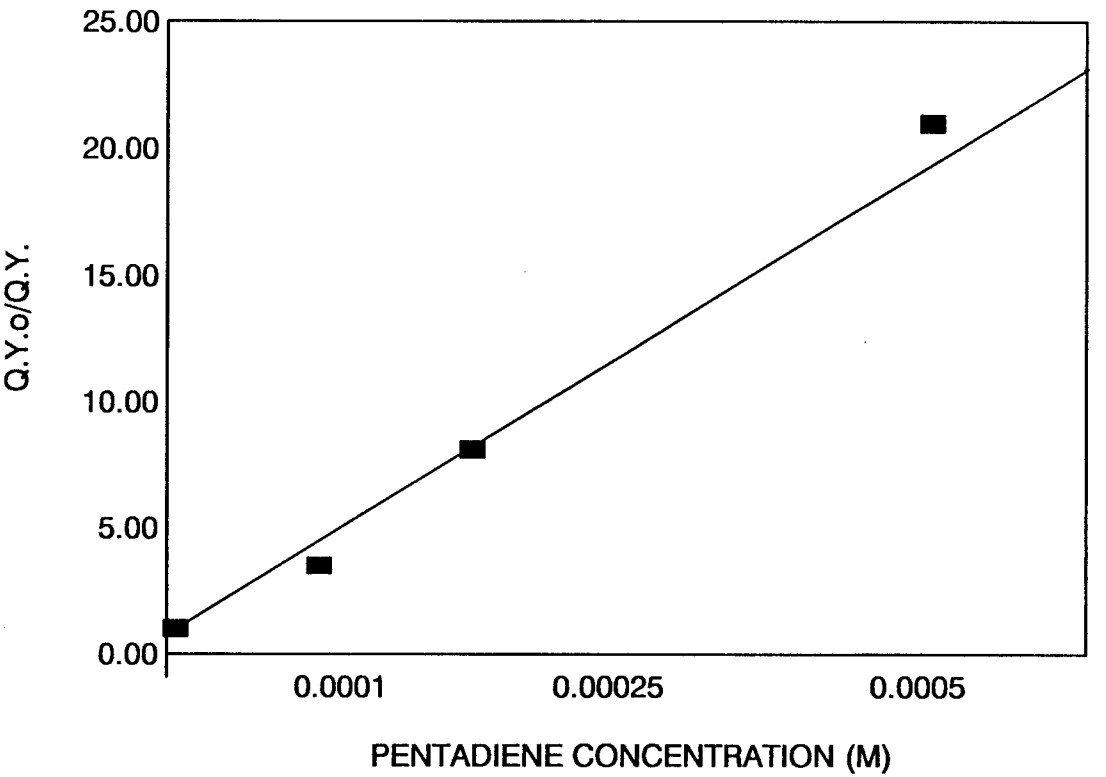

Figure II.27 Stern-Volmer Plot for Product Appearance from Photolysis of 1,3,5,8-Tetrachloronaphthalene at 300 nm.

diene mixture (0.01 M) yielded only products that were consistent with two different cycloaddition compounds for 2 and an additional two cycloadducts for compound 3. That is, the GC/MS indicates a molecular weight that is consistent with cycloaddition to the naphthalene parents. Attempts to isolate

Table II.21 Stern-Volmer Data from Quenching Attempts on 1,3,5,8- and 1,4,6,7-Tetrachloronaphthalene[c] with Fumaronitrile and a Mixture of *cis*- and *trans*-1,3-pentadiene.

Fumaronitrile concentration (M)	Pentadiene concentration (M)	1,3,5,8-TCN[d] Φ_o/Φ [a]	1,3,5,8-TCN[d] Φ_o/Φ [b]	1,4,6,7-TCN[d] Φ_o/Φ [a]	1,4,6,7-TCN[d] Φ_o/Φ [b]
0.0000	0.0000	1.00, 1.00	1.00, 1.00	1.00, 1.00	1.00, 1.00
0.0001	0.0001	2.30, 3.50	0.95, 0.91	1.60, 3.20	0.96, 0.89
0.0002	0.0002	4.20, 8.10	0.68, 0.60	2.30, 5.60	0.69, 0.67
0.0005	0.0005	6.30, 21.0	0.35, 0.25	4.60, 14.0	0.54, 0.34
0.0010	0.0010	none, none	0.14, 0.11	10.5, none	0.22, 0.18
0.0050	0.0050	none, none	0.01, 0.01	none, none	0.01, 0.01

[a] Relative quantum yield for product formation. [b] Relative quantum yield for loss of starting material. [c] 2.3×10^{-4} M. [d] Values are fumaronitrile followed by pentadiene.

these compounds proved fruitless. Since pentadiene is not effective at quenching reactive states of TCNs 2 and 3, another quencher study was attempted using fumaronitrile (Table II.21 and Figures II.28-31). Fumaronitrile has been reported to be an effective low energy triplet quencher.[92] The results are apparently similar to the results obtained in the case of the pentadiene quenching experiments. The addition products could not isolated but the GC/MS in a positive chemical ionization mode exhibited masses that were consistent with cycloaddition. As a result of the inability of the two quenchers

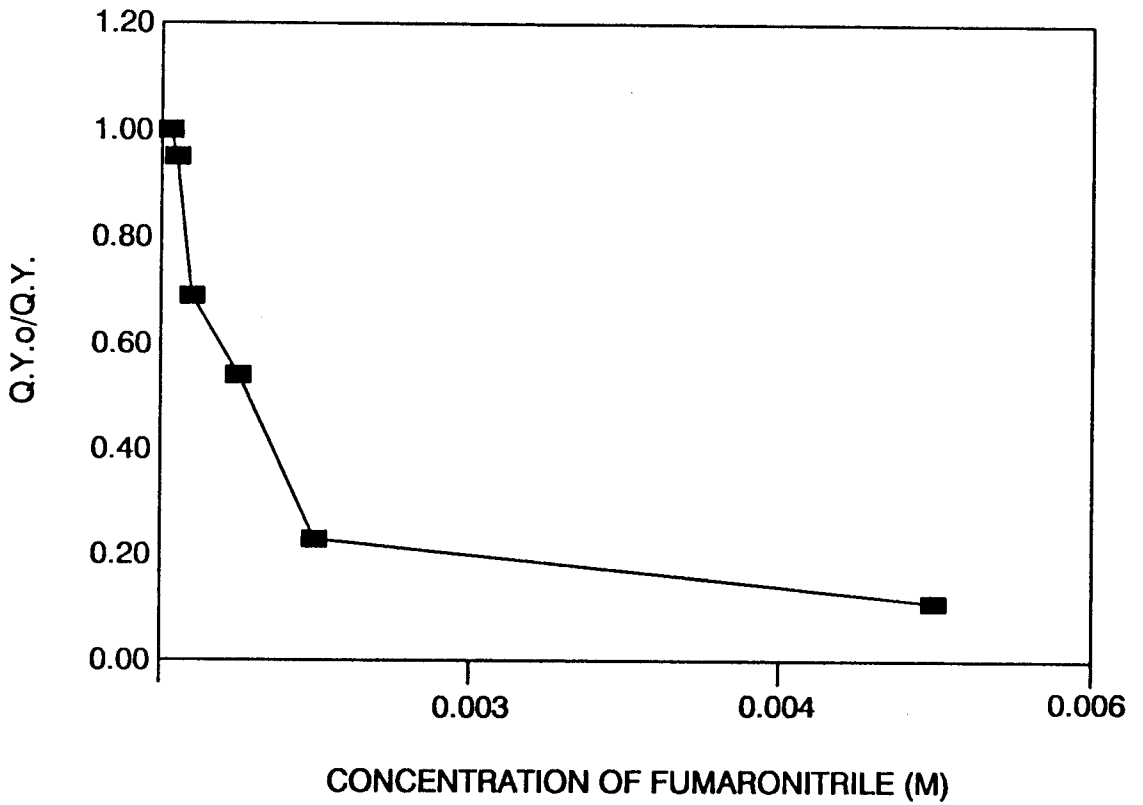

Figure II.28 Stern-Volmer Plot for Loss of 1,4,6,7-Tetrachloronaphthalene in the Presence of Fumaronitrile at 300 nm.

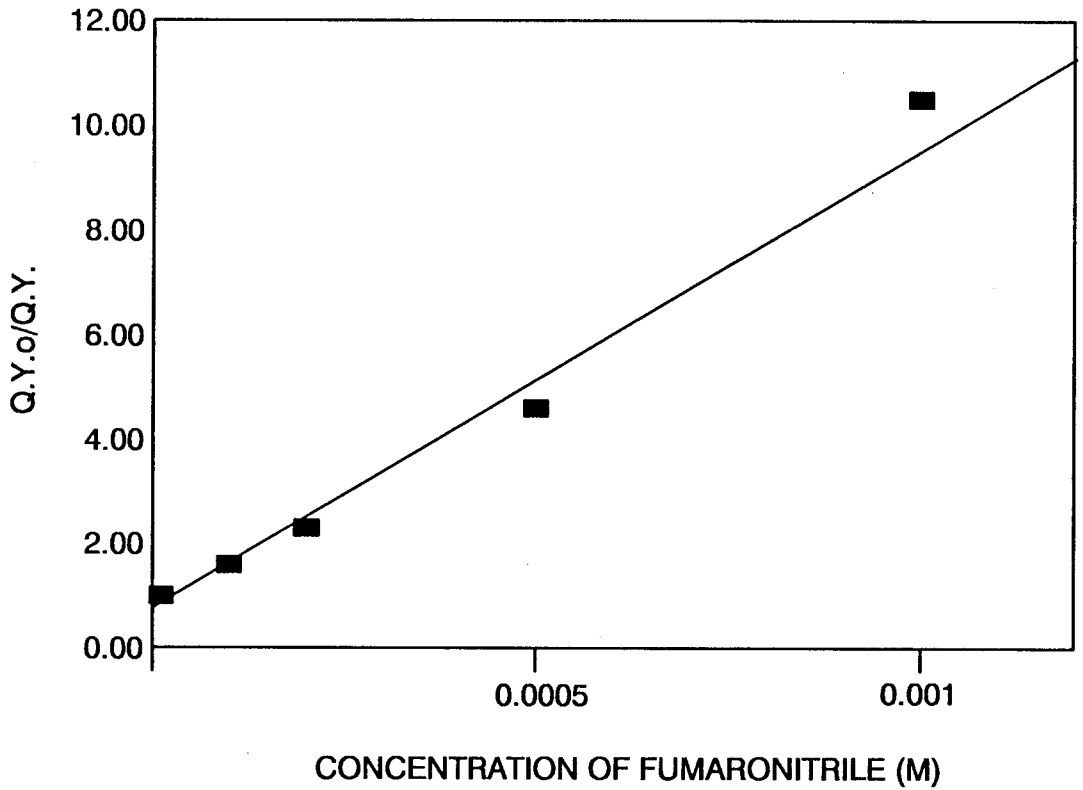

Figure II.29 Stern-Volmer Plot for Product Appearance from Photolysis of 1,4,6,7-Tetrachloronaphthalene at 300 nm.

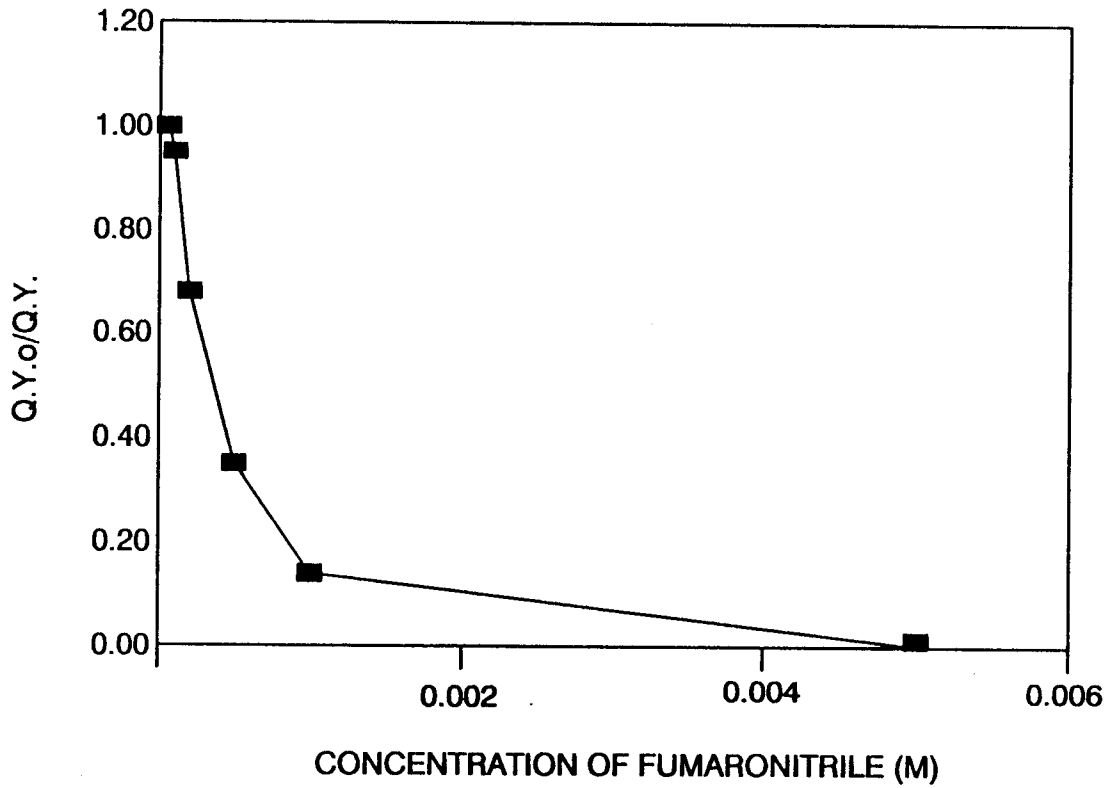

Figure II.30 Stern-Volmer Plot for Loss of 1,3,5,8-Tetrachloronaphthalene in the Presence of Fumaronitrile at 300 nm.

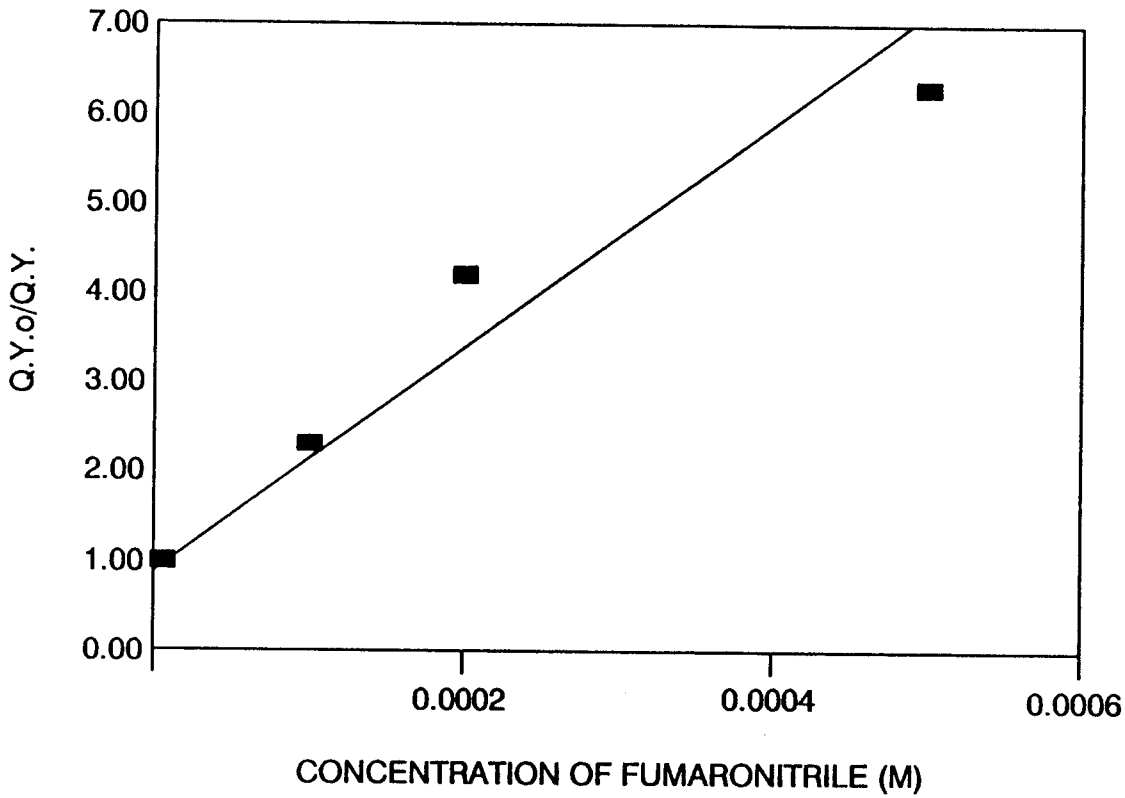

Figure II.31 Stern-Volmer Plot for Product Appearance from Photolysis of 1,3,5,8-Tetrachloronaphthalene at 300 nm.

employed to quench the reactive excited state of the TCNs and the lack of success reported by Ruzo and co-workers[68,69] in trying to quench other chloronaphthalenes, we elected to drop the attempts to find another suitable quencher.

The sole TCN that was quenched by the pentadiene mixture will allow us to make some inferences for our other compounds. The only straightforward Stern-Volmer analysis we were able to perform was carried out on TCN **1** and the pentadiene system (Figure II.22, 23). The analysis yielded an estimate of the triplet lifetime of the TCN at room temperature.[93] The experiment assumes a diffusion controlled rate process calculated from the Equation II.11. Degassed

Equation II.11

$$k_{diff} = 8RT/2000\eta$$

η is equal to the solvent viscosity

pyrex tubes were placed in the "merry-go-round" apparatus and were irradiated in duplicate for 36 h. Since each tube absorbed the same intensity of light, the GC analysis for the amount of product formed provided a direct measure of the relative quantum yield of reaction. The observed Stern-Volmer plots are linear with a positive slope (Figure II.22,23 and Equation II.12). The regression analysis yielded values of 3870 and 3650 for the slopes and 0.12 and 0.22 for the intercepts for product appearance and loss of starting material. The slope should be equal to $k_q \tau$, where k_q is equal to the diffusion controlled rate constant for quenching 2×10^{10} s^{-1}.[94] If quenching is indeed diffusion

Equation II.12

$$\Phi_o/\Phi = 1 + k_q\tau\,[\text{Quencher}]$$

controlled, determination of the slope affords an estimate for a room temperature τ. The triplet lifetime was calculated to be 1.9×10^{-7}s. and 2.1×10^{-7} s. Since this is a composite lifetime inclusive of all the bimolecular and collisional deactivation rates that may take place in room temperature solutions, this τ should not be the same as the one calculated at 77 °K. An interesting sidelight was the discovery that photolyses of the diene mixtures in dilute regions, (diene concentration ≤ 0.001 M) where some dechlorination was observed, trichloronaphthalene alkylation products were observed (Equation II.13). This was another piece of evidence that indeed one of the products of dechlorination is the trichloronaphthyl radical.

Equation II.13

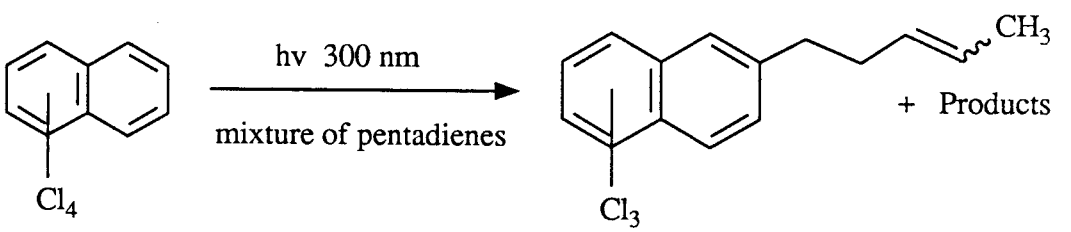

Chemical Dehalogenation

Dechlorination of starting TCNs is accomplished by employment of the lithium salt of the radical anion of p-p'-di-*tert*-butylbiphenyl (LDBB). The reduction potential of p-p'-di-*tert*-butylbiphenyl has been measured to be -2.14

Volts.[95] The proper choice of the donor species makes it possible to generate the radical anion of the starting TCN by an electron transfer process. The requirement for the reaction is that donors have reduction potentials higher than that of the TCN's. The first reduction potentials for 1, 2, and 3 have been measured at -1.39, -1.43, and -1.37 Volts,[96] respectively; therefore, electron transfer from LDBB (-2.12 Volts) is energetically favorable. Dechlorination is accomplished by first generating LDBB by treatment of p-p'-di-*tert*-butylbiphenyl with Li metal in dry THF under an argon atmosphere. TCNs are then syringed into the solution of the LDBB radical anion (Equation II.14). After ten minutes

Equation II.14

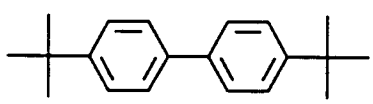

the reaction is quenched by the addition of a small amount of water. The trichloronaphthalene products are extracted with diethyl ether, dried over magnesium sulfate and analyzed by GC and GC/MS. The regiochemistry again was intermediate between the photo-induced electron transfer (TEA) and simple photolysis (Tables II.24-26). Results can be rationalized through differences in solvation and ion pair formations. The inability of the electron transfer to yield the same selectivity as the TEA was thought to arise from a predissociative caged complex and the lithium counter ion. The electron transfer to the TCN yields the radical anion of TCN and a lithium counter ion. The complex can then decompose to a trichloronaphthyl radical and chloride anion. In this case the role of the counterion is questioned. The LBDD electron transfer process

and the subsequent dissociation are chemical processes not an excited state photochemical process; therefore, it may be argued that the observed reactivity can occur from a different reactive manifold. It is our belief that the TEA mediated photolyses yield radical anions that are solvent separated and that the LDBB electron transfer reaction gives a radical anion with a tightly bound lithium counterion. The products of decomposition of the two species are expected to be quite different. Theses differences account for the observed regioselectivity.

Triphenyltinhydride Dehalogenation

Dechlorination of compounds **1**, **2**, and **3** may also be accomplished by employment of the triphenyltin radical generated from the decomposition of AIBN in the presence of triphenyltinhydride (Scheme II.7). As is noted in the introduction, there exists considerable debate about the mechanism of dehalogenation. It has been known for some time that the triphenyltin radical reacts with benzylic halides and aromatic halides to give the the corresponding reduced product. The stannyl radical has been postulated to act as an electron transfer reagent in the reactions of various benzylic iodides.[62,98] In contrast to this is the reactivity observed in substituted benzylic chlorides. The benzylic chlorides have been shown to fit a model that is consistent with a direct atom abstraction.[60,97] In more recent work the stannyl radical has been proposed to transfer an electron to the heteroaromatic system in various chloromethyl substituted heteroaromatics.[98] The mechanism of reduction will undoubtedly continue to be debated. It was our hope that the employment of the

triphenyltin radical would shed some additional light on the intermediate controlling the regiochemistry.

After eight hours in a 70°C oil bath under diffuse light conditions the reaction of compounds 1 and 3 was complete. Compound 2 was only 33% complete. Gas chromatographic analysis indicates that the reaction of 1 and 2 with the tin radical favors the products obtained for the photocatalyzed electron transfer process. If the tin radical transfers an electron to the TCN in question, the observed regiodechlorination would be indicative of the reactivity of the radical anion. The selectivity observed in the reaction of TCN 1 and 2 was not as great as seen in the triethylamine catalyzed dehalogenation but this is to be expected at the elevated temperature. Even though the observed selectivity was not as great, the reactivity of TCN 1 and 2 seems to support an electron transfer process operative prior to dehalogenation. Product analysis for the reaction of 3 demonstrates trichloro products in similar ratios to that which is obtained in the straight photolytic runs (Tables II.24-26). This result does not support an electron transfer process operative in the dechlorination of TCN 3. The higher reaction temperature also tends to muddy the issue of the mechanism of dechlorination. The reactivity of 3 seems to be in contrast to the reactivity of TCNs 1 and 2 under these conditions. It is possible that other factors such as thermodynamics, position of the transition state along the reaction path, and the nature of the counter ion are affecting the product distributions. If the thermodynamics of the products is supplying the driving force for the reaction (late transition state) the energies of the trichloro derivatives are insightful. The calculated energies of the trichloro radicals, trichloro anions, and trichloronaphthlene ground states are found in Table II.23.

Scheme II.7

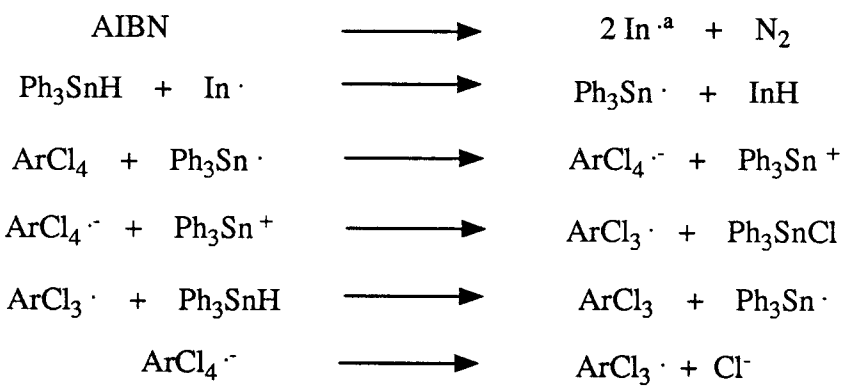

[a] In· is the 1-cyano-1-methylethyl radical.

An examination of Table II.23 shows that there is no clear cut correlation of proposed intermediates to the mechanism of dechlorination *via* the tin radical. Therefore, a more rigorous study of the tin radical is clearly needed.

Elemental Potassium Reductions

After preparing starting materials, it is necessary to prepare the trichloronaphthalene products that will arise from photodechlorination. The simplest and most convienent process proved to be a simple reduction with elemental potassium. Conversions of 30-40% to trichloro products without further reduction to the dichloronaphthalene products is achieved in just two hours. Column chromatography proved difficult, but by preparatory GC trichloronaphthalene products were isolated and characterized. Product ratios were then easily calculated. It is generally assumed that potassium will readily give up an electron and thus transfer it to the tetrachloronaphthalene species.

The incipient radical anion then dechlorinates (Scheme II.8) leading to chloride

Scheme II.8

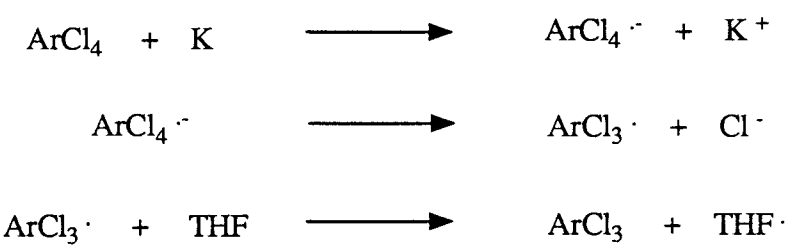

and trichloroarylradicals. The trichloronaphthalenes were identified by gas chromatographic retention times and NMR (^{1}H and ^{13}C). The regiochemistry was then easily identified and calculated. Results appear in the reaction summary tables (Tables II.24-26). There appears to be a good correlation between the lowest calculated energies of trichloronaphthalenes produced and the observed products (Table II.23).

Computational Correlations and Predictive Models

It is apparent that there are at least two different product forming pathways in the dechlorination of the tetrachloronaphthalenes that we set out to study. We attempted to correlate the observed regiochemistry based upon the Wheland intermediate that would be formed if the dechlorination were to occur through a radical anion with a localized sp^3 radical center. Freeman and coworkers made use of the Longuet-Higgins method to calculate coefficients for the NBMO and their charge distributions.[51] Assessment is accomplished by localizing an electron at the eventual site of bond fission (Wheland intermediate)

and summing the charge (Σc_{ix}^2) residing at the carbons that bear chlorine substituents in the remaining odd alternate hydrocarbon.[53] The interaction of negative charge on arene carbon with attached chlorine may be viewed as a destabilizing interaction.[52] Examination of the individual intermediates will demonstrate the largest charge for the least stable intermediate (Σc_{ix}^2) or the smallest charge for the most stable intermediate (Table II.22). The models shown in the Figure II.32 are transition state emulations based upon these ideas and the analogous SRN[1] intermediate.

Table II.22 Longuet-Higgins Summary and AM1 Heats of Formations

TCN	sp^3 position	Σc_{ix}^2 (I-π)[a]	AM1 ΔH_f[b]
1234	1 or 4	0.7272	-31.44
	2 or 3	0.6252	-27.14
1467	1 or 4	0.4545	-32.29
	6 or 7	0.2501	-28.03
1358	1	0.0909	-29.70
	3	0.1250	-22.27
	5	0.5454	-27.89
	8	0.3636	-30.64

[a] Smallest coefficient equals most stable intermediate [b] Kcal/mole

Figure II.32 Wheland Intermediates for Longuet-Higgins Analyses.

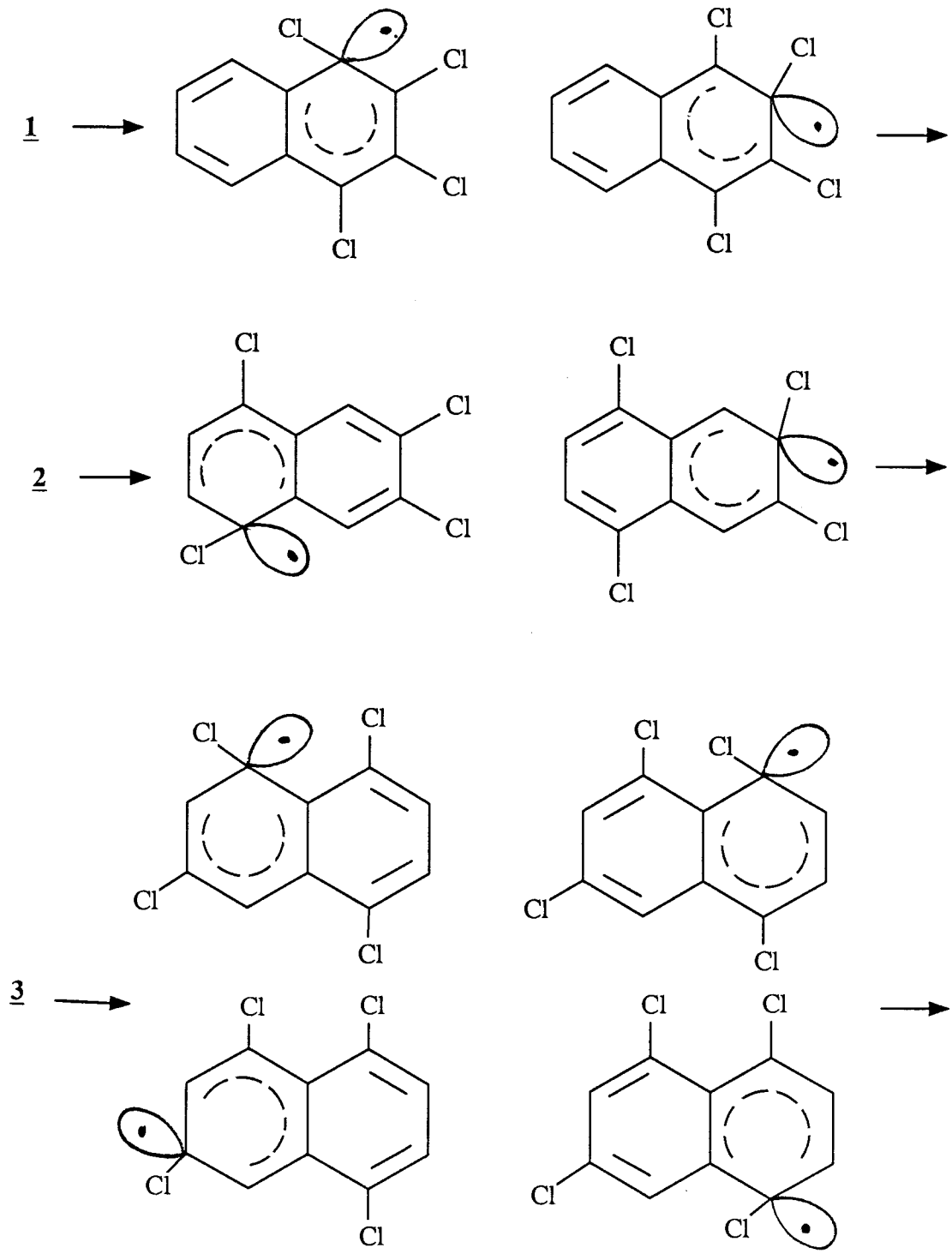

An examination of the table leads one to suggest that compound 1 would lose the chloride located at position 2 the β position, preferentially to position 1 the α position. This would yield the dechlorinated product 1,2,4-trichloronaphthalene in preference to the 1,2,3 trichloro derivative. Compound 2 yields a predicted site of bond cleavage to be most stable from position 6 (β). The loss of chloride from this positions would generate 1,4,6-trichloronaphthalene as the major product of reaction. Compound 3 has four different sites that could lose a chlorine (chloride) and the most stable intermediate that is predicted by this model would be the one that leads to the trichloro derivative 1,4,6-trichloronaphthalene. All three compounds, when photolyzed in the presence of TEA, yielded the predicted trichloro derivative as the major product. Since the photolysis in TEA is expected to produce the radical anion prior to bond cleavage, it appears that this simple approach correctly predicts the observed regiochemistry for preformed radical anions. We have also tried to model this intermediate through the use of AM1 semi-empirical molecular orbital calculations.

The Wheland intermediate is emulated by placing a hydrogen atom at the site of eventual bond cleavage thereby removing that site from conjugation creating an artifical intermediate with an sp^3 center. The results of the calculations, Table II.22, do not agree with the simple Longuet-Higgins analysis and with the regiochemistry observed. Therefore, another approach to evaluation of the transition state for cleavage was undertaken.

The ground state radical anion energies and associated molecular orbitals were calculated by use of the AM1. It was believed that the orbital coefficients in the SOMO would be a possible measure of the instability of the individual

carbon-chlorine bonds. An examination of the coefficients in the calculated SOMO, apparently π*, did not demonstrate agreement with the observed regiochemical dechlorination (Figure II.33). However, an examination of the

Figure II.33 Calculated π* Coefficients in Radical Anions |x| (10^3) Naphthalene Skeleton Only.

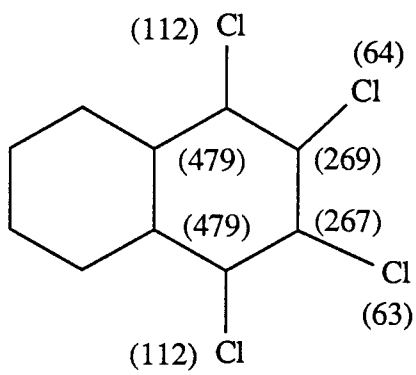

1

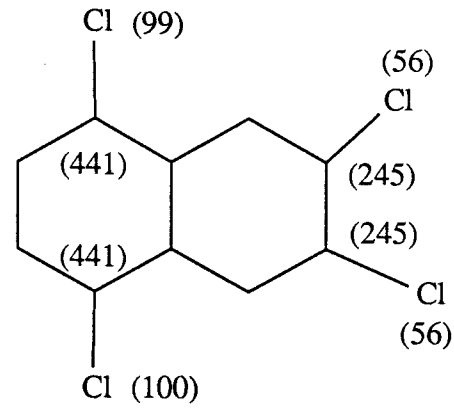

2

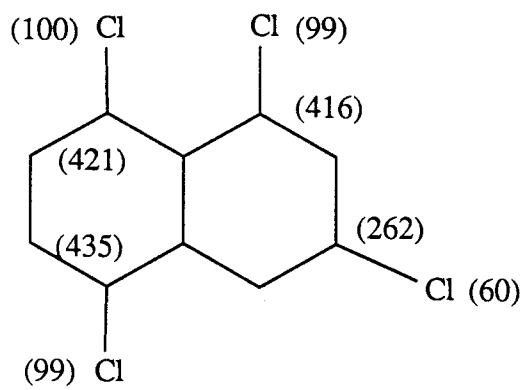

3

lowest molecular orbital identified as σ* did demonstrate a strong correlation between orbital coefficients and the observed site of dechlorination (Figure II.34). The only deviation appears in compound 3 where the strongest coefficients are at carbon-chlorine 3. Since this product is not observed, it could be that relief associated with the loss of chloride from either of the peri

positions (1 or 8) alters the pattern. The strain associated with dichloro 1-8 peri substitution may raise the energy of the system by more than 6 kcal/mole (Table II.8) and, consequently, weaken both carbon-chlorine bonds at positions 1 and 8. Therefore, the two predictive models used to evaluate the site of bond cleavage from an aryl chloride radical anion, the Longuet-Higgins transiton state emulation and the AM1/RHF radical anion σ* coefficient analysis, give reasonable predictions for the three tetrachloronaphthalenes **1**, **2**, and **3**.

Figure II.34 Calculated σ* Coefficients in Radical Anions $|x|$ (10^3) Naphthalene Skeleton Only.

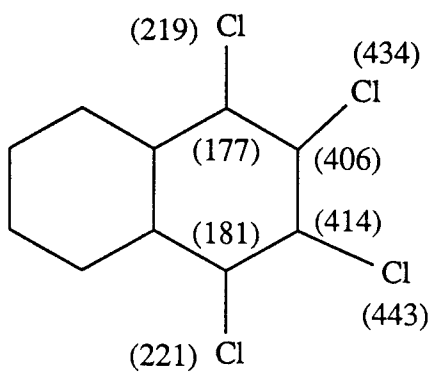

1

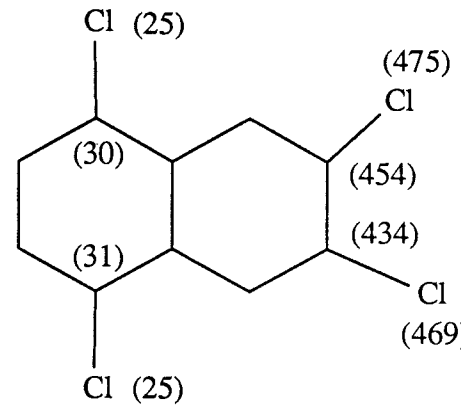

2

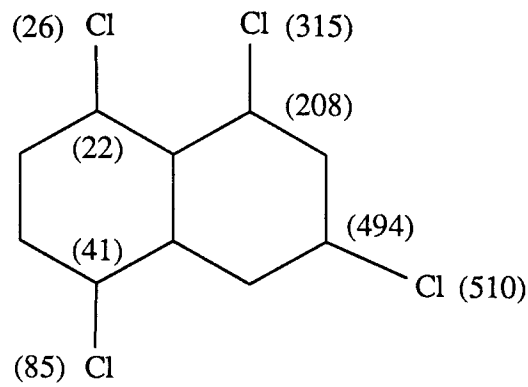

3

It was apparent to us from the plots of quantum yield, the miceller

photochemistry, and the change in regioselectivity observed under electron transfer conditions, that there exists another pathway to product arising from the triplet manifold. The triplet apparently either dechlorinates directly or forms an excimer that then forms dechlorinated products. Since the regiochemistry did not change in the studied region of concentrations, it is inferred that the excimer and triplet dechlorinate with similar regiochemistry. Previous work in our laboratory found very little in the way of solvent effects on the rate of excimer formation; consequently, it can be argued that there exists little charge separation in the excimeric species.[99]

The models used to evaluate the radical anion chemistry (above) could not be used to evaluate the regiochemistry from the triplet manifold, therefore, attempts to model the reaction from a different perspective was employed. AM1 calculations were again used to calculate the energies and molecular orbital coefficients for a triplet excited state species using the keyword "triplet". A similar analysis of the highest semi-occupied molecular orbital (HSOMO) or the lowest semi-occupied molecular orbital (LSOMO) failed to show any correlation with the observed reactivity. Perhaps a correlation with an excited upper vibrational state could be found. Energies of the σ^* triplet TCNs were calculated to be -0.18, -0.25, and -0.17 electron volts for **1**, **2**, and **3**. The calculated energies for the HSOMO for the same compounds were found to be -3.79, -3.84, and -3.84 eVs. Since these are gas phase calculations, it is difficult to address how the upper excited states could participate in the dechlorination process. It is my belief that the computational models are not sophisticated enough to correctly address this problem.

An analysis of the orbital that was identified as the σ^* was conducted

and proved to be quite useful at predicting the site of bond cleavage (Figure II.35). Reasonable agreement is again noted between the observed

Figure II.35 Calculated σ* Coefficients in Triplet Species |x| (10^3) Naphthalene Skeleton Only.

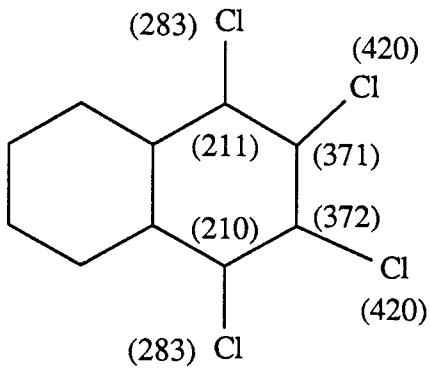

1

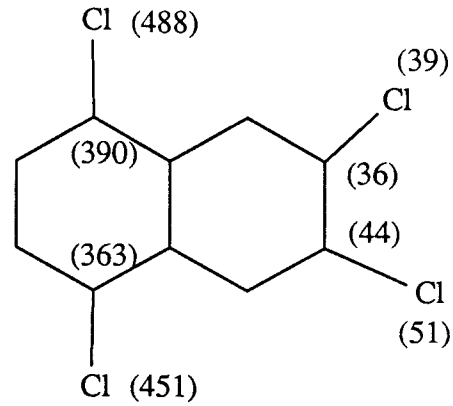

2

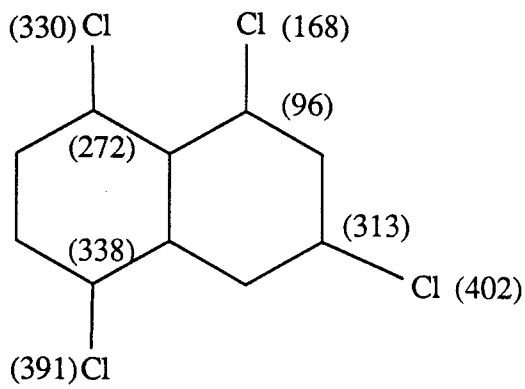

3

regiodechlorination and the coefficients identified in the σ* orbital. The sole dissenter appears to be TCN 3, even though the photolysis of 3 yields all four possible isomers, the loss of chlorine C-8 (peri) was predominate. The Chlorine at C-8 does have a sizeable coefficient but once again an overriding concern is the relief of the steric strain relative to the other regiodechlorination products.

A third model, based upon stabilities of the products, was examined. A homolytic bond cleavage will generate a trichloro naphthyl radical; consequently, energies of trichlornaphthyl radicals were calculated with AM1 (Table II.23). Also, if there is a degree of charge development at the site of bond cleavage prior to homolysis, a model based upon energies of the trichloro anions (sp^2) might reflect the product ratios. The energies of these species are compared the Table II.23.

Table II.23 ΔH_f for Anions ,Radicals, and Trichloro Products Modeled by AM1.

TCN	Anion/Radical	ΔH_f Anion[b]	ΔH_f Radical[b]	ΔH_f[b] Trichloro Product[c]
1234	123 (4)	34.24	84.36	23.55 $\mu = 3.73$
	124 (3)	33.78	85.05	22.97 $\mu = 2.34$
1467	167 (4)	36.52	81.12	20.54 $\mu = 3.39$
	146 (7)	37.64	82.06	20.08 $\mu = 1.37$
1358	358 (1) [a]	37.48	81.12	20.08 $\mu = 1.37$
	135 (8)	38.61	81.00	20.24 $\mu = 1.94$
	138 (5)	40.44	85.26	24.69 $\mu = 2.97$
	158 (3)	44.52	87.36	26.64 $\mu = 1.59$

[a] Renumbering would give 146 TCN. [b] Heat of formation in Kcal/mole.
[c] Trichloronaphthalene heats of formation and dipole moments.

What is obvious is that the energies of the species, inclusive of the radicals, are all very close except for the two trichlornaphthalenes of 1,3,5,8-TCN at the bottom of the column. These two trichloros were rarely observed in dechlorination unless large amounts of starting TCN was consumed. Also, both of these compounds still contain the peri dichloro relationship, thought to be destabilizing. A table of the results from the different reactions accomplished follows.

TABLE II.24 Reaction Summary for 1,2,3,4-Tetrachloronaphthalene.

1234 TCN (1)	REACTION	OBSERVATION 1,2,4- (4) / 1,2,3 - (5)
1	CH_3CN $\xrightarrow{h\upsilon\ 300}$	4.0 / 1.0
2	CTAB / H_2O $\xrightarrow{h\upsilon\ 300}$	4.5 / 1.0
3	CTAB / Et_3N / H_2O $\xrightarrow{h\upsilon\ 300}$	6.5 / 1.0
4	CH_3CN / Et_3N $\xrightarrow{h\upsilon\ 300}$	10 / 1.0
5	p-p'-DTBB $^{\cdot-}$ Li^+ $\xrightarrow{THF}$	3.5 / 1.0
6	elemental K $\xrightarrow{THF}$	3.5 / 1.0
7	Ph_3 Sn H / AIBN $\xrightarrow{70^0}$	3.2 / 1.0

TABLE II.25 Reaction Summary for 1,4,6,7-Tetrachloronaphthalene.

1467 TCN (2)	REACTION	OBSERVATION 1,4,6- (7) / 1,6,7- (6)
1	CH_3CN $\xrightarrow{h\upsilon\ 300}$	1.0 / 4.0
2	CTAB / H_2O $\xrightarrow{h\upsilon\ 300}$	1 .0/ 3.5
3	Na BH_4 CH_3CN / H_2O $\xrightarrow{h\upsilon\ 300}$	2.3 / 1.0
4	CTAB / Et_3N / H_2O $\xrightarrow{h\upsilon\ 300}$	12 / 1.0
5	CH_3CN / Et_3N $\xrightarrow{h\upsilon\ 300}$	50 / 1.0
6	p-p'-DTBB $^{\cdot-}$ Li^+ $\xrightarrow{THF}$	4.0 / 1.0
7	elemental K $\xrightarrow{THF}$	3.5 / 1.0
8	Ph_3SnH / AIBN $\xrightarrow{70^0}$	3.0 / 1.0

TABLE II.26 Reaction Summary for 1,3,5,8-Tetrachloronaphthalene.

1358 TCN (3)	REACTION	OBSERVATION 1,4,6- (7) / 1,3,5- (8)
1 CH_3CN	$\xrightarrow{h\upsilon\ 300}$	1.0 / 2.5
2 CTAB / H_2O	$\xrightarrow{h\upsilon\ 300}$	1.0 / 1.7
3 Na BH_4 CH_3CN / H_2O	$\xrightarrow{h\upsilon\ 300}$	2.3 / 1.0
4 CTAB / Et_3N / H_2O	$\xrightarrow{h\upsilon\ 300}$	4.0 / 1.0
5 CH_3CN / Et_3N	$\xrightarrow{h\upsilon\ 300}$	25 / 1.0
6 p-p'-DTBB $^{\cdot-}$ Li^+	$\xrightarrow{THF}$	4.0 / 1.0
7 elemental K	$\xrightarrow{THF}$	3.5 / 1.0
8 Ph_3SnH / AIBN	$\xrightarrow{70^0}$	1.0 / 1.8

Conclusion

Examination of the plots of inverse quantum yield for direct photolysis in the absence of an electron donor against inverse starting material concentration reveals two slopes. This is indicative of two mechanisms which are operative in the photodehalogenation process. Photodehalogenation occurs directly from the triplet spin state or by formation of a triplet excimer which then can dehalogenate. The regiochemistry of these two competing pathways do not differ significantly in these studies. In the case of photodechlorination induced by an electron donor, exciplex formation rates calculated from a standpoint of a triplet process yield rates that seem to be unreasonably slow while the rates associated with a singlet exciplex appear to be in agreement with reported analogous photochemical processes. Interestingly, the exciplex formed between

starting materials and triethylamine demonstrates a dramatic inversion of regiodechlorination for compounds 2 and 3 while compound 1 shows an increase in selective dechlorination. Also noted is the increase in efficiency of dechlorination. The inversion and enhancement of regioselectivity of major product was rationalized by I_π repulsion theory. The sodium borohydride reductions proved to be intermediate in the regiodechlorination. This intermediacy was rationalized in Scheme II.4 where the radical anion can either diffuse apart to form solvent separated species or remain as an ion pair. It is believed that the two species yield different product ratios. Previous studies have shown that in-cage hydrogen transfer is a major contributor to reaction products.

The results of non-photochemical dehalogenation strongly suggest that an electron transfer to form a charge-transfer complex is responsible for photodechlorination in the presence of triethylamine and sodium borohydride. The nature of the intermediate may be inferred from the regiochemistry of dechlorination. In addition, the regiochemistry observed in the triphenyltinhydride reactions, sodium borohydride photolysis, triethylamine photolysis, and potassium reductions can be rationalized by radical anion and counter ion/radical species formation. The solvent separated and caged-type reactivities are very different. Other factors such as thermodynamics, energies of products, and strain relief of peri interactions may be playing a role in product determination. The almost exclusive formation of a single trichloro isomer in the photolysis of starting TCNs in the presence of triethylamine offers great promise. The fact that regiochemistry can be controlled and predicted suggests to us a possible route to handling and detoxifying other similar chlorinated

aromatic hydrocarbons. The extension of this work to more complicted systems such as the homoaromatic analog to 2,3,7,8-TCDD, 2,3,7,8-tetrachloroanthracene will prove very interesting.

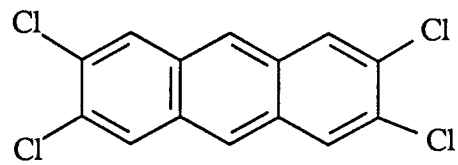

2,3,7,8-tetrachloroanthracene

Chapter III. Structure and Electronic Effects in Some Selected Carbenes

Introduction

Carbene is a term used to describe one of four general classes of carbon centered intermediates. A carbene is a carbon atom intermediate that has only two substituents and thus is divalent. In contrast, carbocations, carbanions and radicals are all trivalent (three substituents) carbon intermediates. Carbocations (**11**) are carbon atoms that possesses no non-bonding valence electrons and bear a formal charge of plus one. Carbanions (**12**) are carbon atoms possessing two non-bonding valence electrons and, therefore, a formal charge of negative one. Radicals at a carbon center (**13**) are again trivalent and possess a single non-bonding valence electron and, therefore, have no formal charge. The divalent carbene (**14**) possesses two non-bonding electrons, but is only divalent, and therefore has no formal charge.

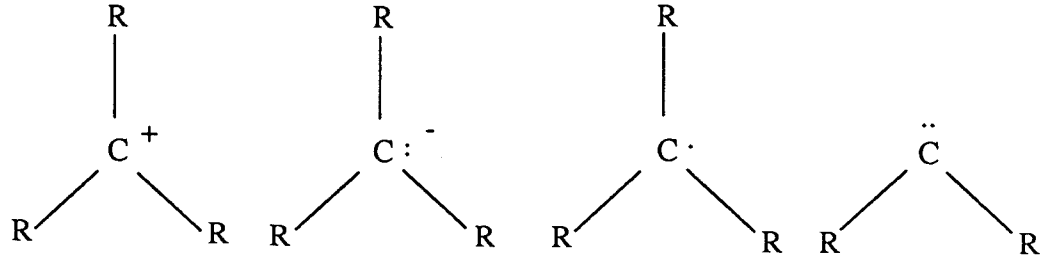

11 **12** **13** **14**

Singlet and triplet are two terms used to describe the spin states assigned to divalent carbon intermediates. If one electron is present in each of the two low lying empty molecular orbitals and the electrons have parallel spins, the spin quantum number s = 1. If the electrons occupy the same orbital they will

have opposite spin and a total spin quantum number s = 0. Multiplicity is defined as 2s + 1, therefore, carbenes will have multiplicities equal to three and one for triplet and singlet spin state carbenes, respectively.[101,102]

The singlet carbene has an empty p-orbital and is considered to be electron deficient. The hybridization at the carbon of a singlet carbene is generally considered to be sp^2. Herzberg has determined the singlet methylene (**15**) H-C-H bond angle to be 102.4 °.[103] Triplet carbenes (**16**) are considered to be diradicals. The mechanisms of many triplet carbene reactions involve the formation of free radicals.[102] The hybridization at the triplet carbene carbon has more s character and in some cases is nearly sp hybridized. Wasserman and co-workers used electron spin resonance (esr) spectroscopy to determine the central H-C-H bond angle of triplet methylene to be 136 °.[104]

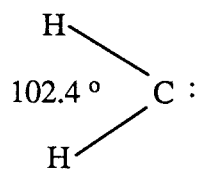

15

Singlet

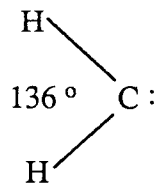

16

Triplet

Historical Background

Divalent carbon is thought to have first been suggested by Geuther in 1862. Guether suggested that the dihalocarbene could be an intermediate in the reaction between chloroform and alkali.[105] In 1897 Nef also suggested that a divalent carbon atom was an intermediate responsible for many reactions.[106] In

1950, Hine provided experimental evidence that dihalocarbene is indeed an intermediate in the basic hydrolysis of haloform.[107] Hine proposed the mechanism depicted in Scheme III.1 for the observed reaction.

Scheme III.1

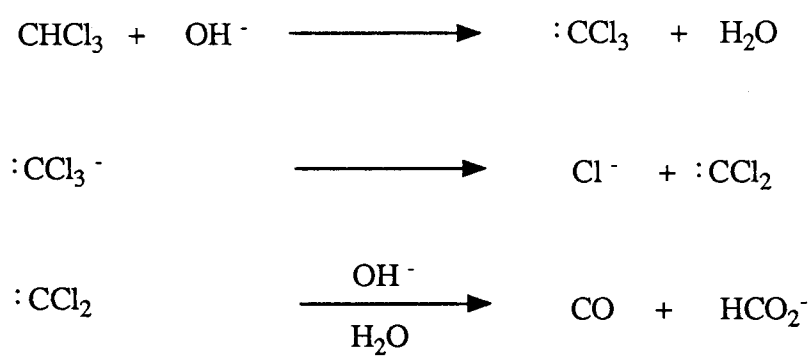

Doering and Hoffman followed the Hine postulate to devise a non-aqueous system that could be employed in synthesis.[108] Employing base and haloform they were able to generate CCl_2 and CBr_2 under conditions designed to enhance addition to alkenes and thus making 1,1-dihalocyclopropanes. Skell and co-workers postulated that the two varieties of carbene, singlet and triplet, should be recognizable by their chemical properties.[109-111] Spin conservation requires that the addition of a triplet carbene to an alkene must produce a triplet state 1,3-diradical intermediate. The intermediate may live long enough to lose the stereochemical integrity of the alkene (E or Z) in proceeding to the cyclopropane. The resulting addition is then considered to be non-stereospecific (Equation III.2). The singlet carbene does not have the same spin conservation requirements as the triplet. The singlet may use the two electrons of the carbene carbon to simultaneously make two bonds to the

alkene. The singlet carbene double bond addition is then considered to be stereospecific (Equation III.1). Singlet carbenes are also known to insert into C-H bonds.

Equation III.1

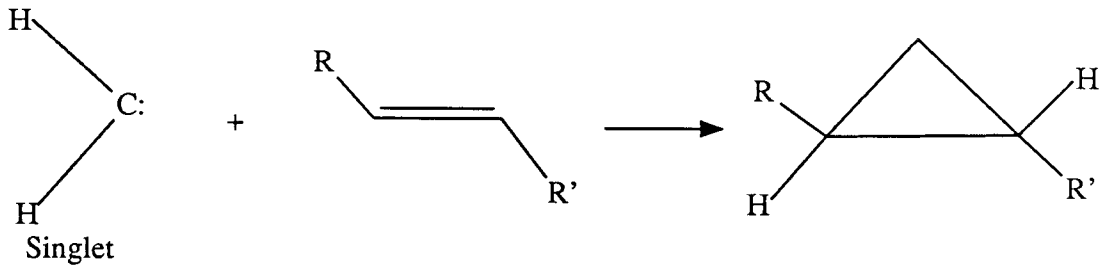

Equation III.2

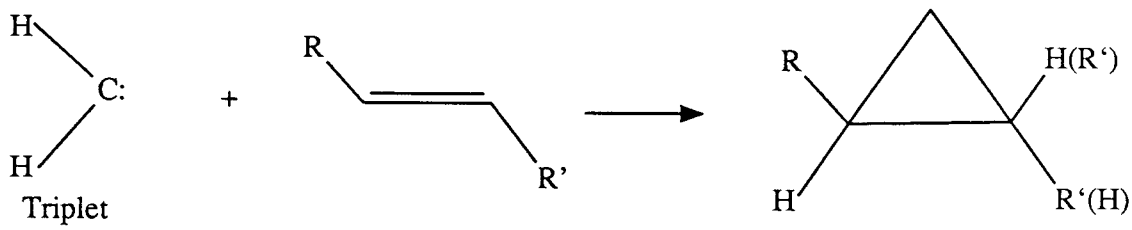

A logical choice for a precursor for the carbene is the corresponding diazo compound. Pyrolysis or photolysis of the diazo compound will release molecular nitrogen and provide a driving force for carbene formation (Equation III.3).

Equation III.3

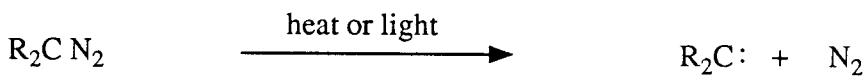

A result of this is that most diazo compounds decompose at room temperature and are, consequently, difficult to handle. With the exception of aromatic diazo compounds, cyclopropyldiazomethane, and dicyclopropyldiazomethane, most diazo compounds have not been isolated. [112,113]

Alkyl- and Dialkylcarbenes

Precursors for alkyl- and dialkylcarbenes can be prepared from the corresponding p-toluene-sulfonylhydrazone (tosylhydrazone). Bamford and Stevens allowed nineteen different tosylhdrazones to react with base in ethylene glycol to form reaction products.[114] Diazo compounds were isolated for all of the arene-substituted tosylhydrazones. It was, therefore, assumed that diazo compounds were intermediates in the decomposition of all tosylhydrazone salts.

It was shown that the rate determining step in the Bamford-Stevens decomposition of tosylhydrazone salts is the unimolecular elimination of the p-toluenesulfinate anion. Decomposition will result in a secondary aliphatic or aromatic diazocompound.[115] If decomposed in aprotic media, the diazo compound will release molecular nitrogen and the corresponding carbene. The carbene will then go on to products (Scheme III.2). Decomposition in protic media was shown to go through a carbocation intermediate.

Intramolecular insertion reactions are known to be typical for carbenes. Alkyl- and dialkylcarbenes are known to have a preference for insertion into the β or γ carbon hydrogen bond.[116] The insertion in the β C-H bond is known as a 1,2-hydride shift and leads to alkenes. Insertion into the γ C-H bond will yield cyclopropane derivatives (Scheme III.3).

Scheme III.2

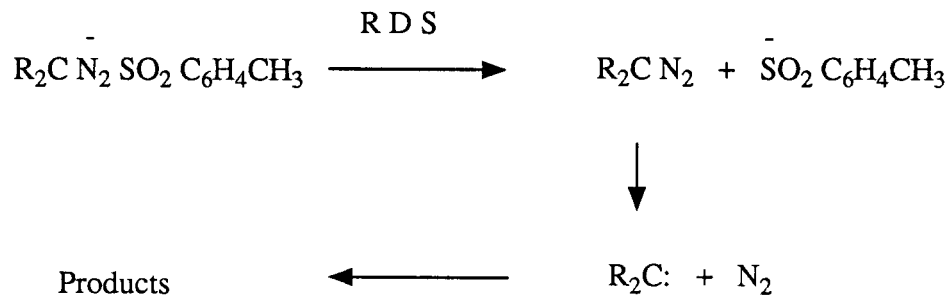

Scheme III.3

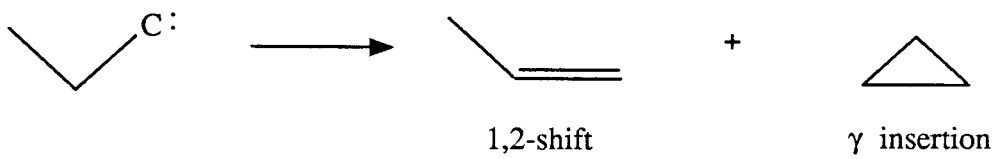

Friedman and Shechter investigated the chemistry of cyclopropylcarbenes by allowing the tosylhydrazones of cyclopropylcarboxaldehyde and cyclopropyl methyl ketone to decompose in the presence of sodium methoxide in diethyl carbitol.[117] Decomposition of the cyclopropylcarboxaldehyde tosylhydrazone to generate cyclopropylcarbene failed to demonstrate normal C-H insertion. C-H insertion would result in the products methylenecyclopropane and bicyclobutane. The products observed were ring expansion to cyclobutene, as the major product, and fragmentation to ethylene and acetylene, as the minor path products (Scheme III.4).[117]

The decomposition of cyclopropyl methyl ketone tosylhydrazone to the carbene gave predominately the ring expanded product 1-methylcyclobutene. Less than 1% vinyl cyclopropane could be isolated. The decomposition of the tosylhydrazones of cyclobutanone and cyclopentanone have also been investigated. The carbene related to cyclobutanone undergoes ring contraction to

Scheme III.4

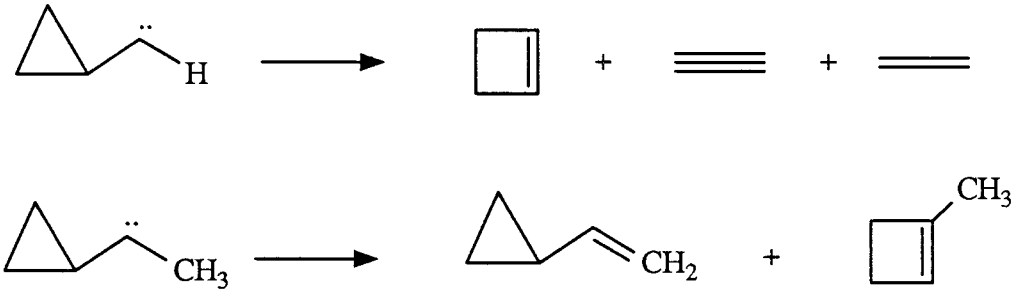

form methylenecyclopropane as the major product (80%) and a 1,2-hydride shift to form cyclobutene. The carbene related to cyclopentanone demonstrates the 1,2-hydride shift to form cyclopentene as the only major product.[117]

In an effort to evaluate the stereoelectronic effects in hydride migration, the carbenes of monodeuterated cyclohexanone tosylhydrazones were decomposed (Scheme III.5).

Scheme III.5

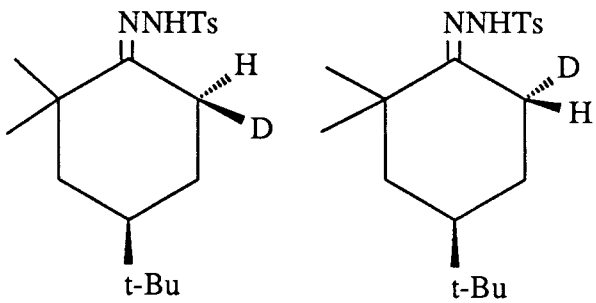

17 **18**

Kyba decomposed tosylhydrazones of **17** and **18**. Axial hydrogen migration / equatorial hydrogen migration was shown to be 1.5. However, the author was able to show that the carbene was flexible enough to achieve alignment from either axial or equatorial hydrogen with the empty p-orbital.[118] Analysis was accomplished through interpretation of MNDO and MINDO/3

calculations of geometric isomers of carbenes derived from **17** and **18**.

Substituent Effects

Substituents present on the divalent carbon in a carbene are known to have a profound effect upon the relative energy levels of singlet and triplet spin states. Mueller and co-workers offered explanations of the observed substituent effects on singlet-triplet energy gaps. Singlet carbenes are stabilized by a substituent with a low lying π orbital able to donate electron density to the vacant p-orbital of the carbene.[119] If the triplet carbene is adjacent to a π donor there is little stabilization from the filled π orbital. However, stabilization may occur when an empty π^* orbital interacts with the one of the singly occupied triplet carbene orbitals.

It has also been shown that the nature of the substituent on the divalent carbene carbon affects the nucleophilic or electrophilic character of the carbene.[120] Incorporation of a vacant p-orbital of a singlet carbene into a π system such that it becomes an integral part of that system has been shown to decrease the electrophilic and increase the nucleophilic nature of the singlet carbene carbon. This is thought to be a result of the added electron density of the π system which now includes the carbene carbon and the vacant p-orbital. If the carbene MOs and the π system MOs could be considered separate, this interaction would be viewed as LUMO-HOMO and net stabilization would result. The same interaction in a triplet carbene would be a SOMO-HOMO interaction and only a small amount of stabilization could result.

Jones and Ennis allowed the tosylhydrazone of tropone to decompose to

form the corresponding carbene (**19**). The only isolated product was shown to be the dimer heptafulvene (**20**) (Equation III.4).[120] There is some debate about

Equation III.4

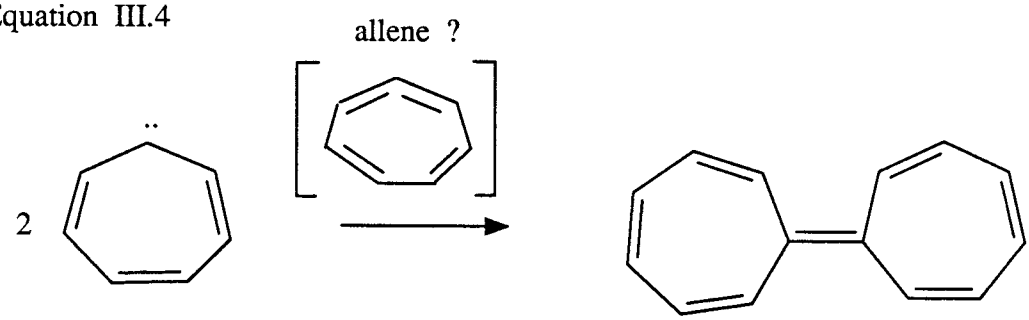

19 **20**

the structure of carbene **19**. The recent work of Waali and coworkers shows that the allene may be a contributor to the structural profile of carbene **19**.[120b] Tropone carbene does not demonstrate a typical reaction with electron rich alkenes. It does, however, undergo addition reactions with electron poor alkenes such as fumaronitrile and maleonitrile. The addition was shown to be stereospecific (singlet). The authors conclude that the carbene is of low electrophilicity (nucleophilic). Dimethoxycarbene has been shown to be nucleophilic as well. This is attributed to the electron donation of the two methoxy substituents. Resonance forms can be drawn to illustrate the donating character of the hetero atoms (Equation III.5).

Equation III.5

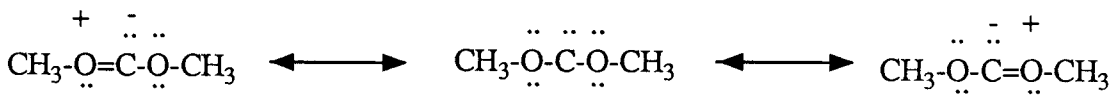

Seyferth and co-workers used a Hammett study to demonstrate the electrophilic character of dichlorocarbene.[121] Dichlorocarbene generated from

$PhHgCCl_2Br$ was allowed to react with a series of para substituted styrenes. The rho value was shown to -0.619 $\pm$ 0.005 which is indicative of a positive charge development on the styrene α-carbon in the transition state.

The structure and electronic interplay of cyclopropane with cyclopropane substituted derivatives have excited chemists for many years. The Walsh model for cyclopropane is envisioned by building the three membered ring from three sp^2-hybridized CH_2's, with the orbitals oriented toward the center of the ring and the three p-orbitals co-planar. If attached to a π system, the cyclopropyl unit

Figure III.1 Walsh Model for Cyclopropane.

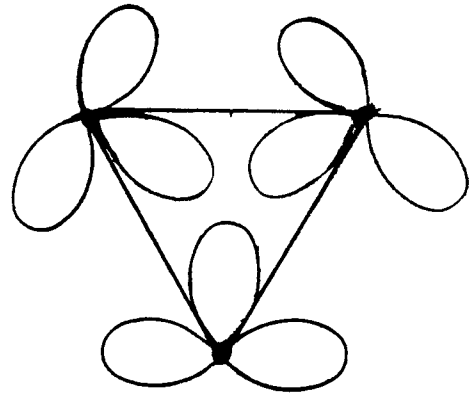

is known to be a good π-electron donor.[122] Because of the π-symmetry associated with the cyclopropyl HOMO, interaction with the adjacent π system is maximized when the orbitals are co-planar. This is normally referred to as a bisected conformation. In the perpendicular conformer the HOMO of the cyclopropyl group is orthogonal to the π-system and the interaction is minimal.[123] For the bisected conformation, the interaction of the cyclopropyl group and a π system is manifested in the reported bond lengthening of the vicinal (C_1-C_2, C_1-C_3) bonds and the shortening of the distal (C_2-C_3) bond.[122] This is attributed to the donation of electron density the cyclopropyl HOMO to

Figure III.2 Orbital Interactions in the Cyclopropylcarbinyl System.

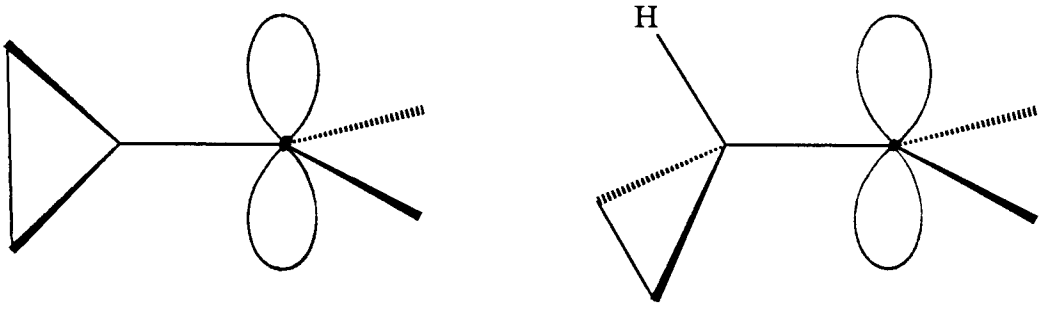

bisected conformation perpendicular conformation

the π system. The result is a decrease in bonding character between C_1-C_2, and C_1-C_3 and a decrease in the antibonding character at the C_2-C_3 bond. In the perpendicular conformation, the cyclopropyl group can act as a π-acceptor. Donation of electron density to the LUMO of the cyclopropyl unit (perpendicular) should result in a lengthening of the vicinal bonds and a shortening of the distal bond. Stabilization is expected to be important only with potent π-donors.[124]

Carbenes are also known to rearrange prior to reaction. Carbene to carbene rearrangements are encountered far less frequently than the analogous carbocation to carbocation or radical to radical rearrangements. Three examples of carbene to carbene rearrangements are the well known phenylcarbene to phenylcarbene (Equation III.6), ketocarbene to ketocarbene (Equation III.7), and the very likely ethynylcarbene to carbene rearrangements (Equation III.8).[125-127]

Equation III.6

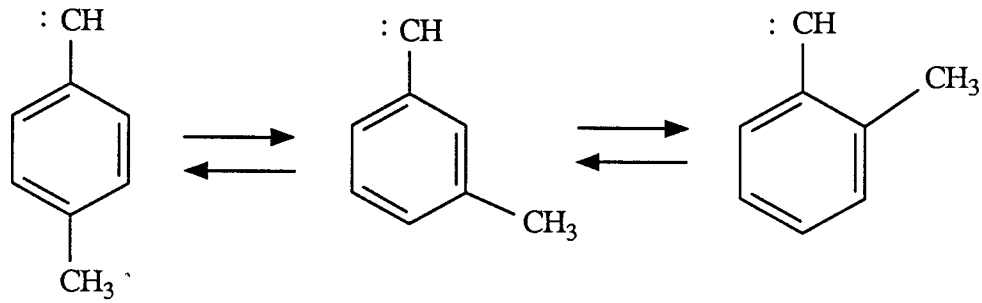

Equation III.7

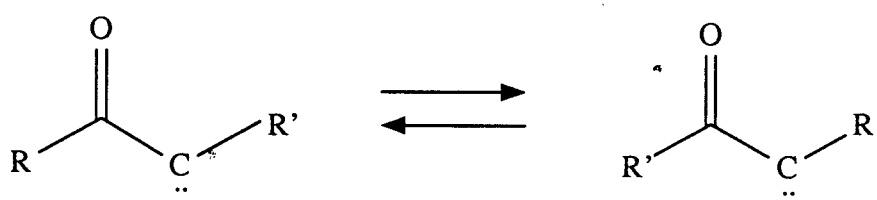

Equation III.8

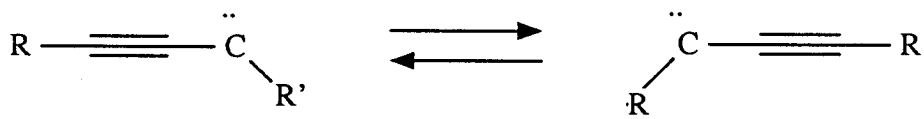

Freeman and Swenson also proposed the carbene to carbene rearrangements for the potentially homoaromatic carbenes **22** and **24** (Equations III.9,10).[128]

Equation III.9

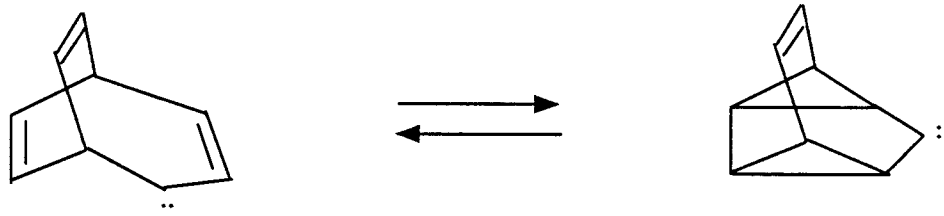

22 **23**

Equation III.10

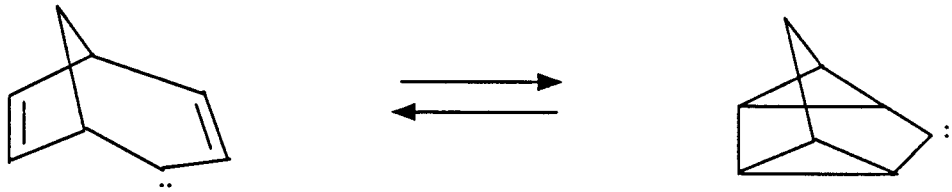

24 **25**

Chapter IV. Results and Discussion of Carbena Reactivity

In this project we have examined the interplay of a carbene center with the cyclopropyl group, conjugation of a carbene center with π systems, and interaction of a carbene center with a remote alkyne group.

Cyclopropane

The effect of cyclopropyl group on the thermodynamics of carbene generation has not been extensively investigated. However, the effect of the cyclopropyl group on the stabilities of carbocations and free-radicals has been well studied.[129,130] The stability of carbocations is greatly influenced by its substituents. The cyclopropane substituent has a greater stabilizing effect than many other alkyl groups.[129b] Both vinyl groups and phenyl groups do not provide as much stability to neighboring cations as does cyclopropane.[130] Roberts *et al.* reported that the rate constant for the solvolysis of cyclopropylcarbinyl chloride in 50% aqueous ethanol at 50°C is 27 times that of β-methylallyl chloride and 40 times that cyclobutyl choride.[126b] This would seem unusual since cyclobutyl chloride is a secondary chloride and cyclopropylcarbinyl chloride is a primary chloride. Roberts proposed a bicyclobutonium cation (Figure IV.1) as the key reactive intermediate (first-formed ion upon solvolysis) but was refuted later by Schleyer and Van Dine.[131]

Schleyer and Van Dine carried out the solvolysis of cyclopropylcarbinyl 3,5-dinitrobenzoates **26**, **27**, **28**. All three compounds demonstrated

Figure IV.1 Bicyclobutonium Cation Orbital Diagram.

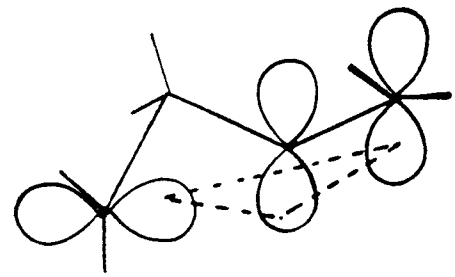

approximately the same rates of solvolysis. The result is not supportive of a bicyclobutonium cation because the positive charge can not be delocalized to all ring carbons. Then if the bicylobutonium ion is a reactive intermediate, the rate of solvolysis of **26** would be greater than that of **27** or **28**.

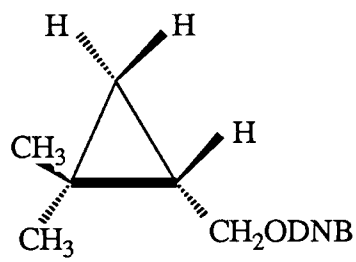

26

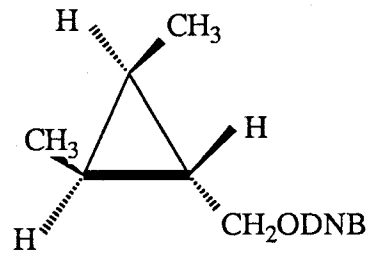

27

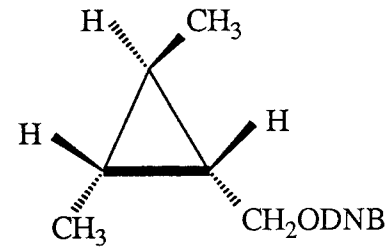

28

It is now generally accepted that the solvolysis will lead to the bisected cyclopropylcarbinyl cation at room temperature, but the debate about the existance of the bicylobutonium ion is far from over. Ab initio calculations performed on the cyclopropylcarbinyl system finds energy minima for the bisected cyclopropylcarbinyl cation and the bicyclobutonium cation are only 0.5 kcal apart.[132] Additional evidence for the possible existence of the bicyclobutonium ion is found in NMR studies done in superacid media.[133] Low temperature NMR studies (up to -132 ^{0}C) indicate that a stable structure of the ion is a set of rapidly equilibrating bicyclobutonium ions, however, additional

resonances appear at higher temperatures. The additional resonances are thought to arise from the bisected cyclopropylcarbinyl cation.[133] The cyclopropylcarbinyl cation would have an orbital diagram as represented in Figure IV.2. The stabilizing effect of the cyclopropyl group is nicely

Figure IV.2 Cyclopropylcarbinyl Cation Orbital Diagram.

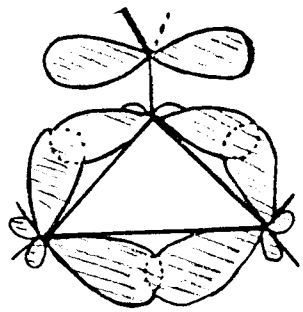

illustrated in a study by Hart and co-workers.[129,134] A series of triisopropylcarbinyl through tricyclopropylcarbinyl *p*-nitrobenzoate (benzoate) esters were allowed to solvolize. Solvolysis rate enhancements are listed (**29**-**32**). Cyclopropane is also effective at stabilizing free-radical intermediates.

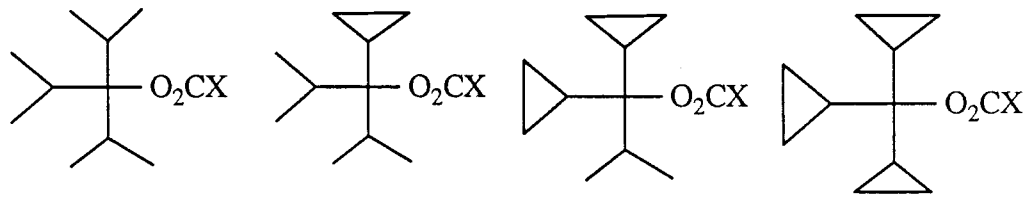

	29	**30**	**31**	**32**
X = $C_6H_4pNO_2$				
k_{rel}	1	246	23500	
X = Ph				
k_{rel}			1	1080

In a similar study to the work of Hart co-workers on carbocations, Martin and

Timberlake measured the rates of decomposition of dialkyl azo substrates 33-36 and observed an increase in decomposition rate with each cyclopropane substituent.[135]

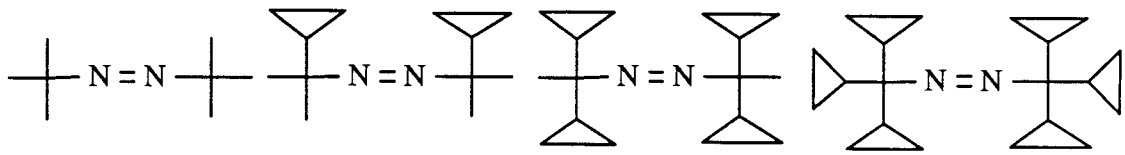

	33	34	35	36
k_{rel}	1	26.8	362	2540

Based upon the carbocation and radical stabilities with cyclopropane substituents, we felt an investigation of cyclopropyl substituted carbenes might help characterize the nature of structure reactivity relationships. The goal of this portion of the study was to evaluate the effect of cyclopropyl in carbene intermediates attached directly to a carbene carbon. We were curious to see what interplay these units would have on the activation parameters for carbene generation from the hydrazone salt. Similar to the studies of Hart and co-workers, isopropyl and cyclopropyl units are the two substituents alpha to the carbene carbon used in this work. Therefore, the carbenes studied were diisopropyl- 37, isopropylcyclopropyl- 38, and dicyclopropylcarbene 39. The potassium salts of the ketone tosylhydrazones (37c, 38c, and 39c) were previously prepared and decomposed in our laboratory by Wuerch. The evolution of nitrogen gas over time was followed. Employment of the program PCNONLIN was used to calculate k_1 and k_2 in the two step decomposition (Scheme IV.1). DMSO was the solvent of choice due to the solubility problems

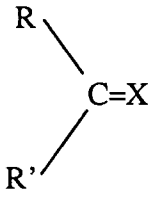

37

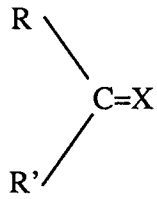

38

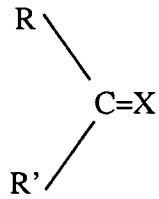

39

37 : R = R' = isopropyl

38 : R = isopropyl, R' = cyclopropyl

39 : R = R' = cyclopropyl

37, **38**, **39** : X = Carbene (:)

a : X = O

b : X = NNHTs

c : X = $NNTs^- K^+$

Scheme IV.1

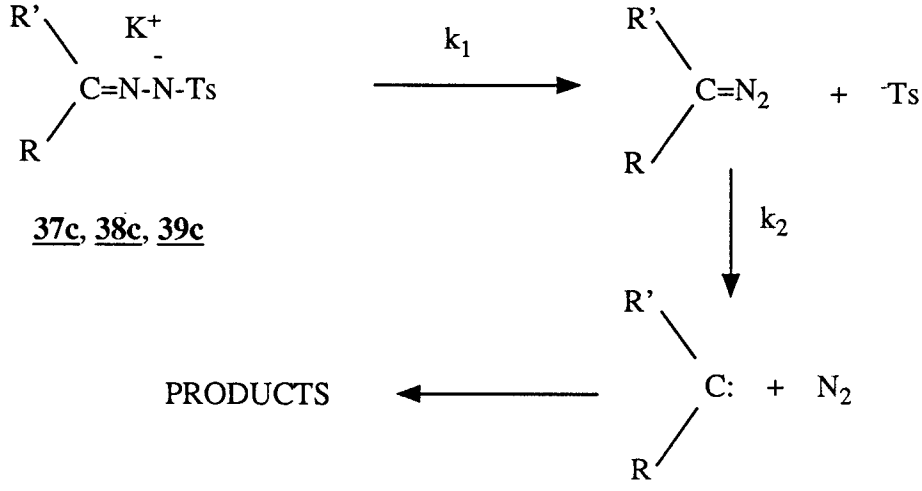

37c, **38c**, **39c**

37, **38**, **39**

associated with the potassium salts of the tosylhydrazones. Wuerch found that a better curve fit could be achieved with a faster first step (k_1) so benzenesulfonylhydrazones were employed rather than tosylhydrazones.

Results and Discussion

The benzenesulfonylhydrazones utilized in this portion of the research are diisopropyl ketone benzenesulfonylhydrazone **40**, cyclopropylisopropyl ketone benzenesulfonylhydrazone **41**, and dicyclopropyl benzenesulfonylhydrazone **42**. These benzenesulfonylhydrazones were prepared by treatment of the corresponding ketones **37a**, **38a**, and **39a** with benzenesulfonylhydrazide in refluxing ethanol (Equation IV.1).

Equation IV.1

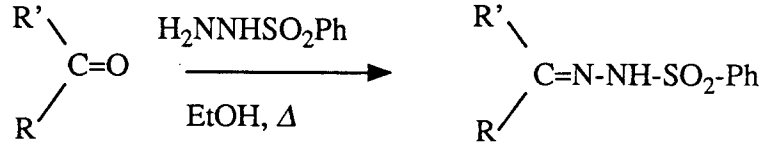

37a, 38a, 39a **40, 41, 42**

The benzenesulfonylhydrazones **40**, **41**, and **42** were treated with potassium hydride in dry THF to generate the potassium salts **43**, **44**, and **45** as shown in Equation IV.2. Each benzenesulfonylhydrazone potassium salt was allowed to decompose in dry DMSO. The proposed mechanism for carbene formation in each system was given in Scheme IV.1. The decomposition temperatures ranged from 110-130 °C.

The isolated carbene products from the decomposition of isopropylcyclopropylcarbene serve to illustrate the reported products of decomposition. Wuerch reported the formation of 1-cyclopropyl-2-methylpropene

Equation IV.2

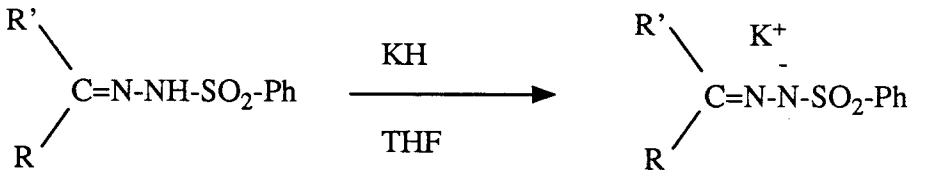

40, **41**, **42** **43**, **44**, **45**

40, **43** : R = R' = isopropyl

41, **44** : R = isopropyl, R' = cyclopropyl

42, **45** : R' = R = cyclopropyl

(**46**), cyclopropyl to cyclobutene ring expansion (**47**), and oxidation to the ketone, as was observed by Oda, to form the corresponding ketone, isopropylcyclopropyl ketone (Scheme IV.2).[136] γ-insertion was not observed in

Scheme IV.2

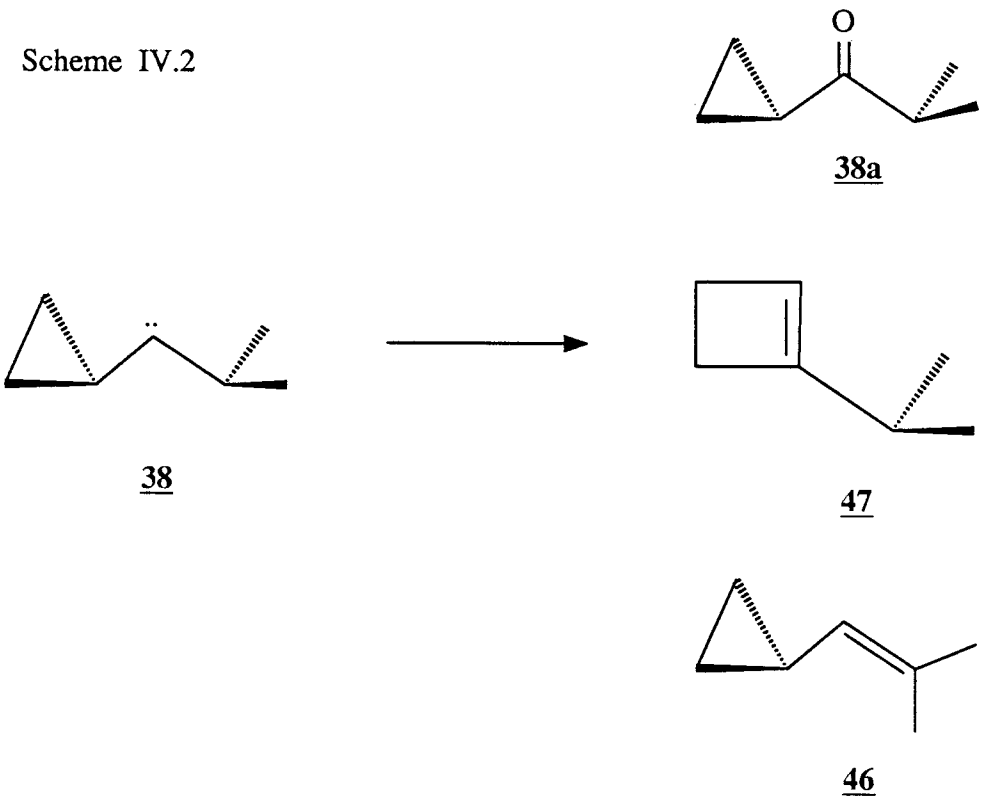

38a

38 **47**

46

any of the three decompositions. Diisopropylcarbene did not show any γ-insertion while isopropylcarbene does exhibit γ-insertion; this seems in contrast to the reported results of Wuerch. The lack of γ-insertion is explained in terms of a more rapid hydride migration leading to the trialkylated alkene (2,4-dimethyl-2-pentene), rather than the disubstituted terminal alkene, isobutylene. Isopropylcyclopropyl carbene also failed to demonstrate any γ-insertion, instead only hydride migration occurs to form 1-cyclopropyl-2-methylpropene (**46**). None of the methylenecyclopropane derivative was observed due to the strained system being formed. The results of the two cyclopropane carbene derivatives are consistent with the findings of Friedman and Shechter,[117] who observed that cyclopropylmethylcarbene preferred ring expansion to methylcyclobutene and hydride migration to vinylcyclopropane rather than the formation of the strained methylenecyclopropane derivative. Békhazi *et al.* observed that dicyclopropylcarbene undergoes primarily ring expansion in benzene or chlorine atom abstraction in carbon tetrachloride.[137] These processes are all consistent with singlet reactivity.[138] There was no evidence for the triplet state hydrogen atom abstraction similar to those found for our later work on 4,4-diphenylcyclohexanylidene and related carbenes.[139]

Kinetics and Activation Parameters

The potassium salts **43**, **44**, and **45** were allowed to decompose in dry DMSO. In each thermolysis a known amount of potassium salt was transferred to a preheated flask containing 30 mL of dry DMSO and N,N-dimethylaniline as an internal standard at the desired temperature. A small amount of solution

was removed at timed intervals and quenched with 1 mL of glacial acetic acid. The samples were cooled in an ice bath prior to analysis. The loss of starting material was plotted over the course of time. The first step of the decomposition of the benezenesulfonyl hydazones (k_1) is a unimolecular decay and consequently is a first-order process. The values obtained for the slopes of the plots give experimental values of k_1 for the thermal decomposition of diisopropyl- and dicyclopropyl- benzenesulfonylhydrazone potassium salts. The values are reported in the tables. The results are in excellent agreement with those calculated by Wuerch.[140]

The thermolyses of the potassium salt of diisopropylbenezensulfonyl hydrazones were carried out 110, 115, 120, 125, 130 °C. The potassium salt of dicyclopropylbenzenesulfonyl hydrazone was decomposed at 130 °C. The potassium salt of isopropylcyclopropylbenzenesulfonyl hydrazone was decomposed at 110 and 130 °C. Each decomposition was run in triplicate to ensure a reasonable data base.

Table IV.1 Calculated Values for Rate Constants.
Diisopropylbenzenesulfonylhydrazone K^+ Salt.

Temp. (°C)	$k_1 \times 10^3\ s^{-1}$
110	0.95 ± 0.01
115	1.53 ± 0.03
120	2.03 ± 0.23
125	3.89 ± 0.13
130	4.09 ± 0.45

Table IV.2 Calculated Values for Rate Constants.
Isopropylcyclopropylbenzenesulfonylhydrazone K^+ Salt[a].

Temp. (°C)	$k_1 \times 10^3\ s^{-1}$	
110	1.20 ± 0.06	1.24 ± 0.12[b]
115	1.78 ± 0.02	
120	2.90 ± 0.04	
125	4.23 ± 0.05	
130	6.13 ± 0.19	6.26 ± 0.35[b]

[a] Wuerch reported results. [b] Results obtained in the present study.

Table IV.3 Calculated Values for Rate Constants.
Dicyclopropylbenzenesulfonylhydrazone K^+ Salt[a].

Temp. (°C)	$k_1 \times 10^3\ s^{-1}$
110	0.578
115	0.699
120	1.52 ± 0.0
125	2.17
130	3.03, 1.94 ± 0.03[b]

[a] Wuerch reported results. [b] Results of the present study.

Table IV.4 Summary of Activation Parameters (k_1) for Decomposition of Hydrazone Salts.

Hydrazone salt (K^+)	E_a (kcal/mol)	$\Delta H^{\neq}$ (kcal/mol)	$\Delta S^{\neq}$ (cal/mol•K)	$\Delta G^{\neq}$ (kcal/mol)
Diisopropyl	28.9 ± 1.4 (27.5 ± 1.2)[a]	28.1 ± 1.4 (26.7 ± 1.2)	0.0 ± 3.6 (3.3 ± 3.1)	28.1 ± 2.0 (28.5 ± 2.5)
isopropylcyclopropyl	25.2 ± 0.6	24.5 ± 0.6	-8.6 ± 1.5	24.7 ± 0.8
dicyclopropyl	27.2 ± 2.9	26.4 ± 2.9	-4.9 ± 7.3	28.3 ± 4.0

[a] Results obtained in the present study are in parenthesis.

All the calculated values demonstrate only a small deviation within each series of compounds. This implies that there is little perturbation of the systems by the substituents on the diazo carbon in the starting potassium salts. The activation energies of interest in this study proved to arise from the second step in the two step decomposition of the salts of the studied hydrazones; diazo to carbene formation (Equation IV.3).

The activation energy derived from k_2 is a measure of the stability of the carbene that is produced relative to the diazo intermediate. The activation energy derived from k_1 is a measure of the stability of the diazo intermediate relative to the hydrazone salt. Values obtained for E_a from k_1 varied only a small amount in each of the reported decompositions. The small variance in E_a indicates that energy profiles for these reactions are nearly identical and insensitive to substituent changes. The other activation parameters calculated are the free energy of activation ($\Delta G^{\neq}$), the enthalpy of activation ($\Delta H^{\neq}$), and the

Equation IV.3

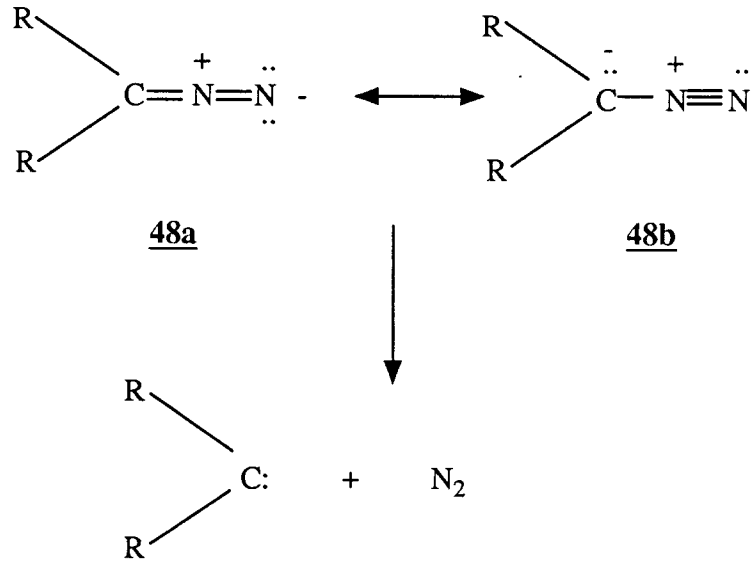

48a **48b**

entropy of activation ($\Delta S^{\neq}$). These values were calculated from the change in energy between the two states in question. In looking at Table IV.4 it is readily noted that there is essentially no difference in the values calculated for all compounds. The results also support the observation that the first step appears to be insensitive to structural change at positions alpha to the carbene carbon.

Most notable when examining Table IV.5 is the values for $\Delta S^{\neq}$ go from positive 28.4 to -30.9 for the series of dicyclopropylcarbene to diisopropylcarbene. The negative entropies are not expected in a dissociation reaction since the transition state in such a reaction would tend toward greater disorder than the ground state diazo compound (unimolecular decomposition). The decreasing entropy terms are thought to arise from the change in dipole moments between comparative states. The AM1 calculations supported this rationale demonstrating changes in dipole moments from diazo to carbene

Table IV.5 Summary of Activation Parameters (k_2).[140]

Diazo compound to carbene (below)	E_a (Kcal/mol)	$\Delta H^{\neq}$ (Kcal/mol)	$\Delta S^{\neq}$ (cal/mol•K)	$\Delta G^{\neq}$ (Kcal/mol)
Diisopropyl	16.4 ± 1.1	15.6 ± 1.1	-30.9 ± 2.8	27.7 ± 1.6
isopropylcyclopropyl	28.5 ± 2.0	27.7 ± 2.0	3.3 ± 5.1	26.4 ± 2.8
dicyclopropyl	37.6 ± 1.8	36.8 ± 1.8	28.4 ± 4.6	25.6 ± 2.5

emulated species. Wuerch argued that the dicyclopropylcarbene generation is entropy controlled. It is argued that the high rate of reaction for formation of dicyclopropylcarbene is due to the large positive value for the corresponding entropy of activation. However, it seems reasonable to view the entropy controlled reaction in a similar way to the 4,4-diphenylcyclohexylidene series;[139] that is, a positive entropy change is indicative of a decreasing dipole moment and negative entropy change is indicative of an increasing dipole moment. AM1 calculated values can be interpreted to follow this observation.

AM1 calculations of the diazo and carbene species (Table IV.6) demonstrate a trend that is in agreement with the dipole moment argument. The observed trends in the dipole moments are consistent with a dipole moment rationale for the trend in the entropies of activation. The diisopropylcarbene generation demonstrated a decrease in entropy of activation while isopropylcyclopropylcarbene generation is neutral and dicyclopropylcarbene shows an increase in entropy of activation. The trends could be a result of the cyclopropanes effect upon the polarity of the diazo compound. The effect of

Table IV.6 AM1 Calculated Heats of Formation (ΔH_f)[a] and Dipole Moments (μ)[b].

Carbene	Diazo ΔH_f	Diazo μ	Carbene ΔH_f	Carbene μ	$\Delta\Delta H_f$	$\Delta\mu$
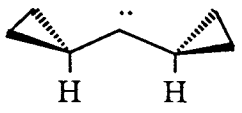	106.74	1.69	125.51	1.18	18.77	-0.51
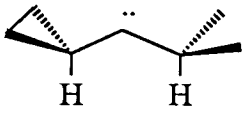	66.88	1.54	85.45	1.69	18.57	0.15
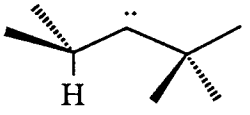	28.12 (27.14	1.69 1.65)[c]	49.60 (50.50	2.12 1.61)	21.48 (23.36	0.43 -0.04)

[a] Heats of formation reported in kcal/Mole. [b] Dipole moments reported in Debye.
[c] Data from both hydrogens down relative to the carbene (180 °).

cyclopropyl group on the polarity of the closely related carbonyl groups is nicely illustrated by the NMR ^{13}C resonances and GC retention times. The observed retention times for diisopropyl ketone is 6.5 min, isopropylcyclopropyl ketone 10.8 min, and dicyclopropyl ketone 20.5 min on a Carbowax gas chromatographic column. The ^{13}C resonances observed for the carbonyl carbon of diisopropyl ketone is found at 218.6 ppm, isopropylcyclopropyl ketone at 214.4 ppm, and dicyclopropyl ketone at 210.6 ppm. The observed resonances are indicative of the electron donating ability of the cyclopropyl substituents. The enhanced polarities attributed to the cyclopropane substitution as well as the ^{13}C NMR resonances can be rationalized by looking at the resonance set F↔G. A similar effect is expected for the diazo compounds. In the carbene generation

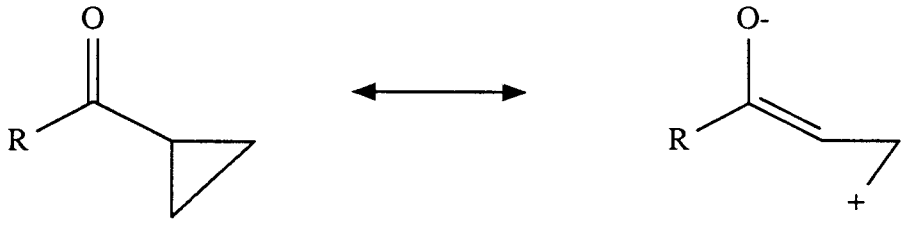

F **G**

step, as the N_2 is stretched, the effect of the cyclopropane is reduced, and the dipole moment is reduced. The reduced dipole leads to less ordering of the solvent and a positive entropy of activation.

Conjugative Effects

Previous work in our laboratory reported decomposition of lithium salts of the tosylhydrazones of 4,4-diphenyl-2,5-cyclohexadienone, 4,4-diphenylcyclohexenone, and 4,4-diphenylcyclohexanone, which generate the corresponding carbenes **49**, **50**, and **51**. The results of the decompositions will

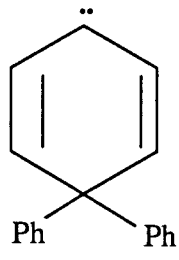

49

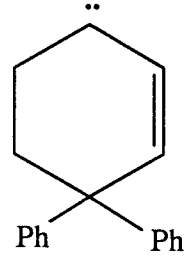

50

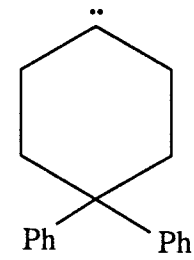

51

be briefly discussed and rationalized in terms of increasing dipole moment in the transition state.

Vinyl carbenes have received considerable attention and study in recent years.[141] Even with the amount of study, the effect of conjugation on the nature of the carbene stability and reactivity remains in question. An attempt to illustrate the effect of conjugation on a carbene center might be undertaken using the series of carbenes carbena-2,5-cyclohexadiene **52**, carbena-2-cyclohexene **53**, and carbenacyclohexane **54**. The 6 membered rings serve to prevent an

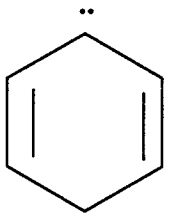

52

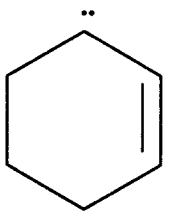

53

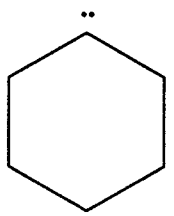

54

intramolecular double bond addition that would generate a cyclopropene derivative. The conjugation effect is expected to result in the increase of the electrophilic character of the carbene carbon as we move up in the series **49**-**51**, **52**-**54**. That is, electrophilic character increases when the π system goes from the four electron five orbital system (**49**, **52**) to a two electron three orbital system (**50**, **53**) to a localized system (**51**, **54**). This is consistent with the results obtained from the MNDO MO calculations for this series of related systems.[142] If one considers the adjacent carbons ability to donate electron density to the carbene center, it is clear that the carbene center is becoming more electron rich with increasing conjugation; decreasing the electrophilicity.

Results and Discussion

Owing to the difficulty of finding suitable precursors, characterization of reaction pathways of carbenes by measurement of reaction rates has been difficult. In the study carried out by Tafesh, products of decomposition were identified and rationalized in terms of competitive rate processes.[139] The product distributions were consistent with electrophilic attack upon the solvent

by the singlet carbene and intersystem crossing to the triplet carbene as the two rate competing processes. The product of the singlet carbene reaction with the solvent is parent ketone. The electrophilicity of the singlet carbenes is nicely illustrated by the ratio of singlet solvent reaction to intersystem crossing to the triplet (Scheme IV.4).

Scheme IV.4

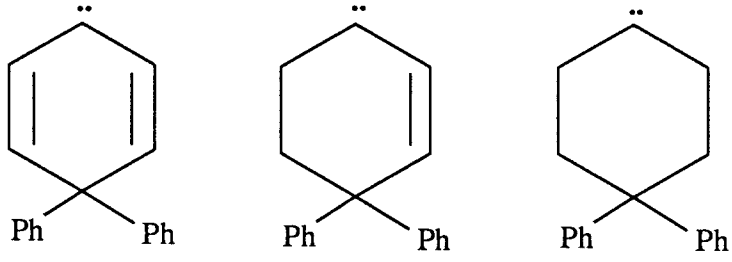

	52	**53**	**54**
$\frac{k_s\ (DMSO)}{k_{isc}}$	1.13	1.71	∞

By measuring the rates of decomposition of tosylhydrazone salt to diazo compound (k_1), decomposition of diazo compound to carbene (k_2), and the rate of loss of starting material independently (k_1) at various temperatures, Tafesh was able to calculate the activation parameters (E_a, $\Delta H^{\neq}$, $\Delta G^{\neq}$, and $\Delta S^{\neq}$) for k_1 and k_2. The free energy and enthalpy of activation ($\Delta G^{\neq}$ and $\Delta H^{\neq}$) were reported to be the same within experimental error for all three compounds.

The negative entropies of activation were at first thought to be unusual but MNDO calculations support these values. The negative entropies of activation are thought to arise from the increased dipole moment in the transition state. MNDO calculations of dipole moments for simplified models of the starting

diazo compound, transition state, and carbene are shown in Scheme IV.5.

Scheme IV.5

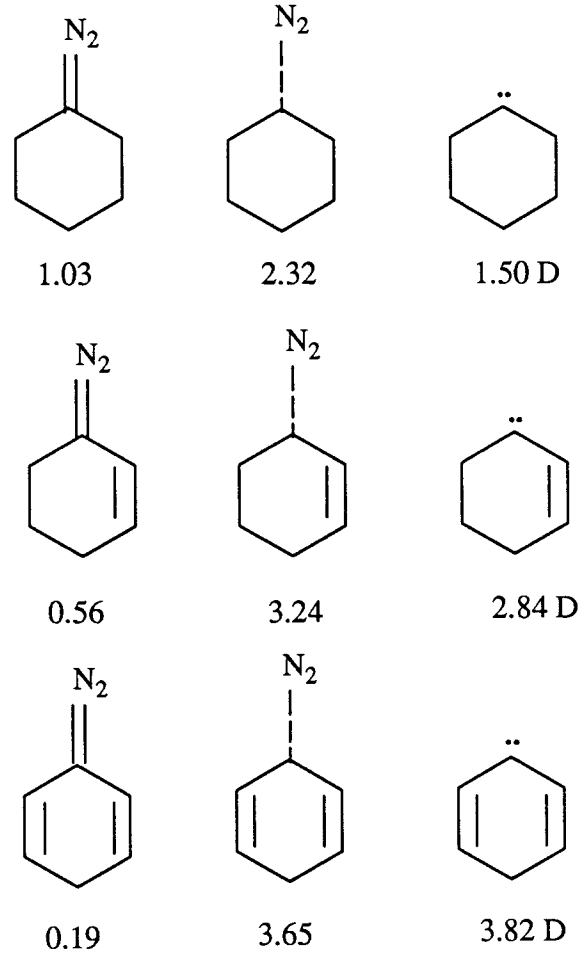

Stretching the carbon-nitrogen bond and allowing full geometric optimization demonstrates a large increase in dipole moment for all compounds modeled. The C-N_2 bond is stretched along the C-N-N axis in increments of 0.15Å. The transition state is assigned to the point where the heat of formation begins to decline and continues to decline to a minimum value. The Scheme IV.5 shows the largest increase in dipole moment is observed in the diene model. The increasing dipole moments are rationalized by considering the

mechanism of nitrogen loss. The magnitude of the overlap integral for the 2p-π interaction is decreased more rapidly than the sp^2-sp σ overlap as the N_2 is removed.[143] Resonance forms seen in the Figure IV.5 are expected to be roughly equal contributors to the ground state of diazo compounds. The disconnection of the 2p-π overlap will favor resonance form **55b** (Figure IV.5) in the transition state. In polar solvents, such as DMSO, the increasing dipole

Figure IV.5

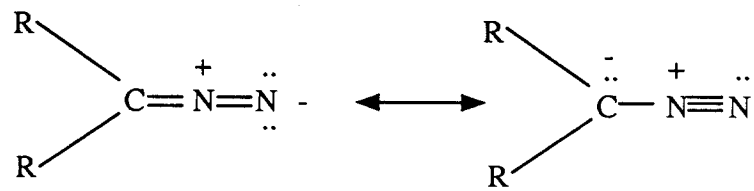

55a **55b**

moment is stabilized by the increasing orientation of the polar solvent molecules. The increased orientation of the solvent may account for the observed negative $\Delta S^{\neq}$ (decreasing entropy).

Kinetics and Activation Parameters

Knowing the rate constants of chemical processes at different temperatures allows for the determination of the activation energy of that process. Step one activation energies, hydrazone salt to diazo compound (k_1), provide little insight into the mechanism of carbene formation. All calculated activation parameters exhibit only a small deviation within the series of compounds. The results support the Tafesh observation that the first step appears to be insensitive to structural change at positions alpha to the carbene carbon. This implies that

there is little perturbation of the systems by the substituents on the diazo carbon in the starting potassium salts or transition states. A similar observation was noted earlier for the reported isopropyl-cyclopropyl hydrazone salt decompositions. The activation parameters of interest in both studies proved to arise from the second step (k_2) in the two step decomposition of the salts of the studied hydrazones; diazo compound transformation to carbene (seen earlier as Equation IV.3).

Equation IV.3

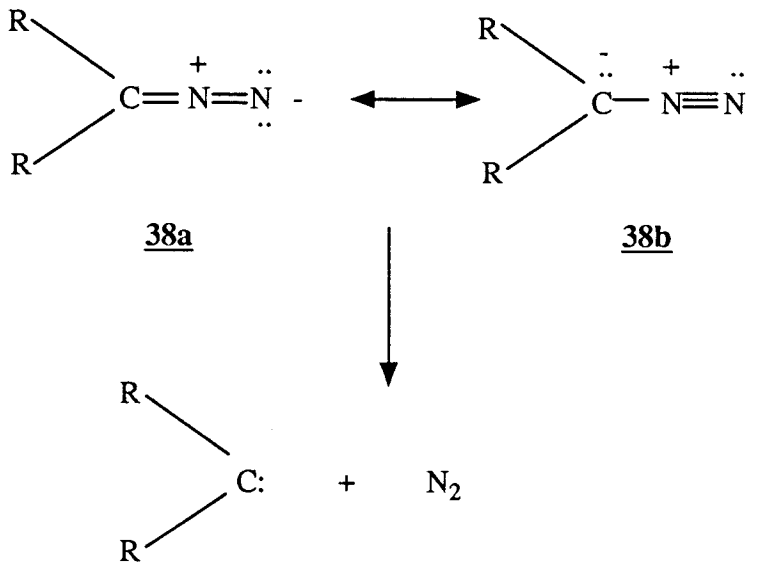

The activation energy derived from k_2 is a measure of the stability of the carbene that is produced relative to the diazo intermediate. Low values of activation energy are indicative of carbene stability.

It is generally assumed that the dissociation of the diazo compound into the two components would demonstrate a positive $\Delta S^{\neq}$. The decomposition of the hydrazone salt into two components is also assumed to have a positive entropy. However, an increase in the ordering of solvent molecules can result

in decrease in entropy terms. The numerical values obtained for the activation parameters derived from k_2 are presented in Table IV.7.

Table IV.7 Summary of Activation Parameters (k_2), Tafesh Results.[139]

Diazo compound to carbene (below)	E_a (Kcal/mol)	$\Delta H^{\neq}$ (Kcal/mol)	$\Delta S^{\neq}$ (cal/mol•K)	$\Delta G^{\neq}$ (Kcal/mol)
4,4-diphenyl-cyclohexylidene	23.9 ± 2.2	23.1 ± 2.2	-10.7 ± 5.7	27.2 ± 3.1
4,4 diphenyl-cyclohexenylidene	23.2 ± 2.2	22.4 ± 2.2	-6.3 ± 5.8	24.8 ± 3.1
4,4 diphenyl-cyclohexadienylidene	22.0 ± 0.6	21.2 ± 0.6	-9.5 ± 1.7	24.2 ± 0.9

Most notable when examining Table IV.7 is that the values for $\Delta S^{\neq}$ are all negative for the series of 4,4-diphenylcyclohexyl derivatives. The negative entropies are not to be expected in a dissociation reaction since the transition state in such a reaction would tend toward greater disorder than the ground state diazo compound. The negative entropy terms are thought to arise from the change in dipole moments between comparative states. The MNDO calculations support this data demonstrating increased dipole moments in both the transition state and carbene emulated species for the 4,4-diphenylcyclohexyl derived species.

Interaction at Remote Sites

Another topic of interest in carbene chemistry is carbene to carbene rearrangements. As was noted in the introduction, carbene to carbene rearrangement is not a frequently encountered carbene reaction. The very likely ethynyl carbene to carbene rearrangement provides a basis for the investigation into the reactivity of homologues.

Results and Discussion

In our laboratory we have decomposed hexanylidene and hexynylidene related species in an effort to evaluate the effect of remote complexation on the reactivity of carbena systems. Previous workers in our laboratory decomposed tosylhydrazone salts of ketones **56**, **57**, **58**, and **59**.

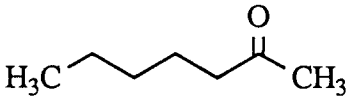

56

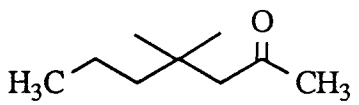

57

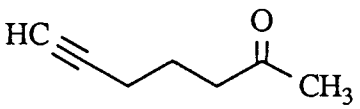

58

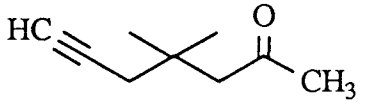

59

It was necessary to decompose the tosylhydrazone salts of **56** and **57** to evaluate the role of the alkynyl unit in the decomposition. The tosylhydrazone salts of **56** and **57** were prepared from the readily available ketones. The salt was generated by addition of methyl lithium or sodium methoxide solution to a

solution containing the previously prepared tosylhydrazone. The solvent is subsequently removed by high a vacuum pump and the salt is then allowed to decompose at the desired temperature. The dry salt of tosylhydrazone of **56** was decomposed at 150 °C at approximately 4 millimeters pressure. The alkene ratios are reported in Table IV.8.

Table IV.8 Decomposition of Tosylhydrazone Salts of 2-Heptanone (**56**) and 4,4-Dimethyl-2-heptanone (**57**).

			yield%		
	salt	temp.	1-alkene	(Z)-2-alkene	(E)-2-alkene
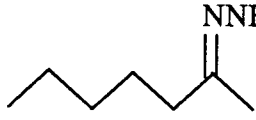 NNHTs	Na	150 °C	4.5 ± 2.2	18.9 ± 2.7	76.5 ± 2.6
	Li	150 °C	2.9 ± 1.2	34.6 ± 3.2	62.5 ± 2.3
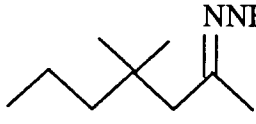 NNHTs	Li	165 °C[44]	7.0	11.8	81.2
	Na , diglyme, Δ		1.6	trace	98.4

An interesting point to make is the lithium salt appears to give different ratios of E and Z 2-alkenes. This result might be expected since it was previously reported that lithium bromide reacts with diazoalkanes to generate an organolithium intermediate which is expected to lead to different product ratios.[144]

The role of the intermediate may be altering the E to Z ratio but the overall trend has similarities. In the case of the lithium salt of the tosylhydrazone of **57**, a similar trend to what was observed in the decomposition of **56** is noted. The trend is supportive of a product determining intermediate that forms alkenes in the anticipated ratios of *trans*-2-alkene > *cis*-2-alkene > 1-alkene.[145]

The sodium and lithium salts of the tosylhydrazones of **58** and **59** were allowed to decompose at 150 °C. The results are summarized in Table IV.9.

Table IV.9 Decomposition of Tosylhydrazone Salts of 2-Heptanon-6-yne (**58**) and 4,4-Dimethyl-6-heptyn-2-one (**59**)

			yield%			
	salt	temp.	cyclic	1-alkene	(Z)-2-alkene	(E)-2-alkene
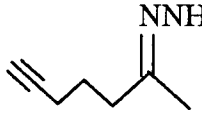	Na	150 °C	47.8 ± 2.2	5.9 ± 0.7 (10.9 ± 0.8)[a]	11.4 ± 1.6 (21.8 ± 3.0)	35.1 ± 1.7 (67.2 ± 2.8)
	Li	150 °C	4.8 ± 2.5	8.1 ± 0.3 (8.5 ± 0.5)	29.9 ± 2.2 (31.4 ± 1.5)	57.3 ± 0.8 (60.2 ± 1.1)
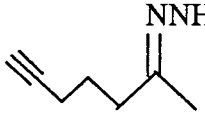	Na[b]	150 °C	72.0	8.7 (31.1)	2.3 (8.2)	17.0 (60.7)
	Li	150 °C	24.6 ± 5.6	9.4 ± 0.4 (12.5 ± 0.5)	4.3 ± 0.6 (5.7 ± 1.1)	61.7 ± 5.8 (81.9 ± 1.6)
	Na[c]	150 °C	34.6	13.2 (20.1)	5.2 (7.9)	47.2 (72.0)

[a] Percent acyclic alkene composition in parenthesis. [b] Results of a previous worker.
[c] Addition of 3.0 equivalents of lithium bromide.

From Table IV.9 it is noted that the lithium salts failed to demonstrate the same propensity for cyclization as the sodium salts. The acyclic alkene compositions remain in close correspondence to the saturated systems. In the saturated systems it was noted that the lithium salts may give organolithium intermediates during decomposition. In order to ascertain the effect of the lithium ion on the reactivity, the sodium salt of the tosylhydrazone of **58** was decomposed in the presence of 3.0 equivalents of lithium bromide (Table IV.9). The results are supportive of the suggestion that the reaction of an intermediate diazo compound with lithium bromide produces a carbenoid that has little propensity to cyclize. It is felt that the cyclization occurs at the free carbene stage of the reaction (Scheme IV.6).

Scheme IV.6

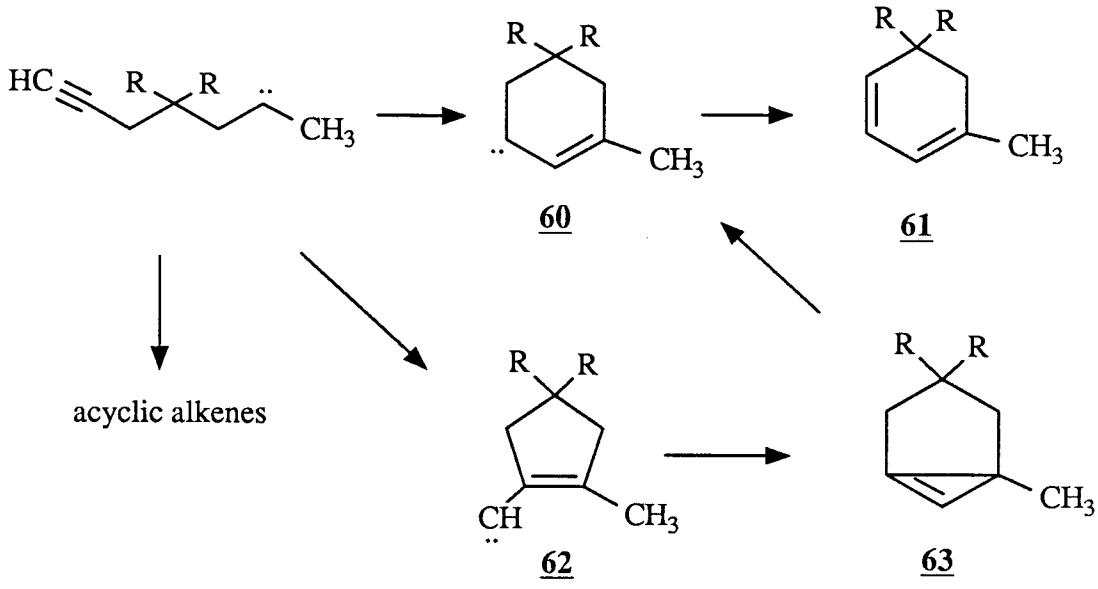

The MNDO calculations were reported to be unable to distinguish between the two pathways depicted in Scheme IV.6.[146] A consideration of the product array for the 2-carbena-6-heptyne intermediates demonstrate that thermal decomposition of the sodium salts produce predominately cyclic products. The lithium salts fail to cyclize to any great extent also; the addition of lithium bromide to sodium salt decomposition retarded cyclization. The acyclic fractions generated in decomposition showed only small deviations. The observed deviations were greatest in the amount of 1-alkene formed the salt decompositions of compound **60**. Perhaps the best explanation for the results is complexation. Lithium complexation with a diazo intermediate will generate a different reactive intermediate and consequently different product ratios.

Conclusion

Free carbene derived from sodium salt decomposition undergoes cyclization; Li salt decomposition gives complexed carbenoid-ion cyclization. Different acyclic alkene ratios for unsaturated sodium salt versus saturated salt decomposition is due to complexation of free carbene with the remote triple bond. The decomposition of tosylhydrazone salts continues to be an efficient way to generate the carbena reactive intermediates. Unfortunately owing to the reactive nature of carbena species the information extracted from carbene generation can only be inferred from rates of decomposition and product identification. The products of decomposition were seen to be singlet type products. Also observed, is that the energies of activation and the calculated activation parameters are dominated by the DMSO solvent-solute interactions. Examination of the calculated dipole moments from AM1 and MNDO provide a rationale for the observed reactivity.

Chapter V. Experimental

Materials

Previously prepared 1,4,6,7-, 1,3,5,8-, and 1,2,3,4-tetrachloronaphalene were recrystallized from methyl alcohol, followed by sublimation. Purity was determined to be greater than 99% by GC analysis. NMR data was seen to be consistent with the structures suggested in the text. The solvents used in the photolyses were dried over CaH_2 and distilled for purification. Purity was greater than 99% by GC analysis. Triethylamine was freshly distilled prior to use. AIBN (Aldrich), triphenyltinhydride (Baker), and sodium borohydride (Aldrich) were used without further purification. Previously prepared isopropyl cyclopropyl ketone, along with 2,4,-dimethyl-3-pentanone and dicyclopropyl ketone, was gently distilled under inert atomosphere for purification. Purity was greater than 99% by GC analysis. The benzenesulfonylhydrazide (Aldrich) was recrystallized from ethanol prior to use. The $NaOCH_3$ was generated from treatment of methanol (Aldrich) with elemental sodium.

General Procerdure for Photolysis

Irradiation of samples were carried out in triplicate in a Rayonet merry-go-round reactor (Southern New England Company) equipped with eight 300 nm Rull lamps while being cooled by an overhead fan to maintain a constant temperature of ≈ 28 °C. The photolysis samples (2 mL) were placed in Pyrex tubes (Ace Glass, 170 mm x 15 mm). Each tube was fitted with a nylon adaptor bushing containing a Pyrex glass sliding stopper valve and was degassed through three freeze-pump-thaw cycles. The tubes were sealed under vacuum

and irradiated at 300 nm for the desired time period. Quantum yield for dependence of 1,2,3,4-, 1,4,6,7-, and 1,3,5,8-tetrachloronaphthalene on concentration of starting material was calculated. A stock solution was prepared and aliquots were removed to make the appropriate dilutions in 10 mL volumetric flasks. Optical densities of TCNs were greater than 2 thus ensuring complete absorption of the incident radiation. If the OD was calculated to be less than 2, a correction for incomplete absorption of light was applied. Three samples of each solution were degassed and irradiated at 300 nm in the presence of an azoxybenzene actinometer.[147] Three actinometer tubes, each containing 1 mL of azoxybenzene solution (*ca.* 0.006 M), were used for each irradiation run. A stock solution of p,p'-di-*tert*-butylbiphenyl (TBBP) internal standard (0.005 M) was prepared by weighing the appropriate mass into a 25 mL volumetric flask. After irradiation (24 h), appropriate volumes of a solution of internal standard (TBBP) were added such that the ratio of internal standard concentration to TCN concentration was approximately 0.5:1.0. Quantum yields of products were determined by using three sets of azoxybenzene actinometry. Reported quantum yields are averages of three samples for each TCN concentration.

Product Analysis and Equipment Employed

Photolysis mixtures were analyzed by GC on a Varian 3300 or 3400 capillary gas chromatograph equipped with an FID, a 30 m x 0.25 cm capillary column (J&W Scientific Inc.), and a Spectra Physics 4290 or 4270 integrator. The capillary column used was DB-225 (50% cyanopropylphenyl-methylsilcone). Helium was employed as the carrier gas at 30 mL/min. The initial injection temperature was set at 150 ^{0}C for a hold of 8 minutes. The column temperature

program was 10 °C per minute to a final temperature of 220 °C with a hold of 15 minutes at the final temperature. The injector temperature was set at 275 °C and the detector temperature was set at 325 °C. The photoproducts were identified by comparing their GC retention times with those of authentic samples, and mass spectral analyses were done with a Finnegan 4023 mass spectrometer fitted to a Finnegan 9610 or a Varian 3400 capillary GC. An internal standard was used to determine quantum yields. High resolution mass spectral data (HRMS, electron impact) was obtained on a Kratos MS-50. NMR data was aquired on either a Bruker AC 300 (300 MHz) or AM 400 (400 MHz) spectrometer. Ultraviolet spectral data was gathered on a Hewlett Packard 8551A diodearray spectrophotometer. Infrared spectra was observed on a Nicollet 5DXB (FT-IR) or a Perkin-Elmer 727B spectrometer. Preparatory GC work was done on a Hewlett-Packard F & M Scientific 700 Laboratory Chromatograph equipped with a thermal conductivity detector and the appropriate choice of column stationary phase, mobile phase, and thermal conditions.

Stern-Volmer Quenching of the Photodechlorination of 1,2,3,4-, 1,4,6,7-, and 1,3,5,8-Tetrachloronaphthalene with *cis* and *trans*-1,3-Pentadiene and Fumaronitrile[88b,92]

Appropriate amounts of a mixture of *cis*- and *trans*-1,3-pentadiene or fumaronitrile were dissolved in 0.0003 M 1,2,3,4-tetrachloronaphthalene, 0.00023 M 1,3,5,8-, or 1,4,6,7-tetrachloronaphthalene (CH_3CN) to give the concentrations shown in Table II.20 and 21 respectively. At the working concentration of tetrachloronaphthalene, it was calculated that all the light was absorbed by the substrate. Photolysis (300 nm, 24 h) and product analyses were carried out as

previously described in the general procedure for photolysis and product analysis. Quantum yields were calculated from triplicate azoxybenzene actinometry.[147] The Stern-Volmer plots were obtained by plotting the ratio of quantum yield of reaction in the absence of the quenchers to that in the presence of the quenchers against the quencher concentration. GC/MS data (positive chemical ionization, CH_4) was found to be consistent with cycloaddition of 1,2,3,4-, 1,4,6,7-, and 1,3,5,8-tetrachloronaphthalene to fumaronitrile (m/z = 341, $M\text{-}H^+$, all Cl_{35}) and 1,4,6,7- and 1,3,5,8-tetrachloronaphthalene cycloaddition to a mixture of *cis* and *trans*-1,3-pentadiene (m/z = 331, $M\text{-}H^+$, all Cl_{35}). The m/z also exhibited a tetrachlorination pattern owing to the natural abundance of Cl_{35} and Cl_{37}. It is interesting to note that the GC/MS analysis (electron impact) of the photochemical quenching of 1,2,3,4-tetrachloronaphthalene with a mixture of 1,3,-pentadienes demonstrated masses consistent with the trapping of a trichloronaphthyl radical by a molecule of 1,3,-pentadiene (m/z = 296, $M^{\cdot+}$, all Cl_{35}). No ground state complexes could be observed by ultraviolet spectroscopy.

Sensitization of *cis* to *trans* isomerization of *cis*-1,3-Pentadiene by 1,2,3,4-Tetrachloronaphthalene[148]

Solutions of *cis*-1,3-pentadiene were prepared with $2x10^{-3}$ M 1,2,3,4-tetrachloronaphthalene in acetonitrile. A set of five tubes were degassed and irradiated for 60 minutes at 300 nm. The amount of *trans* isomer formed was determined by GC analysis on a varian 3700 gas chromatograph equipped with an FID using a series combination of a 10% SE-30 on chromosorb P (80/100) AW/DMCS and a 7% carbowax 20M on chromosorb P (80/100)

AW/DMCS column. The column was programmed for 33 °C to 210 °C at a rate of 25 °C/min. with an increase after a 12 minute hold at the initial injection temperature. The injector port temperature was 250 °C and the detector temperature was 300 °C. The quantum yield of *cis* to *trans* isomerization was determined from the *trans* isomer formed. Corrections for back reactions of the isomers were made according to the method of Hammond and Lamola.[91] For the determination of ϕ_{isc} of 1,2,3,4-Tetrachloronaphthalene,[91] a solution of 0.075 M (128 mg) *cis*-1,3-pentadiene and 0.002 M (133 mg) 1,2,3,4-TCN and 0.001 M (76 mg) of TBBP (internal standard) was prepared in a 25 mL volumetric flask. Several 2 mL samples were degassed and irradiated at 300 nm for 0.25, 1, 2, 11, 18, 25, 40, 50, 60, 84, 108, and 132 h. The *cis/trans* ratios were obtained at 1 h and 132 h and were used to calculate the ϕ_{isc} as follows:

	trans	:	*cis*
1.0 h	0.017	:	1.00
132 h	2.20	:	1.00 (photostationary state)

The quantum yield was determined by the equation described by Hammond and Lamola:

$$\phi_{isc} = \frac{\beta_{t\rightarrow c}}{I} (1 + x)$$

$\beta_{t\rightarrow c}$ = the conversion without back reaction

$$\beta_{t\rightarrow c} = 2.303\ \alpha \bullet \log \left(\frac{\alpha}{\alpha - \beta'} \right)$$

α = the conversion at photostationary state

β' = the conversion measured experimentally at low conversion

x = *cis/trans* ratio at the photostationary state

I = The amount of light absorbed

α = 0.313 ± 0.004

x = 0.455 ± 0.002

β' = 0.017 ± 0.001

β_{t-c} = 0.018 ± 0.003 M reacted

ϕ_{isc} = 1.04 ± 0.01

Phosphorescence and Lifetime Measurements of 1,2,3,4-, 1,4,6,7-, and 1,3,5,8-Tetrachloronaphthalenes

The phosphorescence spectra and lifetime measurements of the triplet states of starting TCNs were obtained at 77 °K using an Aminco-Bowman spectrometer with a rotating cam. The first order decay at 510 nm was monitored by an oscilloscope. A personal computer was used as a time-averaging computer. Two hundred and fifty six sweeps of the output are averaged for total of two hundred and fifty data points.

Photolysis of 1,2,3,4-, 1,4,6,7-, and 1,3,5,8-Tetrachloronaphthalene in the Presence of Triethylamine

Solutions of 1,2,3,4-, 1,4,6,7-, and 1,3,5,8-tetrachloronaphthalene (3×10^{-4} M) that contained variable amounts of freshly distilled triethylamine were prepared. The concentrations of TEA are given in the Tables II.10-12. At 300 nm all the light was calculated to be absorbed by the tetrachloronaphthalene species. Photolysis (300 nm, 2 h) and product analysis were carried out as previously

described in the general procedure for photolysis. Quantum yields were calculated from triplicate azoxybenzene actinometry.[147] Ultraviolet spectra of the individual TCN was unchanged by the addition of triethylamine.

Photolysis of Tetrachloronaphthalene in the Presence of Sodium Borohydride

Stock solutions of $NaBH_4$, 1,4,6,7- or 1,3,5,8-tetrachloronaphthalene in 94% aqueous acetonitrile were prepared. Appropriate amounts of $NaBH_4$ were delivered to 10 mL volumetric flasks and diluted to volume yielding the concentrations seen in the Table II.15,16. Photolysis (300 nm, 3 h) and product analyses were carried out as previously described in the general procedure for photolysis. Quantum yields were calculated from triplicate azoxybenzene actinometry.[147] Ultraviolet spectra of the TCN in question was unchanged by the addition of sodium borohydride.

Photolysis of 1,2,3,4-, 1,4,6,7-, and 1,3,5,8-Tetrachloronaphthalene in 0.1 M Cetyltrimethylammonium Bromide (CTAB)

Solutions of 0.1 M CTAB in 50 mL volumetrics were prepared with 1.75 x 10^{-4} M of TCNs **1**, **2**, or **3** and were allowed to stir overnight. Solutions were photolyzed (300 nm) for 15 h and product analyses was accomplished by extraction with diethyl ether. The micelles solutions were broken by the addition of 180 mL of deionized water, 10 mL of brine, and 2 mL of 10% HCl solution to yield approximately 165 mL of aqueous phase. The aqueous phase was then extracted with three 50 mL fractions of diethyl ether. The ether extracts are combined and dried over $MgSO_4$. The ether was removed in *vacuo* and solvent was exchanged with 2 mL of $CHCl_3$. Products were then analyzed

as described in the general photolysis procedure. Quantum yield was calculated from triplicate azoxybenzene actinometry.[147] Ultraviolet spectra was unchanged relative to the TCN in question.

Photolysis of 1,2,3,4-, 1,4,6,7-, and 1,3,5,8-Tetrachloronaphthalene in 0.1 M CTAB with triethylamine

Solutions of 0.1 M CTAB and 1.75×10^{-4} M TCNs were prepared and allowed to stir overnight. The solutions were then spiked with TEA (0.025 M) and photolyzed for three hours (300 nm). The CTAB miceller solutions were broken by addition of 150 mL deionized water, 10 mL of brine, and 2 mL of 10% HCL to yield approximately 165 mL of aqueous solution. The aqueous solution was then extracted with three 50 mL portions of diethyl ether. The diethyl ether fraction was combined and dried over anhydrous $MgSO_4$. The ether was then reduced in *vacuo* and the solvent exchanged with chloroform. Products were then analyzed as described in the general photolysis procedure. No ground state complex was observed by ultraviolet spectroscopy.

Radical Anion Reduction of 1,2,3,4-, 1,4,6,7-, and 1,3,5,8-Tetrachloronaphthalene Using Lithium p,p'-di-*tert*-butylbiphenylide in THF[149]

A 100 mL, three-necked, Morton flask containing a 2.5 cm glass-covered magnetic stir bar was flame dried under a stream of argon gas. After the flask had cooled under argon, 275 mg (0.395 mol) of p,p'-di-*tert*-butylbiphenyl was added to the Morton flask with 20 mL of dry THF. Lithium ribbon (≈ 6.0 mg, Foote Mineral Co.) was cut into three small pieces and was quickly added to

the stirred solution in the Morton flask. Lithium addition was done under a stream of argon. Owing to the formation of the radical anion of the biphenyl, the solution acquired a green hue within five minutes and turned darker green within thirty minutes. The solution was allowed to stir for another four hours until all the lithium had reacted. A solution of THF containing 15 mg (5.6×10^{-5} moles) of 1,2,3,4-, 1,4,6,7-, or 1,3,5,8-Tetrachloronaphthalene was syringed into the green solution and allowed to stir for five minutes. The reaction mixture was then quenched by adding 10 mL of water. The resulting solution was diluted with 50 mL of water and was extracted with diethyl ether (3 x 20 mL). The organic layer was washed with water and dried over anhydrous magnesium sulfate. After concentration and solvent exchange with chloroform, the ratio of products was determined by GC analysis using a capillary DB-225 column. Standard GC conditions were employed.

Induced Radical Dechlorination of 1,2,3,4-, 1,4,6,7-, and 1,3,5,8-Tetrachloronaphthalene in Benzene Using Triphenyltin Hydride[150]

A mixture of 1,2,3,4-, 1,4,6,7-, or 1,3,5,8-tetrachloronaphthalene (6.0 mg, 0.023 mmol), 0.33 eq. of Ph_3SnH (2.3 mg, 0.0064 mmol), and AIBN (10% of Ph_3SnH, 0.1 mg) was placed in a pyrex tube fitted with a nylon adaptor-bushing and degassed (3 freeze-pump-thaw cycles). The tubes were placed in a 70 °C oil bath and allowed to remain there overnight. After twelve hours the resulting mixture was directly injected into the GC for analysis. Products were identified by retention time under standard GC conditions.

Ultraviolet Data for 1,2,3,4- 1,4,6,7- and 1,3,5,8-Tetrachloronaphtalene

Solutions of 1,2,3,4-, 1,4,6,7-, and 1,3,5,8-tetrachloronaphthalene (2.5×10^{-5} M, CH_3CN) were prepared by dilution from stock solutions. Absorbance was measured (254 and 300 nm) and the corresponding molar extinction coefficients (e) were calculated from the expression A = ebc (Table V.1). The values seen

Table V.1 Calculated Epsilons for TCNs

TCN	e_{254} nm	e_{300} nm
1,2,3,4-	4960	9800
1,4,6,7-	5120	10040
1,3,5,8-	4640	9640

in Table V.1 were used to correct for incomplete absorption of light in the calculation of quantum yield.

Mass Spectral Data for 1,2,3,4-, 1,4,6,7-, and 1,3,5,8-Tetrachloronaphthalene.

HRMS, EI for 1,2,3,4-tetrachloronaphthalene ($C_{10}H_4Cl_4$, $M^{\cdot+}$) Calcd 263.9067, found 263.9068; for 1,4,6,7-tetrachloronaphthalene ($C_{10}H_4Cl_4$, $M^{\cdot+}$) Calcd 263.9067, found 263.9067; for 1,3,5,8-tetrachloronaphthalene ($C_{10}H_4Cl_4$, $M^{\cdot+}$) Calcd 263.9067, found 263.9069. GC/MS for 1,2,3,4-, 1,4,6,7-, and 1,3,5,8-tetrachloronaphthalene was consistent m/z 266 (100) for $C_{10}H_4Cl_4$ ($M^{\cdot+}$). GC/MS conducted upon reaction mixtures found m/z 230 (100) to be consistent with $C_{10}H_5Cl_3$ ($M^{\cdot+}$) for products of reaction.

Preparation of Diisopropyl Ketone Benzenesulfonylhydrazone

A mixture of 8.6 g (0.05 mol) of benzenesulfonyl hydrazide and 5.7 g (0.05 mol) of diisopropyl ketone and a few drops of concentrated HCl was heated reflux for three hours. The reaction mixture was cooled to room temperature and refrigerated. The crystals formed were recrystallized from 95% ethanol. The yield was 8.9 g (0.033 mol, 68%) of a white crystalline product which has the following spectral characteristics. These characteristics are consistent with the proposed structure: ^{1}H-NMR (DMSO-d_6): δ 1.1 (two doublets, 12 H, methyl protons of isopropyl groups), 2.4 - 2.9 (m, 2 H, tertiary isopropyl hydrogens), 10.1 (s, 1 H, NH proton), 7.4 - 8.0 (m, 5 H, aromatic protons). IR (KBr pellet): 3200 cm^{-1} (strong, N-H stretch), 2930 cm^{-1} (strong), 1460 cm^{-1} (medium), 1340 cm^{-1} (strong), 1180 cm^{-1} (strong), 1020 cm^{-1} (medium), 940 cm^{-1} (medium).

Preparation of Dicyclopropyl Ketone Benzenesulfonylhydrazone

A mixture of 8.6 g (0.05 mol) of benzenesulfonyl hydrazide and 5.5 g (0.05 mol) of dicyclopropyl ketone dissolved in 50 mL of 95% ethanol was heated at reflux for twelve hours. The reaction mixture was cooled to room temperature and was then refrigerated. The crystals formed were recrystallized from 95% ethanol. The yield was 6.1 g (0.023 mol, 49%) of a white crystalline product which exhibits the following spectral characteristics. These characteristics are consistent with the proposed structure: ^{1}H-NMR (DMSO-d_6): δ 0.5 - 1.0 (m, 8 H, cyclopropyl ring protons), 1.0 - 1.6 (m, 2 H, cyclopropyl ring protons adjacent to C = N), 10.1 (s, 1 H, NH proton), 7.4 - 8.0 (m, 5 H, aromatic protons). IR (KBr pellet): 3170 cm^{-1} (strong, N-H stretch), 3000 cm^{-1} (weak),

1620 cm^{-1} (medium), 1460 cm^{-1} (medium), 1420 cm^{-1} (medium), 1320 cm^{-1} (strong), 1260 cm^{-1} (medium), 1160 cm^{-1} (strong), 1100 cm^{-1} (medium), 1060 cm^{-1} (medium), 1000 cm^{-1} (medium), 950 cm^{-1} (medium).

Preparation of the Potassium Salts of the Ketone Benzenesulfonylhydrazones

Each of the two ketone benzenesulfonylhydrazones prepared was converted to the corresponding potassium salts using the following general procedure: 2.0 g of 35% wt./wt. KH in mineral oil (0.70 g of KH, 0.0175 mol) was washed four times with dry THF and the KH was allowed to react with approximately 0.0175 mol (4.6 - 4.7 g) of the ketone benzenesulfonyl hydrazone dissolved in 20 mL of dry THF. The THF solvent was removed under vacuum in a desiccator and the solid product was washed with dry THF and redried under vacuum. In each case the product was obtained in greater than 90% yield.

Preparation of Dry DMSO

A three-necked round- bottom flask equipped with a mechanical stirrer and a drierite filled drying tube was charged with approximately 800 mL of reagent grade DMSO and 10 g of calcium hydride. The mixture was allowed to stir for two days and was then distilled under vacuum. The first 100 mL of distillate was discarded and distillation was stopped with 100 mL of material remaining in the distilling flask. The 500 - 600 mL of dry DMSO obtained was stored over 4-Å molecular sieves.

Determination of k_1 for Decomposition of Potassium Salts of Dicyclopropyl, Diisopropyl and Isopropylcyclopropyl Benzenesulfonylhydrazones

A constant temperature oil bath was brought to the desired decomposition temperature. Thirty mL of DMSO was placed in a 100 mL round-bottom flask with a teflon stir bar and then placed in a constant temperature oil bath for thirty minutes. One drop of N,N-dimethylaniline was added to the DMSO (approximately 0.02 g, 2×10^{-4} M) for use as the internal standard. A measured quantity of potassium salt was then added to the stirring DMSO solution. Aliquots of 2 mL were withdrawn at timed intervals and transferred to test tubes in an ice bath. Two drops of glacial acetic acid were added to each aliquot to convert the remaining potassium salt back into the corresponding benzenesulfonylhydrazone. Each aliquot was then analyzed by HPLC using a Waters Associates liquid chromatograph which was equipped with a reversed liquid phase column (Hamilton PRP-1, 150 mm x 4.1 mm) and a Waters Associates model 440 absorbance detector. Absorbance was measured at 254 nm. The solvent used was 60% acetonitrile in water at the flow rate of 2.0 mL/min.

General Procedure for the Syntheses and Pyrolyses of the Tosylhydrazone Lithium Salts of 2-Heptanone, 4,4-Dimethyl-2-heptanone, 2-Heptanon-6-yne, and 4,4-Dimethyl-6-heptyn-2-one (56, 57, 58, and 59)

A carefully weighed amount of the tosylhydrazone was dissolved in 15 mL of dry tetrahydrofuran under nitrogen in a dry, 100 mL, round-bottom flask equipped with a magnetic stirring bar, a Claisen adapter, an addition funnel, and

a condenser with a gas inlet. The funnel was charged with a solution containing one equivalent of methyllithium in diethyl ether using a dry syringe. The methyllithium was added dropwise to the well-stirred tosylhydrazone solution over a time period of 10-15 minutes and stirred for an additional 15-30 minutes at room temperature. The stirring bar was retrieved; the solvent was removed using a rotatory evaporator and further dried by evacuating to 1-3 Torr (oil pump). The solvent was then heated at 65 °C (oil bath) for 45-60 minutes. The flask was connected to two cooled (dry ice/isopropyl alcohol) traps connected in series, evacuated to 1-3 Torr, and heated (oil bath) to the desired temperature for 20-30 minutes. The volatile products were collected from the traps and subjected to GC analyses.

General Procedure for the Syntheses and Pyrolyses of the Tosylhydrazone Sodium Salts 2-Heptanone, 4,4-Dimethyl-2-heptanone, 2-Heptanon-6-yne, and 4,4-Dimethyl-6-heptyn-2-one (56, 57, 58, and 59)

Fifteen mL of absolute methanol under nitrogen was placed in a dry, 100 mL, round-bottom flask equipped with a magnetic stirring bar, a Claisen adapter, a glass stopper, and a gas inlet. A carefully weighed amount of sodium metal (5.0 mmol) was added. After all the metal had reacted, 5.0 mmol of tosylhydrazone was added in one portion and stirred at room temperature for one hour. The stirring bar was removed and the solution was concentrated in the rotatory evaporator to about one-third to one-quarter of its original volume. Ten mL of tetrahydrofuran was added, and the solvent removed in the rotatory evaporator. The process was repeated with two more 10 mL portions of tetrahydrofuran. The dry sodium salt was dried further and pyrolyzed in the

same manner as described for the dry lithium salt.

Stability Test of Products to Reaction Conditions

To test the stability of products to reaction conditions, the product fraction (27.5% cyclic, 9.4% 1-alkene, 58.4% *trans*-2-alkene, and 4.7% *cis*-2-alkene) generated from the decomposition of the dry lithuim salt of 4,4-dimethyl-6-heptyn-2-one tosylhydrazone was added back to the pot residue from the pyrolysis. The mixture was then heated to 150 °C for two minutes; after the two minute heating the volatile fraction was allowed to distill into a trap at 4 mm pressure. The GLC analysis showed a composition of 24.4% cyclic, 10.0% 1-alkene, 60.9% *trans*-2-alkene, and 4.7% *cis*-2-alkene.

Identification of Products from the Thermal Decomposition of Lithium and Sodium Salts of 4,4-Dimethyl-6-heptyn-2-one Tosylhydrazone

Products of decomposition were trapped using a packed column (10 feet x .25 inch copper tube, carbowax 20 M on Chromosorb P NAW 60/80 mesh) on a Hewlett-Packard F & M 700. The products were identified by proton NMR. The first peak was identified as 1,5,5-trimethyl-1,3-cyclohexadiene by comparison of its IR, ^{1}H, and ^{13}C NMR spectra with those of an independently synthesized sample. The second peak was identified as a mixture of 4,4-dimethyl-1-hepten-6-yne and *trans*-4,4-dimethyl-5-hepten-1-yne based on NMR spectra: ^{1}H NMR ($CDCl_3$) δ 0.97 (s, 6 H *gem*-dimethyl of terminal alkene), 1.07 (s, 6 H, *gem*-dimethyl of trans alkene), 1.67 (d, 3 H, $J = 5$ Hz, terminal methyl of *trans* alkene), 1.98 (t, 1 H, $J = 2$ Hz; t, 1 H, $J = 2$ Hz; two triplets superimposed, isomeric alkyne hydrogens), 2.06 (m, 2 H, C-5 of terminal alkene), 2.13 (d, 2

H, $J = 2$ Hz, C-3 of *trans* alkene), 5.01 - 5.10 (2 vbs, 2 H, C-1, terminal alkene), 5.37-5.53 (m, 2 H, C-5, C-6, *trans* alkene), 5.79 (m, 1 H, C-2, terminal alkene). Decoupling resonance at δ 1.67 collapsed 5.37 - 5.53 to absorptions at δ 5.50 and 5.42 (dd, 1 H, 1 H, $J = 15.6$ Hz). HRMS, EI peak 1 for C_9H_{14} ($M^{\cdot+}$) calcd 122.1095, found 122.1096. Peak 2 was resolved into two peaks by capillary GC on a DB Wax column (1-alkene) and (*trans* 2-alkene); for C_8H_{11} ($M - 15^+$) calcd 107.0861, found 107.0858; C_8H_{11} ($M - 15^+$) calcd 107.0861, found 107.0880. The last peak was identified as *cis*-4,4-dimethyl-5-hepten-1-yne from its spectral data: ^{1}H NMR ($CDCl_3$) δ 1.22 (s, 6 H, C-4, *gem*-dimethyl), 1.74 (d, 3 H, $J = 6$ Hz, C-7), 1.98 (t, 1 H, $J = 2$ Hz, C-1), 2.26 (d, 2 H, $J = 2$ Hz, C-3), 5.33 - 5.45 (m, 2 H, C-5, C-6); decoupling resonance at δ 1.74 yielded δ 5.41, 5.34 (dd, 1 H, 1 H, $J = 10.5$ Hz); HRMS, EI for C_8H_{11} ($M - 15^+$) calcd 107.0861, found 107.0867.

Identification of Products from the Reactions of the Lithium Salt of 6-Heptyn-2-one Tosylhydrazone

The products of the vacuum pyrolysis of the lithium salt of 6-heptyn-2-one tosylhydrazone were isolated by preparative GLC and identified by their spectral properties. The first peak was identified as 1-hepten-6-yne. The ^{1}H NMR ($CDCl_3$) exhibited the following peaks: ^{1}H NMR ($CDCl_3$) δ 1.63 (P, 2 H, $J = 7$ Hz, C-4), 1.95 (t, 1 H, $J = 2$ Hz, C-7), 2.09 - 2.20 (m, 4 H, C-3, C-5), 4.97 - 5.08 (3bs, 2 H, C-1), 5.72 - 5.82 (m, 1 H, C-2); HRMS , EI for C_7H_9 ($M - 1^+$) calcd 93.0704, found 93.0714. The third peak was identified as *cis*-5-hepten-1-yne based on the following spectral characteristics: ^{1}H NMR ($CDCl_3$) δ 1.63 (d, 3 H, $J = 6.5$ Hz, C-7), 1.95 (t, 1 H, $J = 2$ Hz, C-1), 2.19 - 2.31

(m, 4 H, C-3, C-4), 5.41 - 5.61 (m, 2 H, C-5, C-6). Decoupling δ 1.63 yielded δ 5.55 (d, 1 H, J = 10.5 Hz, C-6); HRMS, EI for C_7H_9 (M - 1^+) calcd 93.0704, found 93.0684. The second peak was identified as *trans*-5-hepten-1-yne based on the following spectral characteristics: ^{1}H NMR ($CDCl_3$) δ 1.66 (d, 3 H, J = 6.5 Hz, C-7), 1.96 (t, 1 H, J = 2 Hz, C-1), 2.16 - 2.26 (m, 4 H, C-3, C-4), 5.43 - 5.58 (m,. 2 H, C-5, C-6). Decoupling δ 1.66 yielded δ 5.52 (d, 1 H, J = 15.5 Hz, C-6); HRMS, EI for C_7H_9 (M - 1^+) calcd 93.0704, found 93.0714. The fourth product, 1-methyl-1,3-cyclohexadiene, was identified by comparison of its retention time and spectra with those of an independently synthesized sample.

^{1}H and ^{13}C Spectra Reported for Isopropylcyclopropyl Ketone, Dicyclopropyl Ketone and Diisopropyl Ketone

Isopropylcyclopropyl ketone: ^{1}H NMR ($CDCl_3$) δ 2.64 (h, 1 H, J = 7 Hz), δ 1.95 (m, 1 H), δ 1.10 (d, 6 H, J = 7 Hz), δ 0.92 (m, 2 H), δ 0.82 (m, 2 H), ^{13}C NMR ($CDCl_3$) δ 8.18, 10.61, 18.18, 18.55, 21.84, 41.58, 214.59.

Dicyclopropyl ketone: ^{1}H NMR δ 1.92 (m, 2 H) δ 0.94 (m, 4 H) δ 0.82 (m, 4 H), ^{13}C NMR δ 10.33, 20.45, 210.64.

Diisopropyl ketone: ^{1}H NMR δ 2.70 (n, 2 H J = 7 Hz) δ 0.98 (d, 12 H J = 7 Hz), ^{13}C NMR δ 18.66, 38.62, 218.61.

Calculation of Activation Parameters

The relationship between the activation energy (E_a) and the rate constants for the decomposition of the hydrazone salt to diazo compound (k_1) and for the decomposition of diazo compound to carbene (k_2) are given by the Arrhenius equation (Equation V.1).

Equation V.1

$$k_2 \text{ or } k_1 = Ae^{-E_a/RT}$$

Equation V.2

$$\ln k_2 \text{ or } k_1 = -E_a/RT + \ln A$$

The natural log of Equation V.1 generates Equation V.2; A = frequency factor, T = absolute temperature, R = general gas constant = 1.99 cal/mol•K, E_a = activation energy, and k_2 or k_1 = rate constant for the dissociation at temperature T. A plot of the ln k_2 or ln k_1 versus inverse temperature yields a slope of $-E_a/R$. Therefore, the activation energy of the dissociation can be easily calculated. The enthalpy of activation, $\Delta H^{\neq}$, is easily calculated from the E_a by Equation V.3. The entropy of activation, $\Delta S^{\neq}$, is then calculated from Equation

Equation V.3

$$\Delta H^{\neq} = E_a - RT$$

V.4. Calculated values of $\Delta H^{\neq}$ and $\Delta S^{\neq}$ allow for the calculation of the free energies of activation using Equation V.5. The value for T (kelvin) used for

Equation V.4

$$\Delta S^{\neq} = \frac{\Delta H^{\neq}}{T} + R \ln \frac{k_2 \text{ or } k_1}{T} - 47.4$$

Equation V.5

$$\Delta G^{\neq} = \Delta H^{\neq} - T\Delta S^{\neq}$$

each compound in Equations V.3-5 is 393 °K (120 °C). 120 °C is the average temperature of the five temperatures used in the thermolyses. k_2 or k_1 in Equation V.4 is the value established at 120 °C. The value for E_a can be used to determine the enthalpy of activation, $\Delta H^{\neq}$, using Equation V.3. The value for $\Delta H^{\neq}$ is used to determine the entropy of activation, $\Delta S^{\neq}$, using Equation V.4. The calculated values for $\Delta H^{\neq}$ and $\Delta S^{\neq}$ are then used to calculate the free energy of activation $\Delta G^{\neq}$, using Equation V.5. All values are reported earlier in the text in accordance with these relationships.[151]

Table V.2 HPLC Ratios at Timed Intervals.
Decomposition of K^+ Salt of Diisopropylbenzensulfonylhydrazone.

110 °C	Time (sec)	Area ratio	Ln (area ratio)
	60	1.146	0.1359
	120	1.099	0.0953
	180	1.055	0.0531
	260	0.9394	-0.0625
	360	0.8579	-0.1533
	460	0.7767	-0.2527
	560	0.7258	-0.3205

Table V.3 HPLC Ratios at Timed Intervals.
Decompositon of K^+ Salt of Diisopropylbenzenesulfonylhydrazone.

110 °C	Time (sec)	Area ratio	Ln (area ratio)
	60	1.402	0.3382
	120	1.297	0.2602
	180	1.218	0.1973
	260	1.145	0.1356
	360	1.030	0.0294
	460	0.9194	-0.0840
	560	0.8851	-0.1220

Table V.4 HPLC Ratios at Timed Intervals.
Decomposition of K^+ Salt of Diisopropylbenzenesulfonylhydrazone.

110°C	Time (sec)	Area ratio	Ln (area ratio)
	60	1.293	0.2569
	120	1.218	0.1976
	180	1.159	0.1474
	260	1.070	0.0679
	360	0.9812	-0.0190
	460	0.8763	-0.1320
	560	0.8078	-0.2134

Table V.5 HPLC Ratios at Timed Intervals.
Decomposition of K^+ Salt of Diisopropylbenzenesulfonylhydrazone.

115°C	Time (sec)	Area ratio	Ln (area ratio)
	60	1.322	0.2791
	120	1.229	0.2059
	180	1.105	0.1000
	260	0.9836	-0.0165
	360	0.8426	-0.1713
	460	0.7279	-0.3176
	560	0.6137	-0.4882

Table V.6 HPLC Ratios at Timed Intervals.
Decomposition of K^+ Salt of Diisopropylbenzenesulfonylhydrazone.

115°C	Time (sec)	Area ratio	Ln (area ratio)
	60	1.340	0.2927
	120	1.225	0.2028
	180	1.134	0.1259
	260	1.019	0.0189
	360	0.8873	-0.1196
	460	0.7594	-0.2752
	560	0.6162	-0.4842

Table V.7 HPLC Ratios at Timed Intervals.
Decomposition of K^+ Salt of Diisopropylbenzenesufonylhydrazone.

115°C	Time (sec)	Area ratio	Ln (area ratio)
	60	1.202	0.1840
	120	1.131	0.1227
	180	1.019	0.0190
	260	0.9301	-0.0725
	360	0.7848	-0.2423
	460	0.6559	-0.4216
	560	0.5583	-0.5829

Table V.8 HPLC Ratios at Timed Intervals.
Decomposition of K^+ Salt of Diisopropylbenzenesulfonylhydrazone.

120°C	Time (sec)	Area ratio	Ln (area ratio)
	50	1.933	0.6591
	100	1.734	0.5506
	150	1.586	0.4612
	200	1.469	0.3847
	300	1.099	0.0946
	400	0.8746	-0.1340
	500	0.7194	-0.3294

Table V.9 HPLC Ratios at Timed Intervals.
Decomposition of K^+ Salt of Diisopropylbenzenesulfonylhydrazone.

120°C	Time (sec)	Area ratio	Ln (area ratio)
	50	0.9903	-0.0097
	100	0.8964	-0.1094
	150	0.8081	-0.2131
	250	0.6494	-0.4317
	350	0.5293	-0.6362
	450	0.4169	-0.8749
	550	0.3185	-1.144

Table V.10 HPLC Ratios at Timed Intervals.
Decomposition of K^+ Salt of Diisopropylbenzenesulfonylhydrazone.

120°C	Time (sec)	Area ratio	Ln (area ratio)
	50	1.584	0.4600
	100	1.518	0.4171
	150	1.338	0.2912
	250	1.207	0.1878
	350	0.9870	-0.0131
	450	0.8348	-0.1806
	550	0.7036	-0.3516

Table V.11 HPLC Ratios at Timed Intervals.
Decomposition of K^+ Salt of Diisopropylbenzenesulfonylhydrazone.

125°C	Time (sec)	Area ratio	Ln (area ratio)
	50	1.168	0.1556
	100	1.028	0.0272
	150	0.8637	-0.1465
	200	0.7083	-0.3449
	250	0.4598	-0.7771
	350	0.3024	-1.196
	450	0.2137	-1.543

Table V.12 HPLC Ratios at Timed Intervals.
Decomposition of K^+ Salt of Diisopropylbenzenesulfonylhydrazone.

125°C	Time (sec)	Area ratio	Ln (area ratio)
	50	1.166	0.1538
	100	0.9593	-0.0416
	150	0.7933	-0.2316
	200	0.6500	-0.4307
	310	0.5298	-0.6352
	410	0.3545	-1.037
	510	0.2437	-1.412

Table V.13 HPLC Ratios at Timed Intervals.
Decompositon of K^+Salt of Diisopropylbenzenesulfonylhydrazone.

125°C	Time (sec)	Area ratio	Ln (area ratio)
	50	1.318	0.2759
	100	1.092	0.0877
	150	0.9390	-0.0629
	200	0.7869	-0.2396
	310	0.6387	-0.4484
	410	0.4316	-0.8402
	510	0.3061	-1.184

Table V.14 HPLC Ratios at Timed Intervals.
Decomposition of K^+ Salt of Diisopropylbenzenesulfonylhydrazone.

130°C	Time (sec)	Area ratio	Ln (area ratio)
	50	0.5971	-0.5157
	100	0.4664	-0.7627
	150	0.4129	-0.8845
	200	0.3963	-0.9257
	300	0.2634	-1.334
	400	0.2315	-1.463

Table V.15 HPLC Ratios at Timed Intervals.
Decomposition of K^+ Salt of Diisopropylbenzenesulfonylhydrazone.

130°C	Time (sec)	Area ratio	Ln (area ratio)
	50	0.8554	-0.1562
	100	0.7559	-0.2798
	150	0.6588	-0.4173
	250	0.5034	-0.6864
	350	0.3823	-0.9615
	450	0.3024	-1.1 96

Table V.16 HPLC Ratios at Timed Intervals.
Decomposition of K^+ Salt of Diisopropylbenzenesulfonylhydrazone.

130°C	Time (sec)	Area ratio	Ln (area ratio)
	50	0.9066	-0.0980
	100	0.7494	-0.2885
	150	0.6813	-0.3837
	250	0.5423	-0.6119
	350	0.4189	-0.8701
	450	0.3409	-1.076

Table V.17 HPLC Ratios at Timed Intervals.
Decomposition of K^+ Salt of Dicyclopropylbenzenesulfonylhydrazone.

130°C	Time (sec)	Area ratio	Ln (area ratio)
	50	2.165	0.7725
	100	1.968	0.6768
	150	1.723	0.5439
	200	1.671	0.5134
	250	1.437	0.3627
	350	1.205	0.1861

Table V.18 HPLC Ratios at Timed Intervals.
Decomposition of K^+ Salt of Dicyclopropylbenzenesulfonylhydrazone.

130°C	Time (sec)	Area ratio	Ln (area ratio)
	50	2.277	0.8230
	100	1.976	0.6812
	150	1.943	0.6644
	200	1.725	0.5451
	250	1.524	0.4214
	350	1.249	0.2222

Table V.19 HPLC Ratios at Timed Intervals.
Decomposition of K^+ Salt of Dicyclopropylbenzenesulfonylhydrazone.

130°C	Time (sec)	Area ratio	Ln (area ratio)
	50	1.699	0.5299
	100	1.527	0.4231
	150	1.417	0.3483
	200	1.329	0.2841
	250	1.219	0.1976
	350	0.9536	-0.0475

Table V.20 HPLC Ratios at Timed Intervals. Decomposition of K^+ of Isopropylcyclopropylbenzenesulfonylhydrazone.

110°C	Time (sec)	Area ratio	Ln (area ratio)
	50	1.699	0.5299
	100	1.557	0.4428
	150	1.507	0.4101
	200	1.429	0.3569
	250	1.349	0.2994
	350	1.299	0.2616

Table V.21 HPLC Ratios at Timed Intervals. Decomposition of K^+ of Isopropylcyclopropylbenzenesulfonylhydrazone.

130°C	Time (sec)	Area ratio	Ln (area ratio)
	50	1.600	0.4700
	100	1.507	0.4515
	150	1.389	0.3286
	200	1.229	0.2062
	250	1.109	0.1035
	350	0.990	-0.0101

Bibliography

1. Laurent, A. *Ann. Chim. Phys.* **1833**, 2, 275.
2. Aylsworth, J. W. U.S. Pat. 1909, No. 914,222.
3. Aylsworth, J. W. U.S. Pat. 1909, No. 914,223.
4. Aylsworth, J. W. U.S. Pat. 1913, No. 1,111,289.
5. Brinkman, U. A.; Reymer, H. G. M. *Journal of Chrom.* **1976**, *127*, 203.
6. Hutzinger, O.; Safe, S.; Zitko, V. In *The Chemistry of PCBs'* CRC: Cleveland, Ohio, 1974.
7. Beland, F. A.; Geer, R. D. *J. Chromatogr.* **1973**, *84*, 59.
8. Kimbrough, R. D. *Arch. Environ. Health.* **1972**, *25*, 125.
9. Kover, F. D. *Environmental Hazard Assessment Report: Chlorinated Naphthalenes*, 1975, EPA 560/8-75-001.
10. Pudelkiewicz, W. J.; Boucher, R. V.; Callenbach, E. W.; Miller, R. C. *Poultry Sci.* **1959**, *38*, 424.
11. Greenburg, L. *Ind. Bull. N.Y. State Dept. Labor*, **1943**, *22*, 404.
12. Collier, E. *Laneet*, **1943**, *244*, 72.
13. Hansel, W.; Olafson, P.; McEntee, K. *Cornell Vet.* **1955**, *45*, 94.
14. Welsh, D. J. Amer. *J. Med. Technol.* **1957**, *23*, 43.
15. Jones-Thellwell, A. *J. Ind. Hyg. Toxicol.* **1941**, *23*, 230.
16. Höfs, W.; *Dermatol. Wochenschr.* **1957**, *1*, 135.
17. Plewig, G. *Arch. Klin. Exp. Dermatol.* **1970**, *238*, 228.
18. Teleky, L. *Klin. Wochenschr.* **1949**, *27*, 249.
19. Flinn, F. B.; Jarvik, N. E. *Amer. J. Hyg.* **1938**, *27*, 19.
20. Sikes, D.; Bridges, M. E. *Science*, **1952**, *116*, 506.

21. Cornish, H. H.; Block, W. D. *J. Biol. Chem.* **1958**, *231*, 583.

22. Ruzo, L. O.; Safe. S.; Jones, D.; Hutzinger, O. *J. Agr. Food Chem.* **1976**, *24*, 581.

23. Ruzo, L.; Safe, S.; Hutzinger, O.; Platenow, N.; Jones, D. *Chemosphere*, **1975**, *3*, 121.

24. Shelley, W. A.; Kligman, A. M. *Arch. Dermatol.* **1957**, *75*, 689.

25. Hambrick, G. W. *J. Invest. Dermatol.* **1957**, *28*, 89.

26. Ruzo, L. O.; Zabik, M. J.; Schuetz, R. D. *J. Am. Chem Soc.* **1974**, *96*, 3809.

27. Dreeskamp, H.; Hutzinger, O.; Zander, M. Z. *Naturforsch.* **1972**, *27a*, 756.

28. Wagner, P. J. In *Creation and Detection of the Excited State*; Mercel Dekker: New York, 1971; pp 173-212.

29. a) Bunce, N. J.; Safe, S.; Ruzo, L. O. *Can. J. Chem.* **1975**, *53a*, 688. b) Bunce, N. J.; Kumar, Y.; Ravanal, L. *J. Org. Chem.* **1979**, *44*, 2612.

30. Bunce, N. J.; Hayes, P. J.; Lemke, M. E. *Can J. Chem.* **1983**, *61*, 1103.

31. Soumillion, J. Ph.; DeWolf, B. J. *J. Chem. Soc. Chem. Commun.* **1981**, 436.

32. Bunce, N. J.; Safe, S.; Ruzo, L. O. *J. Chem. Soc. Perkin Trans I.* **1975**, 1607.

33. Freeman, P. K.; Ramnath, N. *J. Org. Chem.* **1988**, *53*, 148.

34. Takemura, T.; Aikawa, M.; Baba, H.; Shindo, Y. *J. Am. Chem. Soc.* **1976**, *98*, 2205.

35. Förster T. "The Exciplex"; *Excimers and Exciplexes*: Gordon, W. and Ware W. R. eds., Academic Press, New York, 1975, pp 1-23.

36. Hirayama, F. *J. Chem. Phys.* **1965**, *42*, 3163.

37. Lim, E. C. *Acc. Chem. Res.* **1987**, *20*, 8.

38. Simmons, J. P.; Majer, R. *J. Adv. Photochem.* **1964**, *2*, 137.

39. Wilkinson, F.; Dubois, T. *J. Chem. Phys.* **1963**, *39*, 377.

40. a) Giachino, G. G. *J. Phys. Chem.* **1980**, *84*, 3522. b) Giachino, G. G.; Georger, J. H. J. *Luminescence* **1981**, *27*, 293. c) Akasheh, T. *Chem. Phys. Lett.* **1978**, *59*, 392.

41. Kulis, Y. Y.; Poletaeva, I. Y.; Kuz'min, M. G. *J. Org. Chem. USSR* (Engl. Transl.), **1973**, *33*, 179.

42. Bunce, N. J.; Ruzo, L. O.; Pilon, P.; Sturch, D. J. *J. Org. Chem.* **1976**, *41*, 3023.

43. Barltrop , J. A. *Pure and Applied Chem.* **1973**, *33*, 179.

44. a) Ohashi, M.; Tsujimoto, K,; Seki, K. *J. Chem. Soc. Chem. Commun.* **1973**, 384. b) Tsujimoto, K.; Tasaka, S.; Ohashi, M. *J. Chem. Soc. Chem. Commun.* **1975**, 758.

45. Bunce, N. J. *Chemosphere* **1982**, *11*, 701.

46. Davidson, R. S.; Goodin, J. W. *Tetrahedron Lett.* **1981**, *22*, 163.

47. Bunce, N. J. *J. Org. Chem.* **1982**, *47*, 1948.

48. Barltrop, J. A.; Bradbury, D. *J. Am. Chem. Soc.* **1973**, *95*, 5085.

49. a) Epling, G. A.; Florio, E. *Tetrahedron Lett.* **1986**, *27*, 675. b) Epling, G. A.; Florio, E. *J. Chem. Soc. Chem. Commun.* **1986**, 185.

50. a) Greig, J. B. *Ann. Occup. Hyg.* **1979,** *22*, 11. b) Sax, N. I.; Lewis, R. J. Sr. in *Dangerous Propeties of Industrial Materials*; Reinhold: New York, 1988, pp 3167-8.

51. Freeman, P. K.; Srinivasa, R. ; Campbell, J. A.; Deinzer, M. L. *J. Am. Chem. Soc.* **1986**, *108*, 5531.

52. Streitweiser, A.; Mares, F. *J. Am. Chem. Soc.* **1968**, *90*, 2444.

53. a) Dewar, M. J. S.; Dougherty, R. C. In *The PMO Theory of Organic Chemistry*; Plenum Press: New York, 1975, pp 78-80. b) Burdon, J. *Tetrahedron* **1965**, *21*, 3373.

54. a) Savéant, J. P.; Amatore, C.; Oturan, M. A.; Pinson, J.; Thiébault, A. *J. Am. Chem. Soc.* **1985**, *107*, 3451. b) Rossi, R. A.; Bunnett, J. F. *J. Org. Chem.* **1973**, *38*, 1407. c) Alam, N.; Amatore, C.; Thiébault, A.; Verpeaux, J. N. *J. Org. Chem.* **1990**, *55*, 6347.

55. a) Geer, R. D.; Beland, F. A.; Farwell, S. O.; Callis, P. R. *J. Electroanal. Chem.* **1977**, *78*, 145. b) Savéant, J. P.; Andrieux, C. P.; Su. K. B. *J. Phys. Chem.* **1986**, *90*, 3815. c) Gallardo, I.; Moreno, M.; Casado, J. *J. Electroanal. Chem.* **1987**, *219*, 197. d) Gallardo, I.; Moreno, M.; Bertràn, J. *J. Chem. Soc. Perkin Trans. II.* **1989**, 2017.

56. Symons, M. C. R.; Bowman, W. R. *J. Chem. Soc. Perkin Trans. II.* **1988**, 583. and references cited therein.

57. Maslak, P.; Navaez, J. N.; Kula, J.; Malinski, D. S. *J. Org. Chem.* **1990**, *55*, 4550.

58. a) Maslak, P,; Guthrie, R. D. *J. Am. Chem. Soc.* **1986**, *108*, 2628. b) Maslak, P.; Guthrie, R. *J. Am. Chem. Soc.* **1986**, *108*, 2637.

59. Lorenz, D. H.; Shapiro, P.; Stern, A.; Becker, E. I. *J. Org. Chem.* **1963**, *28*, 2332.

60. a) Kuivila, H. G.; Menapace, L. W. *J. Am. Chem. Soc.* **1964**, *86*, 3047. b) Grady, G. L.; Danylin, T. J.; Rabideaux, P. *J. Organomet. Chem.* **1977**, *142*, 67. c) Gleicher, G. J.; Soppe-Mbang, H. *J. Am. Chem. Soc.* **1981**, *103*, 4100. d) Gleicher, G. J.; Mahiou, B. *J. Org. Chem.* **1990**, *55*, 4466.

61. Walling, C.; Miller, B. *J. Am. Chem. Soc.* **1957**, *79*, 4181.

62. Blackburn, E. V.; Tanner, D. D. *J. Am. Chem. Soc.* **1980**, *102*, 692.

63. Hammond, G. S. *J. Am. Chem. Soc.* **1954**, *77*, 334.

64. Kochi, J. K.; Vogler, E. A.; Tamblyn, W. H. *J. Org. Chem.* **1980**, *45*, 3912.

65. Kuivila, H. G.; Menapace, L. W.; Warner, A. C. *J. Am. Chem. Soc.* **1962**, *84*, 3584.

66. Szychlinski, J. *Rocz. Chem.* **1960**, *34*, 941.

67. Safe, S.; Hutzinger, O.; Jamieson, W. D. *Org. Mass Spectrom.* **1973**, *7*, 169.

68. Ruzo, L. O.; Bunce, N. J. *Tetrahedron Lett.* **1975**, *8*, 511.

69. Ruzo. L. O.; Sunström, G.; Safe, S.; Hutzinger, O. *Chem. Weekbl.* **1976**, *35m*, 422.

70. Bunce, N. J.; Ravanal, L. *J. Am. Chem. Soc.* **1977**, *99*, 4150.

71. QCPE program No. 506 (Ampac 2.1).

72. a) Turner, G. E.; Wynne, P. W. *J. Chem. Soc.* **1941**, 243. b) Günther, H. In *NMR Spectroscopy*; Wiley: New York, 1985 p 119.

73. Lim, E. C.; Chakrabarti, S. K. *Mol. Phys.* **1967**, *13*, 293.

74. Egger, K. W.; Cocks, A. T. *Helv. Chim. Acta.* **1973**, *56*, 1516.

75. Bunce, N. J.; Bergsma, J. P.; DeGraaf, W.; Kumar, Y.; Ravanal, L. *J. Org. Chem.* **1980**, *45*, 3708.

76. Whiffen, D. H. *J. Chem. Soc.* **1956**, 1350.

77. Benson, S. W. In *Thermochemical Kinetics*; New York: 1976, p 281.

78. Wells, P. R. In *Linear Free Energy Relationships*; Academic Press: New York, NY, 1968, Chapter 2.

79. Ruzo, L. O.; Bunce, N. J.; Safe, S.; Hutzinger, O. *Bull. Environ. Contam. Toxicol.* **1975**, *14b*, 341.

80. a) Orbach, N.; Potashnik, R.; Ottolenghi, M. *J. Phys. Chem.* **1972**, *76*, 1133. b) Goldschmidt, C. R.; Potashnik, R.; Ottolenghi, M. *J. Phys. Chem.* **1971**, *75*, 1025.

81. a) Peters, K. S.; Simon, J. D. *Acc. Chem. Res.* **1984**, *17*, 277. b) Peters, K. S.; Goodman, J. L. *J. Am Chem. Soc.* **1985**, *107*, 1441.

82. a) Gould, I. R.; Ege, D.; Mattes, S. L. *J. Am. Chem. Soc.* **1987**, *109*, 3794. b) Gould, I. R.; Moody, R.; Farid, S. *J. Am. Chem. Soc.* **1988**, *110*, 7242.

83. Yang, N. C.; Libman, J. *J. Am. Chem. Soc.* **1973**, *95*, 5783.

84. Mukerjee, P.; Mysels, K. J. In *Creation Micelle Concentrations of Aqueous Surfactant Systems*; Nat. Stand. Ref. Data Ser., Nat. Bur. Stand., 1971, 36.

85. Wolf, T.; Miller, N. *J. Photochem.* **1983**, *23*, 131.

86. Leibner, J. E.; Jacobus, J. *J. Phys. Chem.* **1977**, *81*, 130.

87. a) Pownall, H. J.; Smith, L. C. *J. Am. Chem. Soc.* **1973**, *95*, 3136. b) Shinoda, K.; Soda, T. *J. Phys. Chem.* **1963**, *67*, 2072.

88. a) Turro, N. J.; Gratzel, M.; Braun, A. M. *Angew. Chem. Int. Ed. Eng.* **1980**, *19*, 675. b) Turro, N. J. In *Modern Molecular Molecular Photochemistry*; Benjamin/Cummings: 1978, pp 76-152.

89. Dainty, C.; Bruce, D. W.; Cole-Hamilton, D. J.; Camilleri, P. *J. Chem. Soc. Chem. Commun.* **1984**, 1324.

90. Szwarc, M. In *Ions and Ion Pairs in Organic Solutions*; J. Wiley: New York, 1974, 2, p 45-71.

91. Lamola, A. A.; Hammond, G. J. *J. Chem. Phys.* **1965**, *43*, 2129.

92. a) Wagner, P. J. *Acc. Chem. Res.* **1971**, *4*, 168. b) Wagner, P. J.; Kochevor, I. *J. Am. Chem. Soc.* **1968**, *90*, 2232.

93. Wettack, F. S.; Renkes, G. D.; Renkly, M. G.; Turro, N. J.; Dalton, J. E. *J. Am. Chem. Soc.* **1970**, *92*, 1318.

94. Tyrell, H. J. V. In *Diffusion and Heat Flow in Liquids*; Butterworth and Co. Ltd.: London, 1961, pp 127.

95. Curtis, M. E.; Allred, A. L. *J. Am. Chem. Soc.* **1965**, *87*, 2554.

96. Farwell, S. O.; Beland, F. A.; Geer, R. D. *Analytical Chem.* **1975**, *47*, 895.

97. Gleicher, G. J.; Spurgeon, C. J.; Mahiou, B.; Soppe-Mbang, H.; Bozlee, B.; Minchin, S. A. *J. Mol. Struct.* (Theochem.) **1988**, *163*, 239.

98. Mahiou, B.; Clapp, G. E.; Gleicher, G. J.; Freeman, P. K.; Camaioni, D. *J. Phys. Org. Chem.* (in press).

99. Jang, J-S. *The Photochemistry of Some Polybromobiphenyls*; Oregon State University, 1990, Thesis.

100. Freeman, P. K.; Ramnath, N.; Jang, J-S. *J. Am. Chem. Soc.* **1991,** (in press).

101. Bethell, D. In *Organic Reactive Intermediates*; McManus, S. P., Ed.; Academic Press: New York, 1973; pp 61-126.

102. Kirmse, W. *Carbene Chemistry*; Acedemic Press: New York; 1964.

103. Herzberg, G. *Proc. Roy. Chem. Soc.* **1961**, *262a*, 291-317.

104. Wasserman, E.; Kuck, V. J.; Hutton, R. S.; Yager, W. A. *J. Am. Chem. Soc.* **1970**, *92*, 7491.

105. Geuther, A. *Justus Liebigs. Ann. Chem.* **1862**, *123*, 121.

106. Nef, J. U. *Justus Liebigs. Ann. Chem.* **1897**, *298*, 202.

107. Hine, J. *J. Am. Chem. Soc.* **1950**, *72*, 6162.

108. Doering, W. E.; Hoffman, A. K. *J. Am. Chem. Soc.* **1954**, *76*, 6162.

109. Skell, P. S.; Woodward, R. C. *J. Am. Chem. Soc.* **1956**, *78*, 4496.

110. Skell, P. S.; Garner, A. Y. *J. Am. Chem. Soc.* **1956**, *78*, 3409.

111. Skell, P. S.; Garner, A. Y. *J. Am. Chem. Soc.* **1956**, *78*, 5430.

112. Moss, H. A.; Schulman, F. C. *Chem. Commun.* **1966**, 373.

113. Ensslin, H. M.; Hanack, M. *Angew. Chem. Int. Ed.* **1967**, *6*, 702.

114. Bamford, W. R.; Stevens, T. S. *J. Chem. Soc.* **1952**, 4735.

115. Powell, J. W.; Whiting, M. C. *Tetrahedron* **1959**, *7*, 305-10.

116. Kirmse, W. *Carbene Chemistry* 2nd Ed.; Academic Press: New York, 1971.

117. Friedman, L.; Shechter, H. *J. Am. Chem. Soc.* **1960**, *82*, 1002.

118. Kyba, E. P. *J. Am. Chem. Soc.* **1977**, *99*, 8329.

119. Mueller, P. H.; Rondan, N. G.; Houk, K. N.; Harrison, J. F.; Willer, B. H.; Liebman, J. F. *J. Am. Chem. Soc.* **1981**, *103*, 1049-52.

120. a) Jones, W. M.; Ennis, C. L. *J. Am. Chem. Soc.* **1969**, *91*, 6391. b) Waali, E. E.; Tivakornpannaraai, S. *J. Am. Chem. Soc.* **1986**, *108*, 6058.

121. a) Moss, R. A. *Acc. Chem. Res.* **1980**, *13*, 58. b) Seyferth, D.; Mui, J. Y-P.; Damrauer, R. E. *J. Am. Chem. Soc.* **1968**, *90*, 6182.

122. Tanko, J. M.; Merola, J. S.; Mas, R. H.; Drumright, R. E. *J. Org. Chem.* **1990**, *55*, 4098.

123. Jorgensen, W. C.; Salem, L. *The Organic Chemists Book of Orbitals*; Academic Press: New York, 1973.

124. Clark, T.; Spitznagel, G. W.; Klose, R.; Schleyer, P. v. R. *J. Am. Chem. Soc.* **1984**, *106*, 4412.

125. Jones, M. Jr.; Gaspar, P. P.; Hsu, J-P.; Chari, S. *Tetrahedron*, **1985**, *41*, 1479.

126. a) Roberts, J. D. and references therein *J. Org. Chem.* **1965**, *30*, 23. b) Roberts, J. D.; Mazur, R. H. *J. Am Chem. Soc.* **1951**, *73*, 2509.

127. a) DeFrees, D. J.; McLean, A. D. *Astrophys. J.* **1986**, *308* pt.2 1. b) Hori, Y.; Noda, K.; Kobayashi, S.; Taniguchi, H. *Tetrahedron Lett.* **1969**, 3563. c) Skell, P. S.; Klebe, J. *J. Am. Chem. Soc.* **1960**, *82*, 247.

128. a) Freeman, P. K.; Swenson, K. E. *J. Org. Chem.* **1982**, *47*, 2033. b) Freeman, P. K.; Swenson, K. E. *J. Org. Chem.* **1982**, *47*, 2040.

129. a) Hart, H.; Saundri, J. M. *J. Am. Chem. Soc.* **1959**, *81*, 300. b) March, J. In *Advanced Organic Chemistry* 3rd Ed.; Wiley: New York, 1985, pp. 145, 283-5.

130. Richey, H. G. Jr. "Cyclopropylcarbonium Ion" in *Carbonium Ions*, vol 3; Wiley: New York, 1972, pp. 1201-94

131. Schleyer, P. v. R.; Van Dine, G. W. *J. Am. Chem. Soc.* **1966**, *88*, 2321.

132. Levi, B. A.; Blurock, E. S.; Hehre, W. J. *J. Am. Chem. Soc.* **1979**, *101*, 5537.

133. a) Sauders, M.; Siehl, H. U. *J. Am. Chem. Soc.* **1980**, *102*, 6808. b) Schleyer, P. v. R.; Lenoir, D.; Mison, P.; Liang, G.; Prakash, G. K. S.; Olah, G. A. *J. Am. Chem. Soc.* **1980**, *102*, 683. c) Staral, J. S.; Yavari, I.; Roberts, J. D.; Prakash, G. K. S.; Donovan, D. J.; Olah, G. A. *J. Am. Chem. Soc.* **1978**, *100*, 8016.

134. Hart, H.; Law, P. A. *J. Am. Chem. Soc.* **1964**, *86*, 1957.

135. Martin, J. C.; Timberlake, J. W. *J. Am. Chem. Soc.* **1970**, *92*, 978.

136. Oda, R.; Meino, M.; Hayashi, Y. *Tetrahedron Lett.* **1967**, *25*, 2363.

137. Békhazi, M.; Risbood, P. A.; Warkentin, J. *J. Am Chem Soc.* **1983**, *105*, 5675.

138. a) Sohn, M. B.; Jones, M., Jr. *J. Am. Chem. Soc.* **1972**, *94*, 8280. b) Schoeller, W. W. *J. Org. Chem.* **1980**, *45*, 2161.

139. Freeman, P. K.; Tafesh, A. M.; Clapp, G. E. *J. Org. Chem.* **1989**, *54*, 782.

140. Freeman, P. K.; Wuerch, S. E.; Clapp, G. E. *J. Org. Chem.* **1990**, *55*, 2587.

141. a) Davis, J. H.; Goddard, W. A. III.; Bergman, R. G. *J. Am. Chem.*

Soc. **1977**, *99*, 2427. b) Steinmetz, M. G.; Mayes, R. T. *J. Am. Chem. Soc.* **1985**, *107*, 2111. c) Boger, D. L.; Brotherton, C. E. *J. Am. Chem. Soc.* **1986**, *108*, 6695. d) Honjou, N.; Pancansky, J.; Yoshimine, M. *J. Am. Chem. Soc.* **1984**, *106*, 5361.

142. Dewar, M. J. S.; Thiel, W. *J. Am. Chem. Soc.* **1977**, *99*, 4899.

143. Roberts, J. D. *Notes on Molecular Orbital Calculations*; Benjamin: New York, 1961; 29-30.

144. Goh, S. H.; Closs, L. E.; Closs, G. L. *J. Org. Chem.* **1969**, *34*, 25.

145. a)Mansoor, A. M.; Stevens, I. D. R. *Tetrahedron Lett.* **1966**, 1733. b) Yamamoto, Y.; Moritani, J. *Tetrahedron* **1970**, *26*, 1235.

146. Freeman, P. K.; Danino, J. C.; Stevenson, B. K.; Clapp, G. E. *J. Org. Chem.* **1990**, *55*, 3867.

147. Bunce, N. J.; LaMarre, J.; Vaish, S. P. *Photochem. Photobiol.* **1984**, *39*, 531.

148. a) Stephenson, L. M.; Hammond, G. *Pure Appl. Chem.* **1968**, *16*, 125. b) Stephenson, L. M.; Whitten, D. G.; Vesley, G. F.; Hammond, G. *J. Am. Chem. Soc.* **1966**, *88*, 3665.

149. a) Freeman, P. K.; Hutchinson. L. L. *J. Org. Chem.* **1983**, *48*, 4705. b) Freeman, P. K.; Hutchinson, L. L. *J. Org. Chem.* **1980**, *45*, 1924.

150. Lorenz, D. H.; Shapiro, P.; Stern, A.; Becker, E. I. *J. Org. Chem.* **1963**, *28*, 2332.

151. Streitwieser, A. Jr.; Heathcock, C. H. *Introduction to Organic Chemistry*; Macmillan: New York, 1985, 80.

APPENDIX

GENERAL KINETICS SCHEMES

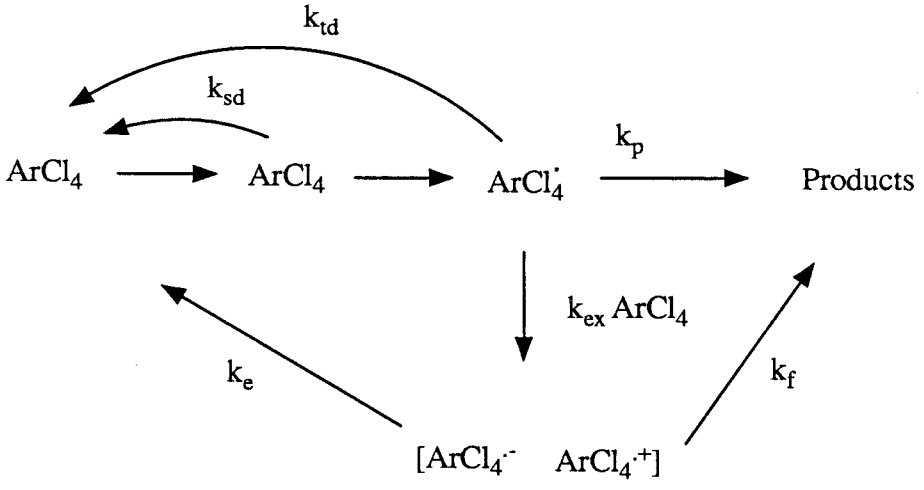

SIMPLE PHOTOLYSES

Rate = I (F) $[ArCl_4]$ ϕ

I = Intensity of Irradiation Light Source

F = Function of the Concentration and Epsilon

ϕ = Intersystem Crossing Yield (ϕ_{isc})

Steady State Assumption employed:

Appearance of Triplet (rate) = Disappearance of Triplet (rate)

$I\,[ArCl_4] = k_{ex}[ArCl_4]\,[T^1] + k_p\,[T^1] + k_{td}\,[T^1]$

$* [T^1] = I[ArCl_4] / k_{ex}\,[ArCl_4] + k_p + k_{ex}$

Rate of Product Formation = dp/dt

$dp/dt = k_p[T^1] + k_{ex}[ArCl_4][T^1]\,(G)$, $G = k_f / k_f + k_e$

$dp/dt = [T^1]\,\{k_p + k_{ex}[ArCl_4](G)\}$

sub * $dp/dt = \{k_p + (G)k_{ex}[ArCl_4]\}\ \{I[ArCl_4] / k_{ex}[ArCl_4] + k_p + k_{td}\}$

ϕ = Quantum Yield = $(dp/dt) / I[ArCl_4]$

$\phi = \{I[ArCl_4] / I[ArCl_4]\}\ \{k_p + (G)k_{ex}[ArCl_4] / k_p + k_{td} + k_{ex}[ArCl_4]\}$

$\phi = \{k_p + (G)k_{ex}[ArCl_4]\} / \{k_p + k_{td} + k_{ex}[ArCl_4]\}$

$\phi^{-1} = \{k_p + k_{td} + k_{ex}[ArCl_4]\} / \{k_p + (G)k_{ex}[ArCl_4]\}$

ANALYSIS IN THE CONCENTRATED REGION

$k_{ex}(G)[ArCl_4] >> k_p$

$\phi^{-1} = \{k_{td} + k_{ex}[ArCl_4]\} / \{(G)k_{ex}[ArCl_4]$

$\phi^{-1} = G^{-1} + k_{td} / (G)k_{ex}[ArCl_4]$

SLOPE = $k_{td} / (G)k_{ex}$, INTERCEPT = G^{-1}

SLOPE/INTERCEPT = k_{td} / k_{ex}

PHOTOLYSES IN THE PRESENCE OF TRIETHYLAMINE

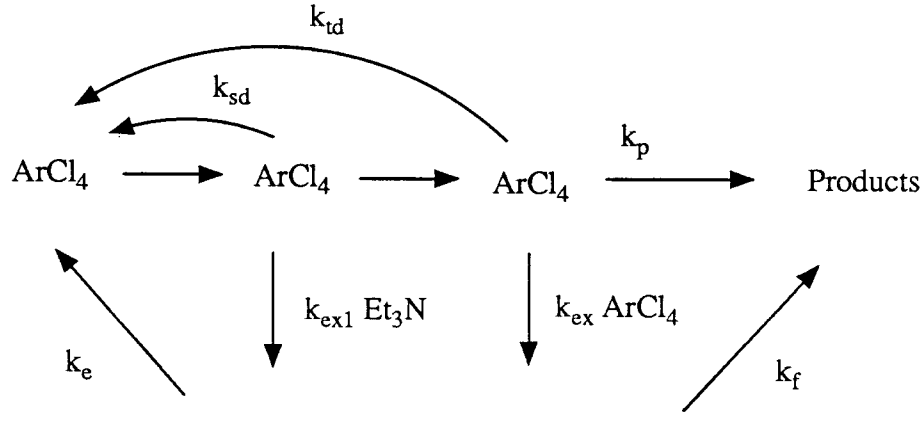

EXCIPLEX VS EXCIMER

PRODUCTS ARISING FROM A SINGLET EXCIPLEX

In the region of high concentration of triethylamine, it is reasonable to expect $k_{ex1}[Et_3N]$ to be the dominate route to product. Quantum yield (ϕ) can then be expressed as follows:

$$\phi = k_{ex1}[Et_3N]\,(G), \text{ where } G = k_f / (k_f + k_e)$$

$$\phi = G^{-1} + (k_{isc} + k_{sd}) / k_{ex1}[Et_3N](G)$$

$$\text{SLOPE} = (k_{isc} + k_{sd}) / k_{ex1}(G), \text{ INTERCEPT} = G^{-1}$$

$$\text{SLOPE / INTERCEPT} = (k_{isc} + k_{sd}) / k_{ex1}$$

$k_{isc} = 1.0$, an estimate of k_{sd} was given by Turro[88b]; $1 \times 10^7\ s^{-1}$ and for k_{ex1} to compete the value would need to be 100 times greater or $1 \times 10^{10}\ s^{-1}$.